NUMERICAL AND EXPERIMENTAL INVESTIGATION OF VARIOUS SURFACTANT AND GAS INJECTION TECHNIQUES FOR IMPROVED RECOVERY IN UNCONVENTIONAL LIQUID RESERVOIRS

A Dissertation

by

FAN ZHANG

Submitted to the Office of Graduate and Professional Studies of
Texas A&M University
in partial fulfillment of the requirements for the degree of

DOCTOR OF PHILOSOPHY

Chair of Committee,	David Schechter
Committee Members,	Mark Everett
	Eduardo Gildin
	Hadi Nasrabadi
Head of Department,	Jeff Spath

August 2020

Major Subject: Petroleum Engineering

Copyright 2020 Fan Zhang

ABSTRACT

In order to extend the economic life of existing horizontal wells and improve oil production for newly drilled wells in unconventional liquid reservoirs (ULR), testing of enhanced oil recovery (EOR) techniques is essential. The interaction of the fluids in the fractures system with the oil stored in the matrix is the key to understanding and implementing all EOR techniques in ULR. This study focuses on investigating the performance of different EOR agents (surfactant, CO_2, rich gas, and foam) through laboratory tests as well as upscaling the experimental data to field-scale through numerical simulation.

A correlated set of Huff-n-Puff and spontaneous imbibition experiments were performed at reservoir temperature using different surfactants, gases, and foam on side-wall core samples from the Wolfcamp and the Eagle Ford formations. The experimental setup was mounted into a Computed Tomography (CT) Unit (CTU) to capture time-lapse CT images which were used to monitor the fluid movement inside the core plugs, track the foam quality in glass beads around the cores, and construct core-scale simulation models. A comprehensive upscale workflow was proposed by combining the results of laboratory data, scaling group analysis, core-scale history match, and field-scale prediction. The scaling parameters are achieved from history-matching laboratory data, which are implemented in the field-scale reservoir model to estimate the production enhancement through surfactant and gas injection EOR techniques.

Different gases (CH_4, a mixture of 85% CH_4 - 15% C_2H_6, enriched gas (50% CH_4 - 50% C_2H_6), and CO_2) were tested to explore the effects of gas composition on the recovery factor in ULR. Enriched gas (50% CH_4 - 50% C_2H_6) showed the most promising potential of improving oil recovery in the Wolfcamp formation. Increasing pressure does not always lead to a higher recovery, such as high pressure (beyond 5,000 psi) CO_2 injection. The primary mechanism of gas injection is multi-contact miscibility, and diffusion has a minor effect on enhancing oil recovery in ULR. Surfactants enhance oil recovery by wettability alteration and interfacial tension (IFT) reduction. Implementing surfactant into completion fluids or re-frac fluids results in additional oil recovered from ULR. From the results obtained, a combination of EOR techniques (foam or sequencing surfactant and gas injection) opens the possibility to achieve optimum oil recovery in ULR.

DEDICATION

To my parents, Hua and Peihua, for your unconditional love and support.

To my wife, Yunfei, for encouraging me to go forward and all your love, supports, and sacrifices.

To my children, Aiden and Emerson, for sharing happiness with me and always giving me the strength to accomplish all the challenges.

ACKNOWLEDGMENTS

I would like to give my dearest gratitude to my committee chair Dr. David Schechter for his guidance, support, teaching, and sharing his knowledge and experience in both research and life. I sincerely appreciate all his support and guidance throughout these years.

I would like to thank my committee member Dr. Mark Everett, Dr. Eduardo Gildin, and Dr. Hadi Nasrabadi, for their guidance, support, and the time they put into this research.

I would like to thank fellow researchers I. Wayan Rakananda Saputra, Imad Adel, Stefano Tagliaferri, Weidong Chen, Rohan Vijapurapu, Jingjing Zhang, Thomas Connor, and the whole Dr. Schechter's research group for their support and contribution in the lab and office.

Thanks also go to my friends and colleagues and the department faculty and staff, especially John Maldonado, for making my life at Texas A&M University easier and a great experience.

Finally, I would like to express my gratitude to the Harold Vance Department of Petroleum Engineering, the Crisman Institute Petroleum Research at Texas A&M University, and Halliburton for funding the research.

CONTRIBUTORS AND FUNDING SOURCES

Contributors

This work was supervised by a dissertation committee consisting of Professor Dr. David Schechter, Professor Eduardo Gildin, and Professor Hadi Nasrabadi of the Department of Petroleum Engineering and Professor Mark Everett of the Department of Geology and Geophysics.

Experimental work was completed by the student, in collaboration with I. Wayan Rakananda Saputra, Imad Adel, Stefano Tagliaferri, Rohan Vijapurapu, Thomas Connor, and John Maldonado of the Department of Petroleum Engineering. The ternary diagram analysis in Chapter V was completed by the student, in collaboration with Weidong Chen of the Department of Petroleum Engineering.

All other work conducted for the dissertation was completed by the student independently.

Funding Sources

This research was supported by the Crisman Institute for Petroleum Research at Texas A&M University.

This research was also made possible in part by Halliburton.

NOMENCLATURE

BPR	Back Pressure Regulators
CA	Contact angle
CT	Computed tomography
CH	Core holder
d	Diameter of core samples
DW	Distilled water
EIA	United States Energy Information Administration
EOR	Enhanced oil recovery
EOS	Equation of state
EUR	Estimated ultimate recovery
$\hat{f}_i^l$	Liquid fugacity of component i
$\hat{f}_i^v$	Vapor fugacity of component i
GC	Gas chromatography
GOR	Gas oil ratio
G_1	Volume proportion of gas in a mixture
HU	Hounsfield Unit
IFT	Interfacial tension
IOR	Improved oil recovery
k	Permeability

k_{ij}	Binary interaction parameter
K_i	K value for EOS
KI	Potassium iodide
L	Length of core samples
MMP	Minimum miscibility pressure
MSTC	Thousand stock tank barrel
OB	Overburden
OD	Outer diameter
OOIP	Original oil in place
O_1	Volume proportion of oil in a mixture
P	Pressure
P_c	Capillary pressure
ΔP_cT	Defined parameter for capillary pressure multiplied by time
ΔP_c	Capillary pressure difference
P_{ci}	Critical capillary pressure of component i
PI	Production interval
PVT	Pressure-Volume-Temperature
q	Production rate
r	Radius of curvature
SASI	Surfactant assisted spontaneous imbibition
Scf	Standard cubic foot
SI	Soak interval

STB	Stock tank barrel
SURF/Surf	Surfactant
S_o	Oil saturation
S_w	Water saturation
S_{wi}	Initial Water saturation
t	Time
t_{mid}	Mean time between two recorded times
T	Temperature
T_{ci}	Critical temperature of component i
ULR	Unconventional liquid reservoirs
USD	U.S. dollar
UV	Ultraviolet visible
V_{ci}	Critical molar volumes for component i
V_{cj}	Critical molar volumes for component j
w_i	Acentric factor of component i
x_i	Liquid mole fractions of a component with index i
y_i	Gaseous mole fractions of a component with index i
σ	Interfacial tension
θ	Contact angle
∅	Porosity
μ_e	Effective viscosity of the two phases
μ_o	Oil viscosity

μ_w	Water viscosity

TABLE OF CONTENTS

Page

LIST OF FIGURES

Page

LIST OF TABLES

Page

CHAPTER I

INTRODUCTION

Unconventional liquid reservoirs (ULR) have contributed to a significant portion of oil production in the United States. Horizontal wells drilled in shale oil formations continue to increase the fraction of crude oil production (Todd et al. 2016). Horizontal wells constituted about 15% of crude oil production in ULR in 2004, but the percentage of oil production from horizontal wells increased to 96% of total production in ULR in 2018 (EIA 2019). Horizontal wells outnumbered vertical wells starting in 2017, however, horizontal wells began to dominate U.S. oil production since 2010. By the end of 2019, oil production from ULR is over 9 million barrels/day. Specifically, the Permian Basin produces more than 50% of oil from ULR with 4.5 million barrels/day followed by the Bakken and Eagle Ford formations (EIA 2020).

A significant volume of hydrocarbons exists in tight oil reservoirs. According to the U.S. Energy Information Administration (EIA), the Permian Basin remains the largest proved reserve in the United States, at about 20 billion barrels. However, the average recovery factors from primary depletion are 5% to 6% of the original oil in place (OOIP) due to the ULR's ultra-low permeability and low porosity (Alharthy et al. 2015, Alvarez et al. 2016b). Furthermore, some researchers claimed primary recovery is ultralow, less than 2% in some areas of ULR in the United States. The North Dakota Council reported that 1 to 2% of oil reserves are recoverable after primary depletion (Alfarge et al. 2017,

Wang et al. 2016). After primary depletion in ULR, the reservoirs may still trap more than 90% of their OOIP.

Multistage hydraulic fracturing along horizontal wells provides high flow paths and large contact areas, resulting in the intense fluid communication between horizontal well and matrix (Tovar et al. 2018, Zhang et al. 2018c). However, the fluid interaction between matrix and fracture system is weak, so production sustainability at a high rate is a common challenge in unconventional liquid reservoirs (Xu et al. 2019a). Although the initial production rate of horizontal wells is high, rapid decline of production rate continues until leveling off at a very low rate due to the low productivity from the matrix. The oil rate is generally less than 10% of initial production after three years of depletion (Xu et al. 2019b). To compensate for the rapid decline in production rates, the current practice is to perform infill drilling in these ULRs and consequently increase oil production in the short term (Alfarge et al. 2017). However, the newly drilled wells also face fast production decline such that infill drilling cannot act as long-term remediation for rapid production decline in ULR. In addition, infill drilling could lead to existing wells (parent well) get frac-hits by stimulation of new well (child well) (Yadav et al. 2017). The parent well that experienced frac hit has the highest risk of cleanouts and reduced production. Even if the parent well is shut-in during the fracturing of the child well, the oil production of the parent well is lower than that before shut-in (Sun et al. 2017). On the other hand, the child well underperforms compared with the parent well by lowering oil recovery factors by 20-40% (Jacobs 2019).

Since primary oil recovery factors range from 1-8% (Alfarge et al. 2017, Thakur 2019) and vast original oil in place for various ULR in the United States, it is imperative to develop the enormous potential of ULR and improve recovery factors by implementing EOR techniques (Thakur 2019). EOR techniques, including chemical injection, gas injection, foam injection, and thermal methods, are well understood and applied widely in conventional reservoirs. However, the EOR methods in unconventional reservoirs are new concepts and still stay at the level of experimental investigation, numerical simulation, and pilot project stage (Alfarge et al. 2017).

ULR is fundamentally different from conventional reservoirs. The shale matrix comprises an inorganic matrix and an organic matrix, with the pore radius typically less than 50 nm and in the range of 2-50 nm (Bai et al. 2013). The porosity of shale reservoirs is generally in the range of 5-10%, and the permeability varies from 0.0001 to 0.1 mD. It is also generally accepted that the initial wettability of ULR like the Bakken, Wolfcamp and Eagle Ford is oil-wet to intermediate-wet. The wettability has been determined by contact angle measurements in each of these reservoirs (Adel et al. 2018b, Alhashim et al. 2019, Wang et al. 2016, Zhang et al. 2017). Since reservoir properties vary in a broad range, it is essential to understand the target reservoir conditions before designing EOR applications.

The difference between conventional and unconventional reservoirs prevents EOR techniques that are extensively used in conventional reservoirs from being directly applied to unconventional reservoirs. EOR techniques that may be feasible to improve oil recovery in ULR are adding surfactant into completion fluids, surfactant injection, miscible gas

injection, hybrid EOR (sequencing surfactant/gas injection), foam injection, and low salinity water flooding (Adel et al. 2018a, Afanasev et al. 2019, Alfarge et al. 2018a, Alvarez et al. 2018a, AlYousif et al. 2018, Atan et al. 2018, Carpenter 2019, Chevallier et al. 2019, Hoffman et al. 2019, Mohanty et al. 2019, Saputra et al. 2019, Valluri et al. 2016, Zhang et al. 2018a, Zhang et al. 2019b).

There is very limited literature on combined EOR techniques (such as sequencing surfactant/gas injection and foam injection) in ULR. It is unknown whether the combined EOR techniques can further improve ultimate oil recovery to achieve optimum oil recovery and recovery mechanisms of these EOR techniques. In addition, there is a lack of EOR numerical simulation workflow of upscaling laboratory data to the field-scale and evaluating the performance of various EOR techniques. Therefore, this study proposes experimental workflows of hybrid EOR and foam injection EOR methods to assess the efficiency of combined EOR techniques. Also, a new modeling workflow for surfactant and gas injection EOR schemes is proposed to unveil the real potential of different EOR methods. In addition, a systematic analysis of experimental data and simulation results is presented to better understand the mechanism of aqueous phase surfactant injection and gas injection for improving production in ULR.

To achieve these objectives, Huff-n-Puff experiments were performed with CT scan technology to compare the performance of various EOR agents and reveal the mechanisms of these EOR techniques. Also, this study combines results of laboratory experiments, scaling group analysis, hydraulic fracturing simulation, core-scale history

match, and field-scale prediction to evaluate and compare the efficiency of various EOR applications in improving oil recovery in ULR. The dissertation is structured as follows:

Chapter II provides a literature review on different EOR applications in unconventional oil reservoirs. The literature review is comprised of three parts: chemical EOR applications, which mainly focuses on surfactant related EOR methods; miscible gas injection, including CO_2, natural gas, and N_2; and hybrid EOR methods with combined EOR methods, such as sequencing surfactant/gas injection and foam. Previous experimental investigation, simulation approaches, and EOR pilot data in ULR are summarized in each part. Chapter III illustrates the methodology of evaluating and comparing the performance of various EOR techniques in ULR. Experimental procedures of chemical, gas injection, and foam EOR are presented as well as the development of different EOR numerical simulation workflows.

Chapter IV describes the workflow of upscaling surfactant experimental data to field-scale. Contact angle, IFT, surfactant adsorption isotherm, and imbibition data are used to screen the efficiency of surfactant formulation and construct capillary pressure curves before and after surfactant treatment. Core-scale and field-scale simulation models are developed by considering CT-scan images, experimental results, and hydraulic fracturing simulation results to achieve upscaling parameters and forecast production after surfactant applications. Two chemical EOR schemes are investigated through reservoir simulation. Chapter V focuses on miscible gas injection investigation in ULR. The primary mechanism of gas injection EOR is studied through analyzing the results of Huff-n-Puff experiments, core-scale history matching, and ternary diagram analysis. In

addition, the critical parameters dominating the efficiency of gas injection EOR are investigated to optimize gas injection design in ULR. In Chapter VI, the feasibility of the hybrid EOR (sequencing surfactant/gas injection) technique is studied through experimental and numerical simulation of the Eagle Ford formation. Time-lapse CT images, the color of produced oil, and experimental observations are analyzed to infer pore size range influenced and target components of hydrocarbons affected by surfactant and gas injection.

Chapter VII assesses the performance of different surfactant formulations, gas mixtures, and foam using core plugs retrieved from the Wolfcamp formation as determined by Huff-n-Puff experiments. The effect of gas composition on MMP and Huff-n-Puff experiments is presented. Moreover, the feasibility of foam injection on improving oil recovery in ULR is also provided. In addition, the potential risks and challenges of foam applications are discussed in this chapter. Finally, important findings and highlighting contributions are summarized in Chapter VIII.

CHAPTER II

LITERATURE REVIEW

This chapter is oriented to review various EOR techniques in ULR, including investigation and application of laboratory experiments, numerical simulation, and pilot performance. First, the current chemical EOR applications in ULR are summarized to demonstrate the mechanisms and efficiency of improving oil recovery in ULR. Next, applications of the miscible gas injection methods are reviewed to recognize the effects of gas composition and pressure. Finally, a review of hybrid EOR studies is illustrated to reveal the potential of future investigation in combined EOR techniques in ULR. The summary of the reference literature listed in this chapter for chemical EOR, miscible gas injection, and hybrid EOR applications are presented in **Table 1-3** separately.

Table 1 – Reference of surfactant EOR applications in ULR.

Author, (Year)	Approach	Formation
Nguyen et al. (2014)	Imbibition Experiment	Eagle Ford/Bakken
Wang et al. (2016)	Experiment & Analytical Upscaling	Middle Bakken
Alvarez et al. (2018b)	Fractured Core-flooding Experiment	Permian
Zhang et al. (2018b)	Imbibition Experiment % Analysis	Permian/Eagle Ford
Whitfield et al. (2018)	Pilot (Pre-load prevent frac hit)	Eagle Ford
Kazempour et al. (2018)	Pilot (Injection)	Middle Bakken
Mohanty et al. (2019)	Fractured Core Experiment	Lower Eagle Ford
Park et al. (2019)	Imbibition Experiment - Salinity	Wolfcamp
Bidhendi et al. 2019	Pilot (Completion and Injection)	Wolfcamp
Saputra et al. (2019)	Imbibition Experiment & Simulation	Eagle Ford

Table 2– Reference of miscible gas injection EOR applications in ULR.

Gas Injection EOR Experimental Investigation			
Author, (Year)	Approach	Formation	Gases
Gamadi et al. (2014)	Huff-n-Puff Experiment	Eagle Ford/Mancos	CO_2
Tovar et al. (2014)	Huff-n-Puff Experiment	Barnett	CO_2
Jin et al. (2017)	Huff-n-Puff Experiment	Bakken	CO_2
Li et al. (2018)	Huff-n-Puff Experiment	Wolfcamp	CO_2, CH_4, N_2
Alharthy et al. (2018)	Huff-n-Puff Experiment	Bakken	CO_2, CH_4, C_1/C_2-85/15%, and N_2
Tovar et al. (2018)	Huff-n-Puff Experiment	Wolfcamp	CO_2 and N_2
Adel et al. (2018a)	Huff-n-Puff Experiment	Eagle Ford	CO_2

Gas Injection EOR Simulation Investigation			
Author, (Year)	Uniqueness	Formation	Gases
Xu et al. (2013)	Effect of Fracture Orientation	Bakken	CO_2
Pu et al. (2016)	Capillary Force and Adsorption	Bakken	CO_2
Sun et al. (2016)	Discrete Fracture Network	Wolfcamp	CO_2
Atan et al. (2018)	Economic Viability	Eagle Ford	Produced Gas
Alfarge et al. (2018b)	Critical Parameters	Bakken	NG/CO_2
Sahni et al. (2018)	Critical Mechanisms	N/A	CO_2
Ning et al. (2018)	Performance of C_2-Enriched Gas	Niobrara	Enriched Gas
Orozco et al. (2019)	Tank Material- Balance Calculation	Eagle Ford	Rich/Dry Gas
Wang et al. (2019)	Impact of Injection Temperature	N/A	CO_2
Ellafi et al. (2019)	Coupled Geomechanical Effects	Bakken	CO_2
Hoffman et al. (2019)	Quantitatively Evaluated Mechanisms	Eagle Ford	Natural Gas

Gas Injection EOR Pilots		
Author, (Year)	Formation	Gases
Todd et al. (2016)	Bakken	Enriched Gas/CO_2
Orozco et al. (2018)	Eagle Ford	Produced Gas
EOG (2019)	Eagle Ford	Produced Gas

Table 3 – Reference of hybrid EOR applications in ULR.

Author, (Year)	Approach	Formation	Method
Pankaj et al. (2018)	Simulation	Eagle Ford	Natural Gas Foam
Katiyar et al. (2019)	Pilot	Woodbine Field	Hydrocarbon Foam

Chemical EOR Applications in ULR

Generally, the chemical scheme has three methods, including polymer, alkaline, and surfactant. Polymer and alkaline flooding are not applicable to improve oil recovery in ULR because fluid cannot be injected through the low permeability matrix. In addition, the wettability of most of the unconventional shale reservoirs is intermediate-wet to oil-wet, meaning water cannot imbibe into the matrix spontaneously and expel oil out. Surfactant additives alter the wettability of rock surface from oil-wet to water-wet and reduce IFT, which implies surfactant is a promising EOR agent in ULR (Alvarez et al. 2016a, Nguyen et al. 2014).

Improving oil recovery using surfactant has caught the attention of the oil industry. Several researchers have investigated the efficiency of surfactant EOR for application in ULR. A review of previous literature regarding chemical EOR applications is presented in the next section.

Nguyen et al. (2014) investigated the potential of surfactants to improve oil recovery in shale reservoirs. Spontaneous imbibition experiments were performed using outcrop core samples from the Eagle Ford and Bakken formations using preserved core plugs in Amott cells at reservoir temperature. Porosities of the Eagle Ford and Bakken

cores vary from 8 to 14% and 5 to 6.5%, respectively. The temperature and permeability of the two reservoirs are in the range of 194-248 ^{o}F and 0.003 to 0.09 mD. Different types of surfactants, including cationic, anionic, nonionic, zwitterionic, and blends with concentration 0.1 to 0.2 wt.%, were tested to the effectiveness of surfactant formulations. Brine was the base aqueous solution, and the salinity of brine for Eagle Ford and Bakken is 2 wt.% and 27 wt.%. All types of surfactants improved oil recovery through imbibition tests using Bakken core plugs. The highest oil recovery was achieved using a nonionic surfactant. The cationic surfactant had the least oil enhancement effect. On the other hand, anionic surfactants showed the best performance in the Eagle Ford samples, recovering up to 48% of the OOIP. Similar to the test on Bakken cores, the cationic surfactant failed to improve oil recovery effectively. The authors concluded that wettability alteration was the dominant mechanism for the experiments reported, it was also reported that no clear correlation was observed between IFT and recovery factor in this study. In addition, they also reported the high salinity in Bakken reservoirs might be a challenge for surfactant applications because high salinity reduces the effects of wettability alteration and IFT reduction.

Wang et al. (2016) investigated surfactant performance on improving oil production, imbibition rate, and invasion depth in the Middle Bakken formation. The porosities and permeabilities of the core samples are from 4 to 8% and from 0.009 to 0.09 mD. The highest oil recovery obtained from the spontaneous imbibition is 32% OOIP, which is 20% beyond the brine base case. Experimental results indicated that the surfactants had the promising potential for improving oil recovery in the Middle Bakken

formation. The authors reported that the imbibition rate decreased as time went on, and most of the oil recovered from the core in the first few hours of spontaneous imbibition experiments. They then upscaled the experimental results to the field scale using an analytical method. They concluded surfactant could not increase oil recovery if the reservoir only contained hydraulic fractures because of limited invasion depth of surfactant into the matrix. However, the authors suggested the surfactant was a promising EOR agent for shale reservoirs with high intensity of pre-existing natural fractures.

Alvarez et al. (2018b) evaluated the ability of surfactants for improving oil recovery in ULR through experimentally representing surfactant soak during the fracture treatment by surfactant imbibition in Wolfcamp core plugs. Core-flooding experiments were performed using the Wolfcamp side-wall cores at a reservoir temperature of 165 ^{o}F. The porosity and permeability of the core samples range from 6 to 7% and from 0.0001 to 0.0002 mD, respectively. The highest recovery factor achieved from these core flooding-imbibition experiments is 13.3% OOIP using an anionic surfactant at a concentration of 2 gpt. Time lapse CT scanning was implemented throughout the duration of experiments to monitor fluid movement and penetration depth inside the core plugs. The authors concluded that surfactants alter the wettability of rock surfaces and moderately reduce IFT.

Zhang et al. (2018b) investigated the correlation between contact angle, IFT, and calculated capillary pressure with recovery factors as well as scaling approach for spontaneous imbibition using ULR cores. The authors reported that the recovery factors from spontaneous imbibition experiments had a negative trend with contact angle that

lower contact angle results in larger recovery factors and a positive correlation with capillary pressure that recovery factor increases as capillary pressure increases. In addition, no strong correlation was observed between the recovery factor and IFT. Hence, they proposed a surfactant selection method for improving oil recovery in ULR. The authors also developed a scaling model to characterize the flow behavior of spontaneous imbibition in ULR.

Mohanty et al. (2019) investigated the ability of a developed chemical blend to improve oil recovery and fracture permeability through fractured-core experiments using shale samples from Lower Eagle Ford. The blend could recover up to 30% of OOIP from the contacted shale and improved the permeability of the matrix at the fracture face by 25 to 100% due to the wettability of the fracture surface was altered to water wet. In addition, the authors mentioned field trials were designed in several horizontal wells in the Eagle Ford formation, but not carried out. However, surfactant mixed with 20,000 ppm brine as a preload was applied in several wells to mitigate fracture hits.

Whitfield et al. (2018) investigated pre-load as a frac hit management tool and production response after pre-load. A pre-load volume of 3,000 to 20,000 bbl. was injected at a constant rate of 2 to 5 bbl/min to mitigate frac hits. The cumulative oil production increment was 12,000 bbl during 8 months of production after 5 weeks of the shut-in. However, the authors reported that oil recovery improvement could be a result of pressure maintenance.

Park et al. (2019) performed spontaneous imbibition experiments at a reservoir temperature of 155 ^{o}F to evaluate the effects of different surfactant types and salinity on

the contact angle, IFT, and oil recovery using Wolfcamp core samples. Two different lithologies were tested; quartz-rich and carbonate-rich. Five types of surfactants at nine salinity levels were tested to identify the optimum salinity for wettability alteration and IFT reduction as well as the efficiency of improving oil recovery by spontaneous imbibition. Recovery factors of imbibition tests were determined by the wettability of rock surfaces. As the wettability changed from oil-wet to intermediate-wet and then to water-wet, recovery factors increased from 5 -10% to as high as 25% and eventually increased by up to 40%. Maximum wettability alteration occurred at salinity between 20,000 and 30,000 ppm. Surfactant and salt blends decreased IFT fast (from 25 mN/m to 12 mN/m) at low salinity and changed to slow (from 12 mN/m to 11 mN/m) as the salinity reached 30,000 ppm. The authors concluded the most favorable salinity range for surfactant application is from 20,000 to 33,000 ppm, which effectively decreases IFT and provides the greatest wettability alteration.

Kazempour et al. (2018) investigated the performance of customized chemical formulations for boosting oil recovery in the Middle Bakken formation through experiments, numerical simulation, and a field trial. Spontaneous imbibition experiments were performed on the preserved core plugs from the Middle Bakken formation at 115^{o}C. Two types of chemical formulations and two salinities (4% and 22%) were used in the tests. The recovery factor increased up to 40% OOIP by using chemical additives, and the recovery factor was only 2% using brine alone. Then, a field trial was carried out on a horizontal well in the Middle Bakken formation. The authors predicted an additional 25% of EUR would be recovered after 5 years of post-production, and about 8.3% of

incremental oil recovery was observed by the time of publication. They concluded this chemical Huff-n-Puff treatment significantly increased oil production that made this a potential economic IOR process in ULR.

Bidhendi et al. (2019) investigated the effect of surfactant on wettability alteration and oil production enhancement in the Wolfcamp formation. Laboratory experiments, chemical Huff-n-Puff field trials, and two completion trials were conducted in this study. Results of experiments indicated wettability alteration is a key mechanism to improve oil recovery in oil-wet shale reservoirs rather than ultra-low IFT. The most effective IFT for wettability alteration was from 1 to 5 dynes/cm. The authors observed a 39% cumulative oil production increment in the first 180 days and increased oil cut compared to the type curve of the formation. However, the production data of chemical Huff-n-Puff was not published in the paper.

Saputra et al. (2019) compared the oil production of wells with and without surfactant additives in the same area**.** The oil production was normalized based on the injected volume of proppant to eliminate the effect of completion design. The author demonstrated that adding surfactants to completion fluids improved oil recovery in the Wolfcamp formation.

In addition to the listed existing literature regarding chemical EOR applications, this research published two papers (Zhang et al. 2018b, Zhang et al. 2019c) to develop a chemical EOR simulation workflow accounting for experimental data, hydraulic fracturing, and history match.

Miscible Gas Injection EOR Applications in ULR

Gas injection is one of the most promising EOR techniques in ULR. Several research organizations and companies have investigated the efficiency of gas injection on improving oil production in unconventional reservoirs using experiments, numerical simulation, and field testing. Although different gases, such as CO_2, N_2, CH_4, produced gas, and enrich natural gas, were tested since the last decade, the majority of studies focused on CO_2 because of its widespread application for EOR in conventional reservoirs and a lower minimum miscibility pressure (MMP) than other gases. In the meantime, readily available produced gas and enriched natural gas has provided an alternative to CO_2, due to ample supply, easy accessibility, and low price. Currently, there is scant research on the potential and mechanisms of produced gas and enriched natural gas in ULR.

Considering the difficulty in performing gas injection experiment using shale cores, there is inadequate literature regarding experimental investigation of gas injection in ULR. The majority of the gas injection studies were conducted using numerical simulation to understand the mechanisms and performance of gas injection process.

Gamadi et al. (2014) performed CO_2 Huff-n-Puff experiments at a reservoir temperature of 95 ^oC using core samples from the Eagle Ford and the Mancos shale to investigate the efficiency of CO_2 injection on improving oil recovery in these reservoirs. Core samples were saturated with synthetic oil (decane to tridecane). The experiments studied the effect of pressure and soak time with recovery factors. The authors reported

the cyclic CO_2 injection increased recovery factors up to 95% of OOIP in the Eagle Ford cores. They also concluded the miscibility was the dominant parameter of cyclic CO_2 injection and increasing pressure beyond the MMP does not further improve recovery factor. In addition, the authors found recovery factors showed a positive correlation with injection pressure and soaking time.

Tovar et al. (2014) performed CO_2 injection experiments at reservoir temperature using preserved sidewall cores from the Barnett shale to study the potential of CO_2 injection in the Barnett reservoir. A novel configuration of gas injection experiments was developed to physically simulate hydraulic fracture and matrix system using core-holder to represent reservoir conditions. Glass beads were packed to surround core samples and act as high permeability fractures. CT scan technology was applied to the experiments to monitor fluid movement inside shale cores. The authors reported recovery factors of gas injection experiments between 18 to 51%.

Jin et al. (2017) investigated the effect of high-pressure CO_2 to enhance the diffusion-dominated flow in the matrix and extract additional oil from the Bakken reservoirs. Core samples were collected from two Bakken wells targeting from the Upper Bakken to Three Forks formations. CO_2 experiments were performed at reservoir conditions of 230 ^oF and 5,000 psi, and produced oil was collected throughout the duration of the experiments. Results from the experiments indicated that up to 99% of the oil was recovered in the cores from Three Forks the and Middle Bakken formations and up to 68% of OOIP was extracted from the Lower and Upper Bakken core samples. The authors

concluded pore-throat size and total-organic-carbon (TOC) were correlated with recovery factors. Low TOC and large pore-throat size results in higher oil recovery.

Li et al. (2018) performed Huff-n-Puff experiments using CO_2, CH_4, and N_2 at 2,000 psi to investigate the performance of gas injection on enhancing oil recovery in the Wolfcamp formation. The highest recovery factor was achieved using CO_2 after 6 Huff-n-Puff cycles, which was 65%.

Alharthy et al. (2018) investigated the effect of injection gas compositions on improving oil recovery in the Bakken formations. Experiments were performed at reservoir conditions of 230 ^oF and 5,000 psi using CO_2, CH_4, solvent mixture C_1 (85%) and C_2 (15%), and N_2 on the core samples from the lower and Middle Bakken formations. The experiments recovered up to 95% of oil by using CO_2, CH_4, solvent mixture C_1 (85%) and C_2 (15%) from core plugs and the oil recovery rate of CO_2 was faster than the other gases. In the Lower Bakken cores, the recovery factors decreased to nearly 40%. The authors concluded the primary mechanism of gas injection was miscible mixing and solvent extraction in the narrow region near the interface of fracture and matrix.

Tovar et al. (2018) investigated the efficiency of gas injection in the Wolfcamp formation using CO_2 and N_2. The core samples were cleaned utilizing the Dean-Stark method and re-saturated using the oil from corresponding wells at 10,000 psi for more than three months. The gas injection experiments were performed at reservoir temperature of 165^oF with different pressure from 2,100 to 3,500 psi. Up to 40% of OOIP was recovered from CO_2 injection experiments at 3,500 psi. However, recovery factors of N_2 Huff-n-Puff were 0% even when the experimental pressure was increased to 5,000 psi.

Recovery factors increased as both the soak time and pressure increased. The authors concluded the N_2 is much less effective than CO_2 in shale reservoirs and encouraged the use of methane/ethane mixtures for EOR in ULR. They also suggested the gas Huff-n-Puff injection in ULR operated at the highest possible pressure.

Majority of gas injection EOR in ULR studies were using numerical simulation because it is easier to conduct, less time-consuming, and less expensive compared to experimental investigation. Numerical simulation is an economical method to examine the effects of different parameters in gas injection and upscale laboratory data to the field-scale. Simulation results can provide some insights into the gas injection application design.

Xu et al. (2013) investigated the effect of hydraulic fracture orientation for gas injection EOR in the Bakken formation. Simulation results indicated CO_2 injection increased the recovery factors from less than 10% to almost 28% in both transverse and longitudinal fracture cases. The transverse fracture results in higher oil production, but faster breakthrough time and less injection efficiency compared to longitudinal fracture. Overall, the longitudinal fracture is a more effective method than the transverse fracture. The authors also concluded permeability of hydraulic fractures had a minor influence on increasing oil recovery, and the dual-porosity model is more suitable to represent unconventional reservoirs.

Pu et al. (2016) developed a simulation model considering capillary force and adsorption using pore size distribution from core measurement to study CO_2 EOR process in the Bakken. The authors reported that capillarity and adsorption should be applied to

gas injection simulation in ULR to capture the differentiation of production driving mechanism (considering capillarity and adsorption or not). They also concluded a substantial oil production improvement was observed when the model considered capillarity, adsorption, and pore size distribution properly.

Sun et al. (2016) developed a discrete fracture network model to evaluate the performance of CO_2 injection using the Huff-n-Puff protocol in ULR. The diffusion coefficient was achieved from history matching of experimental data and implemented into the field-scale model as a scaling parameter. Diffusion is a dominant parameter of gas injection process in the core-scale simulation. However, diffusion is negligible in the field-scale due to the short duration of the process. The authors concluded incremental oil was sensitive to reservoir properties but was not sensitive to soak time and capillary pressure.

Atan et al. (2018) investigated the technique and economic viability of gas injection EOR technique using produced gas in the Eagle Ford reservoirs. A compositional, dual-porosity, and dual-permeability reservoir model was developed to simulate the primary depletion and gas injection EOR process. The simulation results indicated cyclic gas injection EOR using produced gas has the potential of leading to incremental oil recovery of 41% in the Eagle Ford formation. The authors concluded containment of the injected gas is the highest risk to the gas injection EOR project based on the sensitivity analysis in this study. They found rotating the compressors as a function of pad performance and economic variables could result in an economic EOR project at low oil prices. In addition, the authors suggested that this study provided insight and guidance for a surveillance design.

Alfarge et al. (2018b) studied the main parameters for different gases in miscible gas injection process in ULR. The authors reported the porosity and fracture intensity were the dominant parameters to determine the success of CO_2 EOR and the effect of production enhancement in shale formations. They found molecular diffusion had different behavior in CO_2 and natural gas injection due to various properties of the gases. The penetration depth of natural gas is sensitive to the diffusion coefficient. Any increase in the diffusion rate leads to deeper natural gas penetration depth. CO_2 would penetrate deeper into the matrix even diffusion rate at a relatively low due to the larger concentration difference. In addition, the authors concluded natural gas possessed better performance than CO_2 on improving oil recovery in ULR when the permeability fall in the range of 10 nD - 1 mD. Because natural gas has a lower molecule weight and smaller size than CO_2, resulting in natural gas penetrates deeper into the matrix compared to CO_2.

Sahni et al. (2018) investigated the critical mechanisms of the miscible EOR process for optimal field test design in unconventional reservoirs. The authors indicated gas vaporization and IFT reduction was the primary recovery mechanisms, and molecular diffusion had no significant effect on incremental oil for the studied reservoir. They also concluded that the injected CO_2 volume determined the incremental oil recovery from the miscible EOR process, and soak time had a minor impact on oil production improvements in ULR.

Ning et al. (2018) evaluated the performance of ethane-enriched gas injection on enhancing oil recovery in Codell and Niobrara reservoirs using a dual-porosity reservoir model. The author reported ethane is a beneficial supplement to CO_2 in designing gas

injection EOR in ULR, and a mixture of 20% methane, 50% ethane, and 10% butane showed the highest incremental oil production with 1MMscf/day injection rate from results of sensitivity analyses. They also concluded the oil recovery enhancement was triggered when the diffusion coefficient was larger than 10^{-4} cm^2/s.

Orozco et al. (2019) developed a reservoir model considering tank material-balance calculation to evaluate the performance of gas injection EOR in the Eagle Ford reservoirs. The reservoir model was calibrated by history match of production data during primary depletion and gas injection treatment period. The results indicated the gas injection process was a feasible EOR method to significantly improve oil recovery in the Eagle Ford formation. They also concluded that rich gas could further improve oil production compared to dry gas through gas injection in shale reservoirs.

Wang et al. (2019) developed a non-isothermal compositional reservoir simulator for the CO_2 EOR process. The authors investigated the impact of injection temperature on the production from unconventional reservoirs. They concluded cold CO_2 injection could effectively increase the injectivity in the unconventional reservoirs.

Ellafi et al. (2019) investigated production mechanisms in unconventional reservoirs using reservoir simulation, which coupled geomechanical effects with diffusion/adsorption. The molecular diffusion mechanism is the dominant energy to expel oil from the matrix by oil swelling, and adsorption controls the storage capacity of the matrix surface when it contains high TOC and clay. The authors reported that deformation in the shale reservoirs resulted in higher recovery factors, but the change in porosity and stress yielded in the CO_2 injection process lower incremental oil recovery. They also

concluded CO_2 EOR could improve oil recovery in ULR and reliable storage of CO_2 with minimal environmental footprint.

Hoffman et al. (2019) quantitatively evaluated recovery mechanisms for gas injection in shale reservoirs. Four gas injection EOR mechanisms (vaporization, oil swelling, viscosity reduction, and pressure maintenance) were investigated in the study. The authors indicated the recovery had a strong function of the gas-oil ratio (GOR) with the highest recovery for black oil, and gas injection resulted in 40% incremental oil production as a percentage of the primary recovery over a three-year production. They also found vaporization is the dominant mechanism for high GOR reservoirs (>6,000 scf/STB), and oil swelling is the primary mechanism for low GOR reservoirs (500-2,000 scf/STB) during gas injection process in unconventional liquid reservoirs. In addition, the authors concluded that pressure maintenance contributed about 10% of total production, and viscosity reduction had a minimum impart of gas injection EOR process.

After introducing previous experimental and numerical simulation investigations of gas injection EOR in ULR, a review of gas injection EOR pilots in ULR is listed next. Most of the gas injection field pilots were performed in the Eagle Ford and Bakken formations using produced gas and CO_2. Significantly improved oil recovery was observed from produced gas injection pilots in the Eagle Ford formation.

Todd et al. (2016) reported four gas injection field pilots in the Bakken formation, in which three of them injected CO_2, and the fourth injected enriched gas. The two CO_2 Huff-n-Puff pilot wells did not encounter injectivity problems but failed to show significant oil production improvement from gas injection processes. CO_2 cyclic injection

in a vertical pilot was conducted with a 300-500 Mscf/day injection rate for 20-30 days. CO_2 was observed in a well 900 ft away, then the pilot was stopped. The last field pilot injected enriched natural gas with 55% CH_4, 10% N_2, and 35% C_{2+} at 3,500 psi for 55 days. Incremental oil production was observed in all four offset wells. Although all the CO_2 injection pilots failed to display sufficient production uplift in the Bakken formation, CO_2 injection might effectively improve oil recovery in other unconventional reservoirs. In addition, enrich natural gas has great potential as an EOR agent in ULR.

Orozco et al. (2018) reported a gas injection pilot in the Eagle Ford formation. Five Huff-n-Puff cycles were performed after 30 months of primary depletion. The author indicated that the recovery factor increased to 12.8% OOIP after five cycles, and the recovery factor of primary depletion for the same production period was 7.4%. They also concluded that gas injection is a promising EOR technique for boosting oil recovery in Eagle Ford reservoirs.

EOG Resources was the first company to disclose that it had recovered from 30% to 70% more oil from Eagle Ford shale wells using the natural gas injection method. Additional capital costs of the gas injection process were about $1 million per well on average, and the EOR process used associated gas from its wells. In addition, gas injection EOR is a fast process that production response is in 2-3 months (as shown in **Fig. 1)** and is an economical method that invested $1 adds $2 to net present value. EOG reported 150 EOR wells had been converted since the start of the program, and strong results were observed from these EOR wells (EOG 2019).

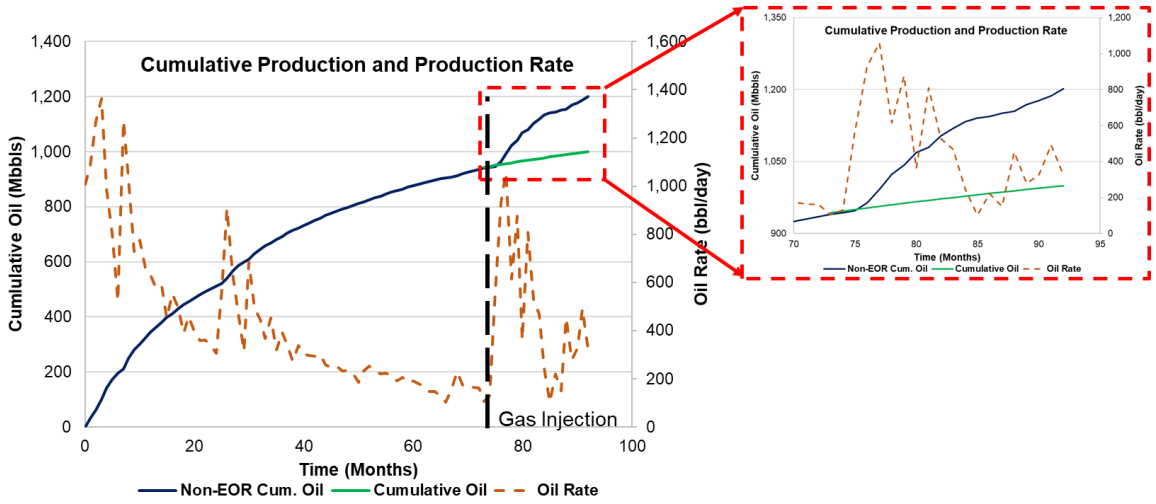

Figure 1 – Cumulative oil production and oil rate of gas injection pilots in Vincent Unit (Eagle Ford).

In addition to the listed existing literature regarding miscible gas EOR applications, this research published two papers (Zhang et al. 2018a, Zhang et al. 2019a) to develop a gas injection EOR simulation workflow and investigate the primary mechanism of gas injection EOR in ULR through experimental work and numerical simulation.

Hybrid EOR Applications in ULR

Field observations, along with laboratory experiments, have proven the potential of improving oil recovery in unconventional liquid reservoirs through chemical and gas injection methods. Different components of the oil are recovered from chemical and gas injection EOR techniques due to the various dominant mechanisms of these EOR methods. Therefore, a hybrid EOR technique (a combination of chemical and gas injection EOR

techniques) opens a possibility to chase optimum oil recovery through sequencing chemical/gas injection and foam in ULR. Currently, there is a significant lack of literature on hybrid EOR techniques in unconventional liquid-rich reservoirs, the most relevant previous publications regarding the evaluation of hybrid EOR in ULR are illustrated below.

Pankaj et al. (2018) investigated the impact of the natural gas-based foam on hydraulic fracture geometry and productivity in the unconventional reservoirs using numerical simulation. The authors concluded that natural gas foam fracturing fluids were characterized by rapid wellbore clean-up, low formation damage, relative permeability improvement, and less requirement of water for hydraulic fracturing. They also reported that natural gas foam fracturing fluids could improve proppant transport at least 10% farther in the hydraulic fractures than linear gel due to its increased effective viscosity. In addition, the authors concluded that improving relative permeability through surfactants and delivering proppant to farther distance could result in higher oil recovery in unconventional reservoirs.

Katiyar et al. (2019) investigated the performance of a hydrocarbon foam EOR pilot in a hydraulically fractured reservoir in the Woodbine field. The EOR pilot comprised of one horizontal injector and two surrounding horizontal producer pads. Brine and produced gases were injected alternately as well as co-injection protocol into the target formation. The authors reported the pilot met all of the success criteria for EOR purpose, which included mobility and injection control, out of zone injection elimination, increased oil production rates, increased gas utilization ratio, and sustained production after

cessation of surfactant injection. They also indicated that oil production of the well increased for at least six weeks after completing surfactant injection, and more than 2,000 bbl. of incremental oil was recovered from foam EOR operation.

In addition to the listed existing literature regarding miscible gas EOR applications, this research published two papers (Zhang et al. 2018a) to investigate the mechanism and efficiency of hybrid EOR (sequencing surfactant and gas injection) through laboratory experiments and numerical simulation. In addition, a novel experimental workflow of foam injection using Huff-n-Puff protocol was developed to evaluate the effectiveness of foam injection on enhancing oil recovery in unconventional liquid reservoirs. The details of the experimental workflow are available in Chapter III, and the results of foam experiments are presented in Chapter VII.

CHAPTER III

METHODOLOGY [*]

This research investigates the mechanisms and potentials of chemical, gas injection, and hybrid EOR techniques to improve oil recovery in unconventional liquid reservoirs through laboratory experiments and numerical simulation. These objectives are achieved by performing Huff-n-Puff experiments at reservoir conditions, analyzing experimental data of surfactant related tests (performed by colleagues), and executing numerical simulations. Chemical and gas injection EOR numerical simulation workflows are developed to upscale the experimental data to the field and evaluate the performance

---

[*] Parts of the methodology presented in this chapter have been reprinted from:

"Enhanced Oil Recovery in Unconventional Liquid Reservoir Using a Combination of CO_2 Huff-N-Puff and Surfactant-Assisted Spontaneous Imbibition" by Fan Zhang, I.A. Adel, K.H. Park, I. W. R. Saputra, and D.S. Schechter. SPE Paper 191502. Copyright 2018 by the Society of Petroleum Engineers (SPE). Reproduced with permission of SPE. Further reproduction prohibited without permission.

"Upscaling Laboratory Result of Surfactant-Assisted Spontaneous Imbibition to the Field Scale through Scaling Group Analysis, Numerical Simulation, and Discrete Fracture Network Model" by Fan Zhang, I. W. R. Saputra, G. Niu, I.A. Adel, and D.S. Schechter. SPE Paper 190155. Copyright 2018 by the Society of Petroleum Engineers (SPE). Reproduced with permission of SPE. Further reproduction prohibited without permission.

"Experimental and Numerical Studies of EOR for the Wolfcamp Formation by Surfactant Enriched Completion Fluids and Multi-Cycle Surfactant Injection" Fan Zhang, I. W. R. Saputra, S.G. Parsegov, I.A. Adel, and D.S. Schechter. SPE Paper 194325. Copyright 2019 by the Society of Petroleum Engineers (SPE). Reproduced with permission of SPE. Further reproduction prohibited without permission.

"Numerical Investigation to Understand the Mechanisms of CO_2 EOR in Unconventional Liquid Reservoirs" by Fan Zhang, I.A. Adel, I. W. R. Saputra, W. Chen and D.S. Schechter. SPE Paper 196019. Copyright 2019 by the Society of Petroleum Engineers (SPE). Reproduced with permission of SPE. Further reproduction prohibited without permission.

"Numerical Investigation of EOR Applications in Unconventional Liquid Reservoirs through Surfactant-Assisted Spontaneous Imbibition (SASI) and Gas Injection Following Primary Depletion" by Fan Zhang, I.A. Adel, I. W. R. Saputra, and D.S. Schechter. SPE Paper 196055. Copyright 2019 by the Society of Petroleum Engineers (SPE). Reproduced with permission of SPE. Further reproduction prohibited without permission.

of various EOR methods in improving oil recovery in ULR. In addition, a novel experimental workflow of foam injection experiments using the Huff-n-Puff protocol in ULR is presented to evaluate the efficiency of foam on improving oil recovery from liquid-rich shale reservoirs.

This chapter begins with an introduction of the core preparation process. Then, the experimental procedures of gas Huff-n-Puff experiments and MMP determination are illustrated. Details of hybrid EOR (sequencing gas injection/chemical EOR) and foam injection experimental workflows are then demonstrated. The development of chemical and gas injection EOR simulation models and the methods of acquiring input data are presented at the end of this chapter.

Core Preparation

To ensure the accuracy of chemical, gas injection, and hybrid EOR related laboratory experiments, the sidewall core plugs and oil samples were retrieved from the same well in liquid-rich shale reservoirs. A robust workflow of core plugs preparation procedure was conducted to restore the cores to the original reservoir conditions.

Rock samples were cleaned using the Dean-Stark method (Dean et al. 1920) and were then vacuum dried. After the cleaning and drying process, the core plugs were saturated with the reservoir oil under 10,000 psi for over three months until cores reached ultimate oil saturation that no more oil could soak into the core plug. Core samples were weighted and CT-scanned periodically throughout the aging process. Original Oil In Place

(OOIP) of each core plug was determined through the density of oil and weight difference before and after the saturation process (Zhang et al. 2018a, Zhang et al. 2019c).

Experimental Procedure of Gas Injection EOR Evaluation

In order to evaluate the mechanisms and efficiency of gas injection process on enhancing oil recovery in ULR, the MMP measurements and gas injection experiments were conducted to achieve these objectives. In this section, an introduction of MMP determination and gas injection experimental procedure is illustrated as follows.

Minimum Miscibility Pressure Determination

The slim tube method is used to determine the MMP in this research, which is believed the most accurate method. The recovery factors were calculated based on injecting 1.2 pore volume (PV) of gas. The effluents were collected and measured throughout the duration of the MMP test to determine the recovery factor at each pressure. The recovery factors of each pressure were plotted, and separated into two regions were identified as the immiscible region and the miscible region (Adel et al. 2016). The MMP of each sample was determined at the intersection point of the trend lines of the two regions. The schematic of the MMP apparatus is presented in **Fig. 2**.

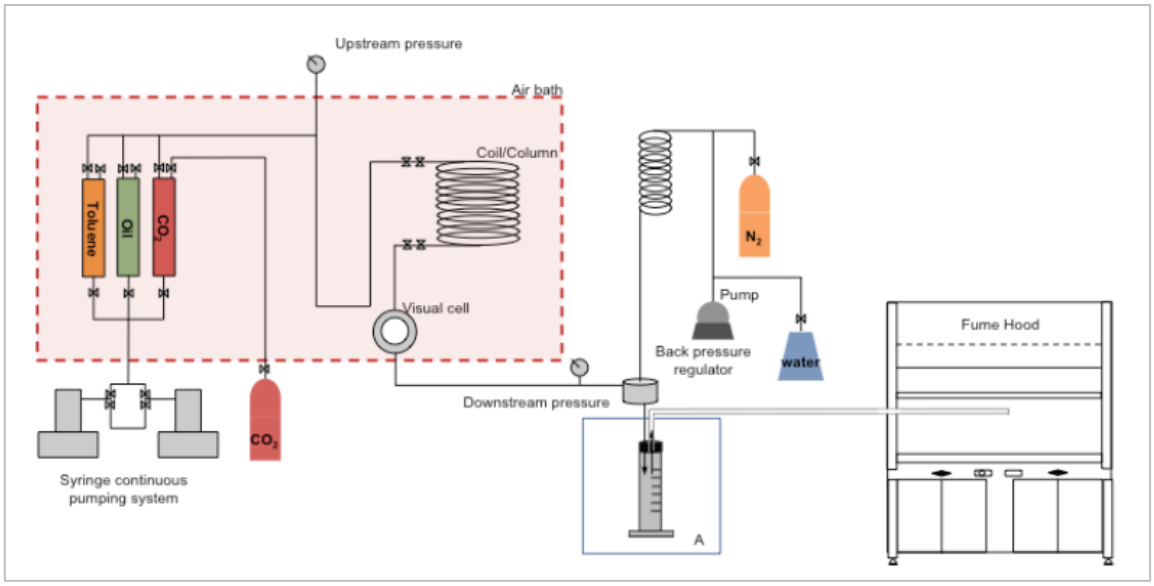

Figure 2 – Schematic of the MMP measurement setup

A significant increment in oil production is observed when the injection pressure is above the MMP. Therefore, it is essential to determine the MMP of the oil and the injected gas before performing the gas injection experiments.

Gas Injection Experiment

A physical representation of a hydraulic fracture was obtained by surrounding a side-wall shale core plug with 1 mm diameter glass beads inside an aluminum core-holder. This configuration closely reproduces field conditions by containing a high permeability fracture in direct connection with the matrix, which has permeability in the nano darcy range. All of the experiments were performed in core-flooding equipment coupled to a

CT-scanner, which enabled time-lapse to be taken during the tests. The apparatus was able to reach reservoir temperature and pressure.

Once the core holder was packed and connected to the core flooding rig, a vacuum was applied to remove the trapped air in the core-flooding system. Then, gas was injected from an accumulator to the core holder until reaching the designed pressure. At this point, soak time started at constant pressure for 10-72 hours. During the soak period, CT-scans were performed regularly to track the density changes and fluid movement inside core plug. When the soak period was completed, gas was injected into the core holder to displace the soaked gas and the oil out of the core holder with a constant flow rate. The effluents were collected at the outlet of the system. The described procedure constitutes one Huff-n-Puff cycle. The ultimate oil recovery was achieved by repeating several cycles until no more oil was produced (Zhang et al. 2018a, Zhang et al. 2019c).

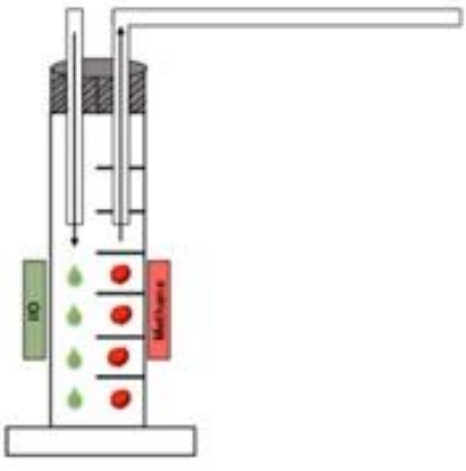

Figure 3 – Modified graduate cylinder designed for hydrocarbon injection tests.

When hydrocarbon gases were used during the tests, due to safety reasons, a stopper was mounted to seal the top of the graduated cylinder used to collect the effluents. The stopper had two holes, one allowing the produced oil to flow in and the other allowing the produced gas to evacuate into the fume hood. The modified graduated cylinder acted as a separator, as shown in **Fig. 3**. The stopper had two holes, one allowing the produced oil to flow in and the other allowing the produced gas to evacuate into the fume hood.

However, the fume hood was not accessible in the CT room. A vacuumed accumulator acted as the fume hood for all the gas injection experiments using hydrocarbon gases in the CT room, and the set-up of the gas disposal system is presented in **Fig. 4**. The produced gas was collected in an empty vacuumed accumulator that was later purged in the fume hood.

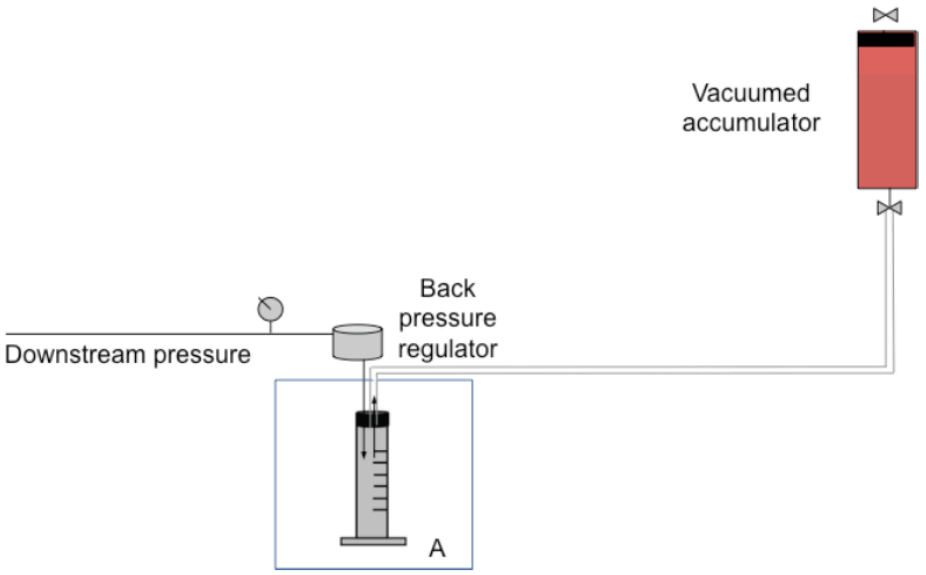

Figure 4 – Hydrocarbon gases purging set up for gas injection experiments performed in the CT room.

Experimental Procedure of Hybrid EOR Evaluation

Hybrid EOR technique is a combination of both chemical and gas injection EOR techniques to chase a further oil recovery improvement in ULR, which is a new EOR scheme in shale reservoirs. This research investigates two types of hybrid EOR schemes, sequencing gas injection/surfactant EOR and foam injection EOR. A novel workflow of foam injection using Huff-n-Puff protocol is included in this section.

Sequencing Gas/Surfactant EOR Experiment

To observe the effectiveness of combining gas and surfactant EOR techniques to recover additional oil, core plugs used on the spontaneous imbibition experiments went through the gas injection tests. The core plug was retrieved and directly placed in the modified Amott Cell set-up after the last cycle on the gas injection experiment. These tests were performed following the experimental procedures of spontaneous imbibition and gas injection experiments, which were described in the previous sections. Typically, the ultimate recovery factors of gas injection experiments are larger than those from spontaneous imbibition tests. A higher recovery factor could be expected if operated spontaneous imbibition experiment followed by a gas injection test. However, it is difficult to determine whether the hybrid EOR technique could further improve oil recovery compared to gas injection EOR. Therefore, gas injection experiments were performed before imbibition tests. The primary objective of this hybrid EOR test was to investigate

the feasibility of this hybrid EOR technique. One type of surfactant was used in the imbibition experiment to eliminate the effect of different surfactant formulations on recovery factors.

Foam Injection Experiment

Foam Huff-n-Puff experiments were performed at 5,000 psig and reservoir temperature of 155 ^{o}F. Hydrocarbon gases and one type of surfactant solution were co-injected into the core holder with a 70% gas/liquid ratio. The configuration of the core holder was the same as for the gas injection experiments. The schematic of the foam injection experiment setup is presented in **Fig. 5**. Hot water was circulated through the overburden of the core-holder to maintain the reservoir temperature, while heating tape was used for the lines and the connections. CT images of core plugs were taken regularly to track fluids movement inside the core plugs and to monitor the foam quality in glass beads during the experiments. The workflow of the foam experiments is the following:

- Pressurizing the core holder to 4900 psi with gas.
- Heating lines up using heating tape in order to avoid methane hydrate formation when the gas mixes with the surfactant solution.
- Isolating the core holder by closing the inlet and outlet.
- Setting BPR to 4950 psi.
- Injecting gas at 4.44 cc/min through the bypass until a stable pressure difference (PD) is observed.

- Co-injecting surfactant solution through bypass at 1.8 cc/min until the stable foam is observed at the outlet.
- Increasing the flow rate to 5.9 cc/min and 13.9 cc/min for the surfactant solution and the gas respectively, until stable foam production is observed at the outlet and a constant PD is achieved.
- Closing bypass and opening inlet of the core holder.
- Injecting foam into the core holder and waiting until the foam is produced at the outlet.
- Closing inlet of the core holder and leaving outlet open to monitor the pressure inside the system.
- Adjusting the overburden pressure to maintain a minimum of 600 psi pressure difference inside the core holder.
- Waiting until the temperature stabilizes, in the meantime, injecting gas through the bypass to clean the lines at 3 cc/min. As the gas expands inside the core holder, it will be produced from the outlet.
- After 30 minutes, closing the outlet of core holder, open inlet, increase BPR to 5,000 and use gas to maintain a constant pressure for 72 hours.
- After completing soak time, displacing the fluids inside of core holder by fresh hydrocarbon gas and collecting the oil using the modified graduate cylinder.

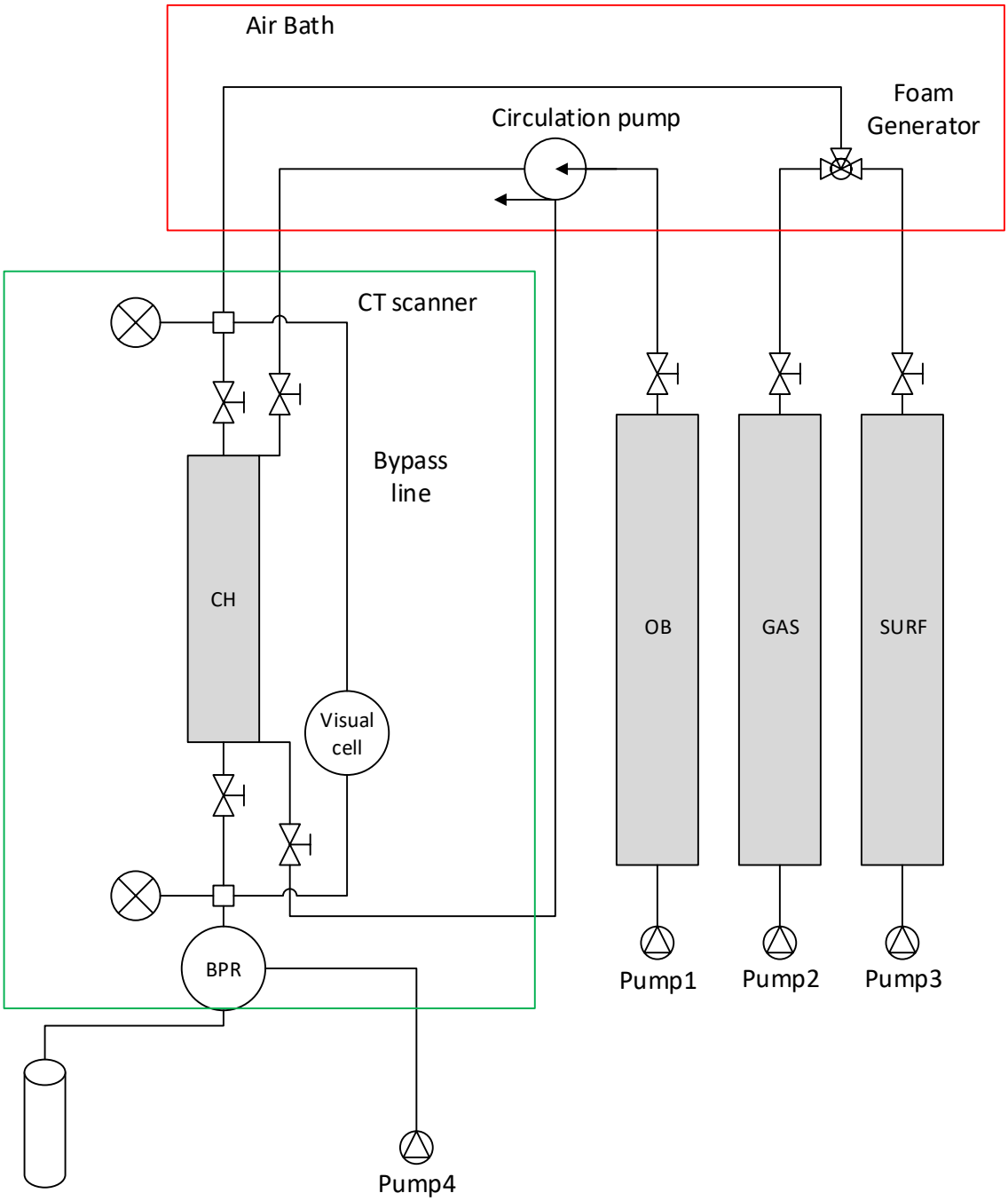

Figure 5 – Schematic of foam injection experiments.

Chemical EOR Numerical Simulation Workflow

In this study, numerical simulation is utilized to upscale experimental results of surfactant imbibition laboratory tests to the field, and then evaluate the potential of chemical EOR applications on improving oil recovery in ULR. PVT properties, capillary pressure, and relative permeability are modified to history match the oil production from laboratory experiments using the core-scale model. Then, the set of properties that the best match laboratory data is applied to the field-scale model to provide an insight into the efficiency of chemical EOR on the well-per-well basis. The hydraulic fracturing simulation results are implemented into the field-scale model to describe the geometry and permeability in hydraulic fractures better. This section contains the details of the core-scale model, capillary pressure curve, permeability curve, and field-scale model development.

Core-Scale Modeling

Heterogeneity is a universal nature of shale rock samples. Since the quality of the field-scale results is strongly dependent on the accuracy of the core-scale model, heterogeneity is included in the core-scale grid model. The core-scale model was constructed using CT-scan technology to capture the heterogeneity of shale cores. CT number has a linear correlation with density, indicating that a higher CT number results in a larger density. The density distribution of the core is converted into porosity

distribution, allowing for the inclusion of heterogeneity into the core-scale model. The dimensions of the core-scale model and fluid properties are precisely the same as the imbibition experiments.

Capillary pressure and relative permeability are critical inputs for numerical simulation, which are modified in order to match the oil recovery of imbibition tests. Initial and final capillary pressure is derived from scaling group analysis, and the details of capillary pressure generation are illustrated in the next section. The relative permeability curves of before and after surfactant treatment are constructed by trial-and-error of implementing multiple sets of curves on the core-scale numerical model. The adsorption isotherm of the surfactant is utilized as a weight factor of wettability alteration in simulation. The capillary pressure and relative permeability curves of each grid are determined from surfactant adsorption volume that interpolation of initial and final curves. Capillary pressure and relative permeability curves, and surfactant adsorption isotherms are applied to the field-scale model.

Capillary Pressure and Relative Permeability Curves

The interaction of surfactant with the oil-water-rock system alters the wettability of the rock surface from oil-wet to water-wet, and it reduces IFT, resulting in the transformation of the capillary pressure and the relative permeability curves. A reliable set of these two curves not only can simulate fluid flow in the reservoir close to the real state, but it also increases the accuracy of predicting surfactant performance in the field. In this

study, the capillary pressure profiles are estimated from scaling group analysis of experimental data, and relative permeability curves are generated from history-matching the oil recovery of laboratory-scale imbibition experiments (Zhang et al. 2019c).

The spontaneous imbibition process is dominated by capillary pressure, which is defined by the Young-Laplace equation presented as **Eq. 1** (Young 1805), where r is pore radius.

$$P_c = \frac{2\sigma\, cos\theta}{r} \quad \text{..... (1)}$$

Leverett (1939) defined a correlation between radius with porosity and permeability as:

$$r \propto \sqrt{\frac{k}{\emptyset}} \quad \text{..... (2)}$$

The capillary force could be rewritten in term of the Leverett radius, porosity, permeability, interfacial tension, and contact angle by:

$$P_c = \frac{2\sigma\, cos\theta}{\sqrt{\frac{k}{\emptyset}}} \quad \text{..... (3)}$$

In order to generate a capillary pressure profile of spontaneous imbibition process, a scaling group considering capillary pressure and laboratory data is defined as **Eq.4**, where $P_c\mathrm{T}$ is a newly defined parameter standing for capillary pressure multiplied by time.

$$P_c\mathrm{T} = \mathrm{t}\frac{2\sigma\ cos\theta}{\sqrt{\frac{k}{\emptyset}}} \quad \text{..... (4)}$$

The values of porosity, permeability, IFT, and contact angle are all determined in the laboratory. Hence, $\Delta P_c\mathrm{T}$ of each time step during spontaneous imbibition experiments is calculated for constructing the capillary pressure curve next. In addition, ΔP_c of each interval is calculated from **Eq.5**, where $\mathrm{t_{mid}}$ is the mean time between two recorded times in the experiments. By considering oil recovery curves obtained from spontaneous imbibition experiments, initial water saturation and ΔP_c, the capillary pressure profile can be generated for spontaneous imbibition process.

$$\Delta P_c = \frac{\Delta P_c\mathrm{T}}{\mathrm{t_{mid}}} \quad \text{..... (5)}$$

The capillary pressure curves of before and after surfactant treatment are estimated by analyzing the imbibition experimental data of the surfactant case and base case (brine/distilled water alone). In addition, the set of capillary pressure curves is applied to the core-scale and field-scale model for history match and evaluating the efficiency of chemical EOR on recovery improvement.

Relative permeability curves are constructed by trial-and-error of implementing multiple sets of curves on the core-scale numerical model. Different sets of relative permeability curves are tested to match the oil recovery of imbibition tests, and the curves are determined from the best history match results.

Hydraulic Fracturing Modeling

The reservoir model is constructed considering a physics-driven hydraulic fracturing model to simulate applications of EOR methods on the field scale (Parsegov et al. 2018b). The baseline conductivity attribute for each fracture was imported into a field-scale reservoir model. In **Fig. 6**, the effective fracture half-length defined by conductivity cutoff is greatly smaller than fracture half-length achieved from that of proppant placement. Smaller fracture half-length creates local pressure drawdown during production and may change the efficiency of the proposed EOR techniques. It is essential to take into account the proppant embedment and cruising, and other damaging mechanisms in fracturing simulation. Although the large volumes of fluid pumped during completion, hydraulic fractures exhibit limited height (~100 ft) from simulation results (Zhang et al. 2019c).

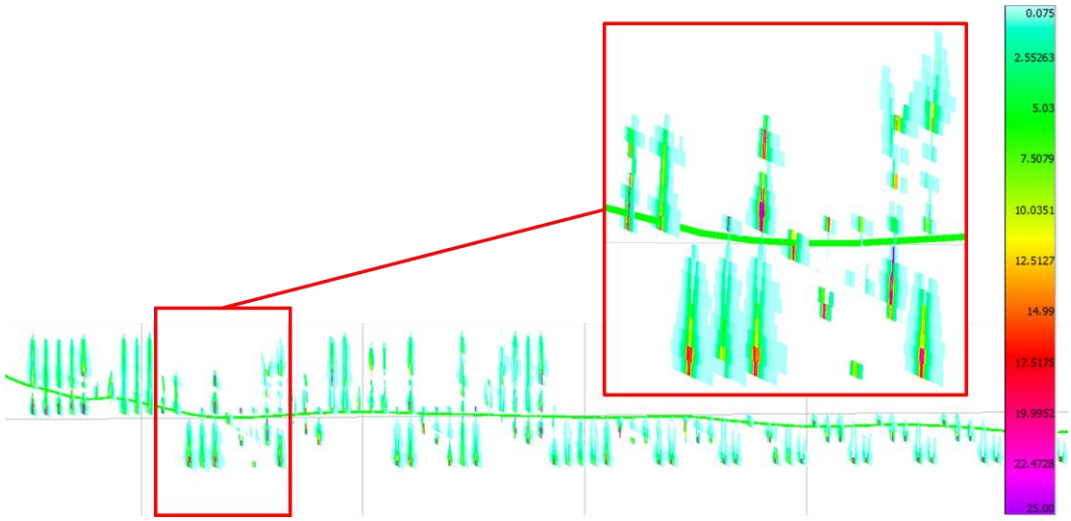

Figure 6 – Effective conductivity for the well with zoom in Stages 4 and 5. Reprinted with permission from Zhang et al. (2019c).

Field-Scale Modeling

The field-scale simulation model is constructed by considering the results of laboratory experiments, scaling group analysis, and core-scale history match, and hydraulic fracturing modeling. Chemical EOR modeling algorithm used on the core-scale model is also applied to the field-scale model to represent the mechanisms of surfactant EOR in ULR. The orientation, position, and perforation location of the well were determined based on real well data. Physics-driven fracturing simulation results provided the conductivity distribution in hydraulic fractures. Permeability for each hydraulic fracture grid is converted from the conductivity to achieve a more realistic hydraulic fracture system (Rubin 2010). The permeability distribution of hydraulic fractures in the reservoir model is presented in **Fig. 7**.

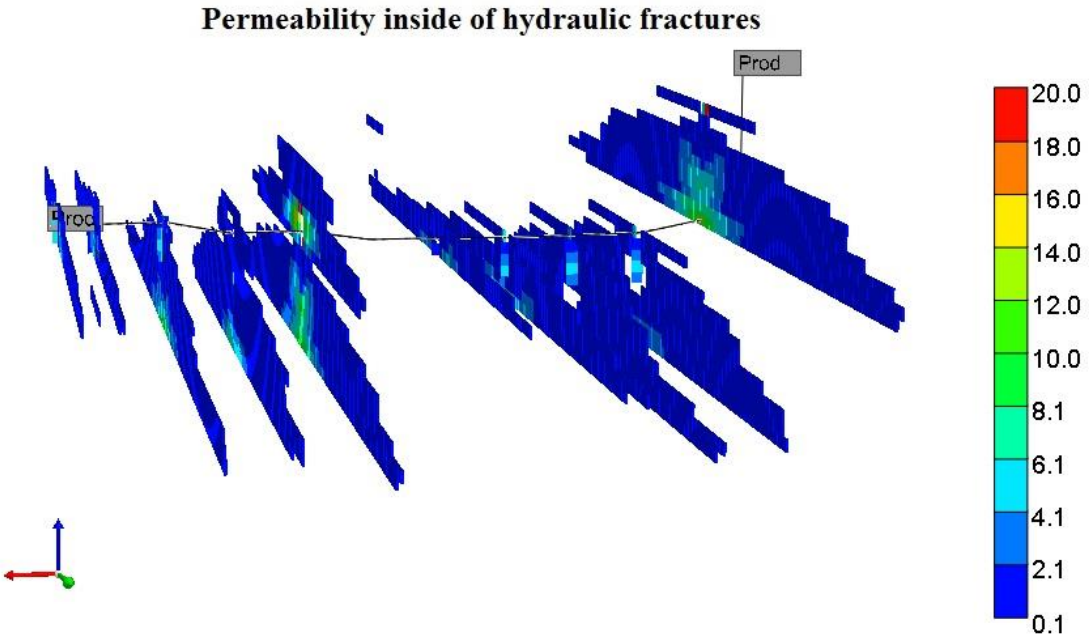

Figure 7 – Equivalent permeability in hydraulic fractures based on effective fracture conductivity shown in Fig. 10. Reprinted with permission from Zhang et al. (2019c).

A mixed gridding structure is utilized in the reservoir model to decrease the total grid number and ensure the accuracy of the simulation results. The grids close to hydraulic fractures are equally distributed in all three directions, and other grids are constructed following a logarithmic distribution, as depicted in **Fig. 8**. In addition, the ratio of two grids next to each other is less than 1.5, which decreases simulation errors.

Allocation of production from each fracture stage was approximated equal by analyzing previously-published data (Parsegov et al. 2018a). Therefore, two neighboring fracture stages out of the total 30 stages were modeled to save computational time. Production was normalized and assigned correspondingly for history-match purposes.

This cropped reservoir model has a dimension of 600 ft length, 2,000 ft width, and 200 ft height with 500 ft fracture half-length.

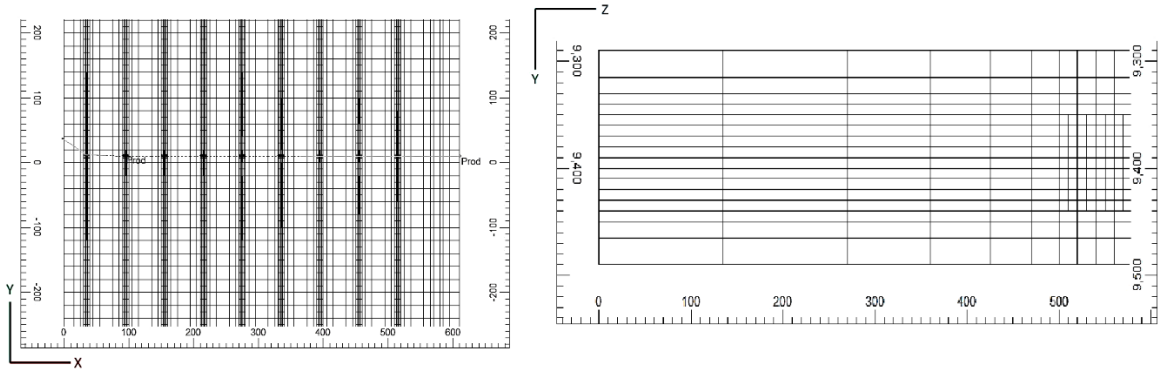

Figure 8 – Gridding structure for all three directions. Reprinted with permission from Zhang et al. (2019c).

All the undetermined reservoir parameters (such as permeability, porosity, natural fracture spacing, etc.) of the field-scale model are validated from the history match of actual production data. Then, different chemical EOR scenarios are investigated to observe the efficacy of each method on improving oil recovery in ULR.

Gas Injection EOR Numerical Simulation Workflow

Numerical simulation is an economical and less time-consuming approach to investigate the mechanisms of gas injection EOR and predict the performance of the gas injection process on enhancing oil recovery in ULR. PVT properties and diffusion coefficients are dominant parameters to describe the effect of gas injection. A core-scale

history match is performed to achieve those parameters for upscaling gas injection experimental results to the large reservoir scale. Results of gas injection simulation provide insight into the primary mechanism of gas injection process and guidance of gas injection EOR design in ULRs.

Core-Scale Modeling

The grid-base core-scale model is converted from CT images of the core plug to capture the heterogeneity of shale cores. Different porosity and permeability estimated from CT number are assigned for each grid block to demonstrate the heterogeneity of the core plugs accurately. The dimensions of the model, fluid properties, injection pressure, and soak time are precisely the same as the gas injection experiments. A slim tube model is developed and matched the MMP data from the laboratory to validate PVT properties for gas injection simulation.

The mechanisms of gas injection EOR technique include multi-contact miscibility, diffusion, and oil swelling. Related parameters are modified to history match laboratory data using the core-scale model. Diffusion coefficients of gas and hydrocarbons at different pressure are determined from the best history match results. However, the diffusion coefficient is the only available tuning parameter in the simulator, which controls the effect of gas injection on improving oil recovery in ULR. The impact of the multi-contact miscibility process is not sufficiently represented in numerical simulation to capture the actual mechanisms observed in the laboratory. The discrepancy between

diffusion coefficients achieved from the simulation compared with those measured in the laboratory to reveal a better representation of the dominant mechanism of gas injection in unconventional liquid reservoirs.

Field-Scale Modeling

A large-scale reservoir model is developed by coupling results of hydraulic fracturing simulation, experimental results, and core-scale history matching. Diffusion coefficients achieved from core-scale history matches are implemented into the field model to represent the effect of gas injection EOR. The gridding structure of the gas injection reservoir model is the same as the chemical EOR field-scale model. Since oil and water production from each stage is almost the same, two adjacent stages out of 14 stages were constructed to represent the whole well. The dimensions of this cropped reservoir model are 600 ft in length, 1,600 ft in width, and 100 ft in thickness with a 500 ft fracture half-length along the width direction. The field-scale model is validated by history match with actual production data. Reservoir parameters (such as porosity, fracture spacing, initial water saturation, etc.) are determined from the results of the best history match case. The effect of injection pressure and injection start time are investigated to provide insight into gas injection design. In addition, the potential of gas injection on recovery in ULR is evaluated using this reservoir model.

CHAPTER IV

CHEMICAL EOR IN UNCONVENTIONAL RESERVOIRS [*]

Surfactant additives possess the potential of improving oil recovery for different chemical EOR schemes (addition of surfactant into completion fluids and chemical injection process). In this chapter, two types of surfactants (named as Surf1 and Surf2) are used to investigate the recovery performance of various chemical EOR applications in ULR. Experimental data of surfactant related tests are referenced from (Zhang et al. 2019c).

The mechanisms of chemical EOR in unconventional liquid reservoirs are illustrated using relative permeability change of each mechanism. Next, capillary pressure and relative permeability curves are determined from dimensionless scaling group analysis and core-scale history match of experimental data. Finally, the potential of various chemical EOR applications is studied using the calibrated field-scale model to evaluate the efficiency of chemical EOR and provide insight into chemical EOR design in unconventional reservoirs.

---

[*] Parts of the methodology presented in this chapter have been reprinted from "Experimental and Numerical Studies of EOR for the Wolfcamp Formation by Surfactant Enriched Completion Fluids and Multi-Cycle Surfactant Injection" Fan Zhang, I. W. R. Saputra, S.G. Parsegov, I.A. Adel, and D.S. Schechter. SPE Paper 194325. Copyright 2019 by the Society of Petroleum Engineers (SPE). Reproduced with permission of SPE. Further reproduction prohibited without permission.

Mechanisms of Chemical EOR in ULR

The mechanisms of chemical EOR on improving oil recovery in unconventional liquid-rich reservoirs are wettability alteration and IFT reduction. In ULRs, wettability alteration plays a more significant role than IFT reduction on oil production enhancement (Zhang et al. 2018b).

Wettability alteration causes the sign of capillary pressure to change from a negative value to a positive value based on the Young-Laplace equation (**Eq. 1**), resulting in water is spontaneously imbibed into the matrix and expel oil from ULR. In the meantime, the relative permeability of oil is promoted, but the relative permeability of oil is suppressed (Monsalve et al. 1984, Morrow 1976). The relative permeability curves change caused by wettability alteration is shown in **Fig. 9**. This change of relative permeability results in a higher oil rate and consequently improve oil production.

Figure 9 – The change of relative permeability as the wettability altered from oil-wet to water-wet.

On the other hand, the IFT reduction leads to an uplift of relative permeability that both oil and water rates increase as IFT decreases (Schechter et al. 1994), as presented in **Fig. 10**. As the water rate increases, more water is produced from the matrix to the fracture system resulting in the water saturation increase in the fracture system. The oil production is determined by the transport capability of the fracture system. Oil production decreases as water saturation increases. Therefore, IFT reduction leads to an increase in oil relative permeability, but an increase of water-saturation in fractures may occur at the same time, especially in high initial water saturation reservoirs. The effect of improving oil recovery from IFT reduction is less than wettability alteration.

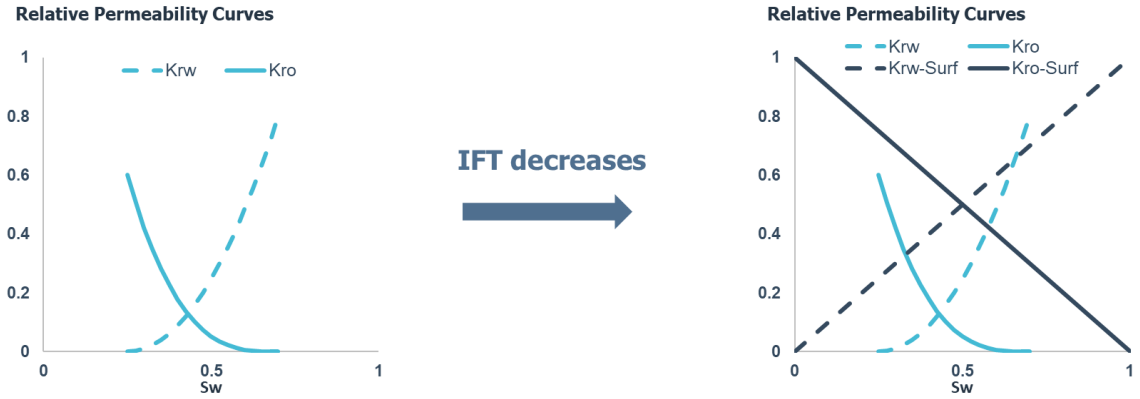

Figure 10 – The change of relative permeability from IFT reduction

Capillary Pressure Determination

Capillary pressure curve is a crucial input for reservoir simulation, especially modeling the wettability alteration process. To ensure the accuracy of the capillary pressure curves, these curves for all three fluid (water, Surf1 solution, and Surf2 solution)

systems were estimated using a scaling group analysis method. The $P_{c\ max}$ of each fluid was calculated by using **Eq.4** and **Eq. 5**, in which the contact angle (θ) and IFT (σ) were achieved from laboratory measurements. The constructed capillary pressure curves (in **Fig. 11**) of all fluid systems were then applied to the core-scale model to history match experimental results of imbibition experiments.

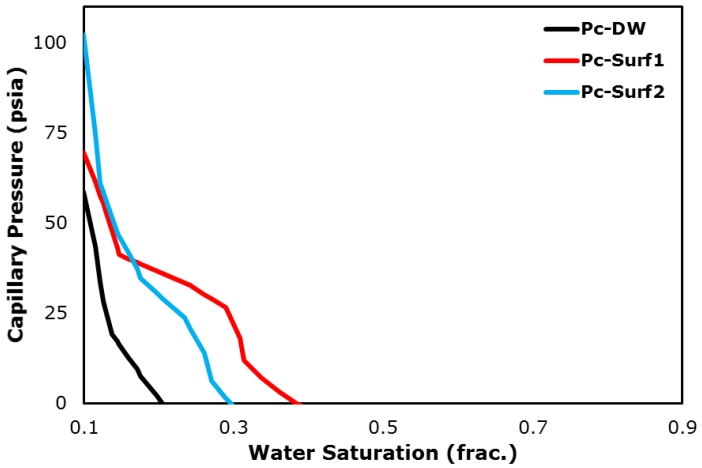

Figure 11 – Capillary pressure curves of all three fluid systems from scaling analysis. Reprinted with permission from Zhang et al. (2019c).

Core-Scale History Match

Previously, the capillary pressure curves were generated using scaling group analysis, and these curves would be implemented to the core-scale model. The relative permeability curves were determined by modeling the imbibition experiment and matching the oil recovery from the tests. Due to the highly heterogeneous nature of shale core samples, the integration of this heterogeneity into the core-scale model is essential to

confirm the accuracy of the relative permeability curve for the imbibition process. Core-scale models were developed by converting the density distribution of CT images to porosity and permeability for each core. A comparison of the grid-based core-scale model to the 3D CT image of rock samples is presented in **Fig. 12**. Multiple unique features (such as bedding planes) of core plugs observed from CT images are accurately implemented in the core-scale model.

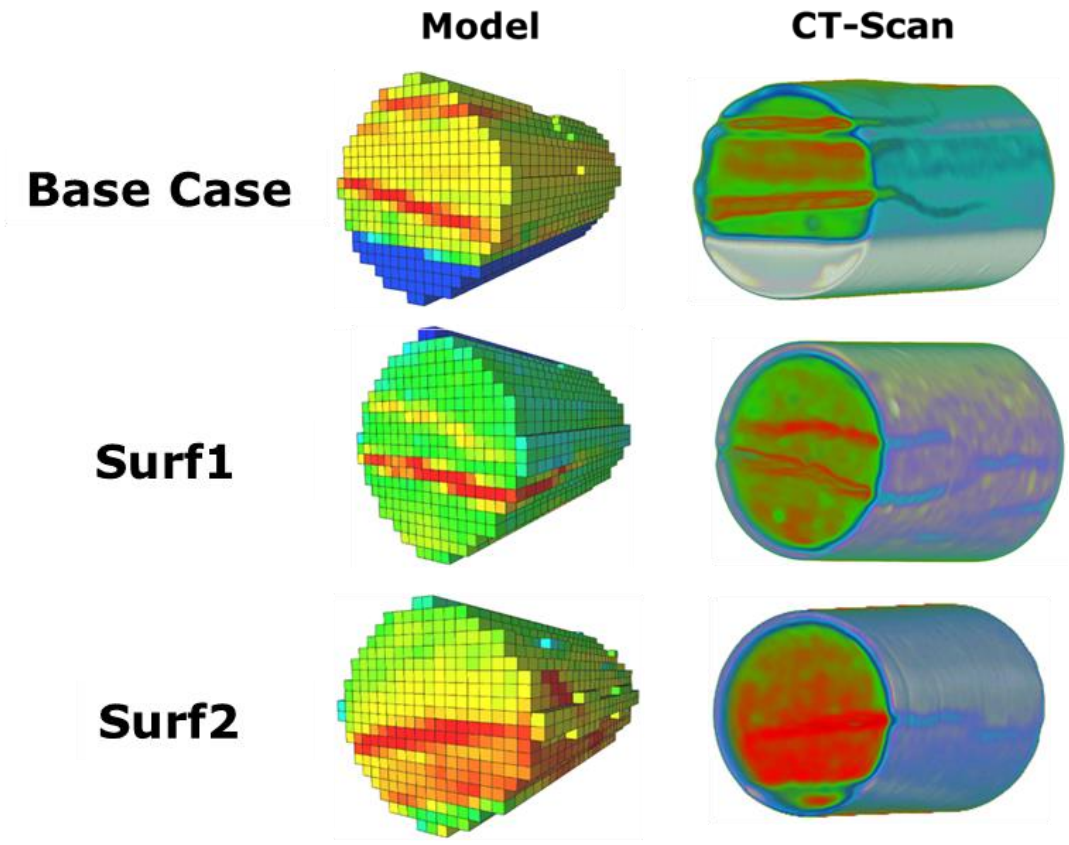

Figure 12 – Comparison of the 3D CT-scan image and core-scale model for porosity distribution. Reprinted with permission from Zhang et al. (2019c).

The core-scale model was developed to simulate the laboratory conditions of the imbibition experiment accurately. The core grid model was positioned in the middle of a water bath, corresponding to the core plug that was submerged into the aqueous solution in an Amott Cell during the imbibition experiment. Similar to the initial condition of the imbibition test, surfactants were only present outside of the core plug. Initially, the wettability of all core plugs was oil-wet. As more surfactant solution imbibed into the rock, the wettability of rock was altered gradually from oil-wet to water-wet. Therefore, the capillary pressure and relative permeability curves switched to the set of curves for the water-wet condition. The degree of alteration of the two curves was controlled by the amount of surfactant adsorbed in each grid block. This chemical EOR modeling algorithm was believed to be the most accurate method to depict the effect of wettability alteration and oil recovery improvement by surfactant additives.

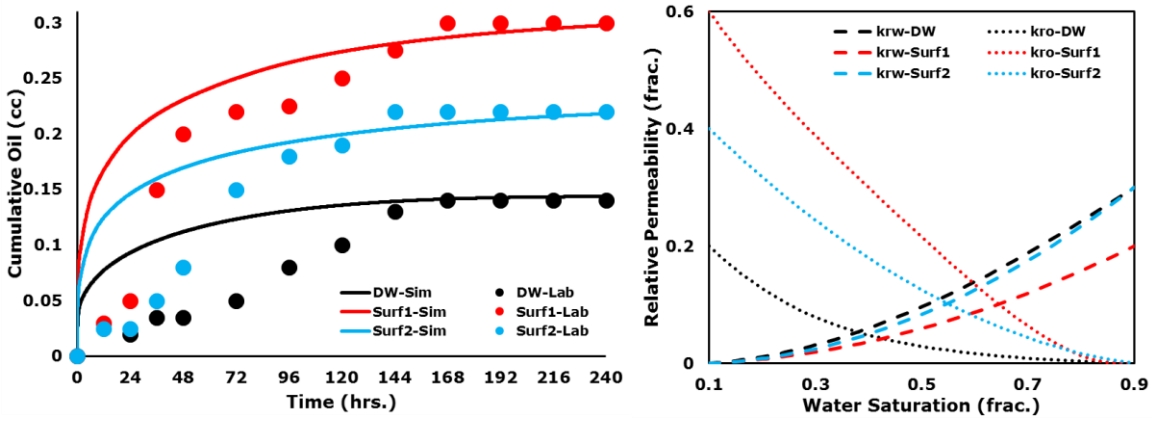

Figure 13 – The history-matching results of all three imbibition experiments (left) and corresponding relative permeability curves (right). Reprinted with permission from Zhang et al. (2019c).

History matching of imbibition data was performed on each experiment with numerous relative permeability curves. IFT and contact angle values were considered in the design of the relative permeability curves to ensure the tested relative permeability curve following the mechanisms of wettability alteration and IFT reduction. The results of the best history match case are presented in **Fig. 13**, in which the best-match oil recovery curve presented in the left and the corresponding relative permeability curves are shown in the right.

An apparent relation between relative permeability and IFT was observed where a lower IFT led to a higher maximum relative permeability. Although the ultimate oil recovery is in an agreement between laboratory and the simulation data, oil recovery from the simulation is overestimated compared to the laboratory data during the first few days. The produced oil attached to the rock surface was observed at the early time of most of the imbibition experiments, resulting in the recorded oil recovery from experiments that may be lower than the actual value. The experimental procedure dictates that oil droplets produced are recorded as they float to the top of the Amott cell. Even though the droplets are produced, they may not be measured until they detach from the core surface. The delay in that measurement could account for the mismatch. This observation verifies matching the ultimate recovery is the valuable part of this exercise. The relative permeability curves obtained from the best history match results and the capillary pressure curve constructed previously are implemented into the field-scale model.

Field-Scale Model

The field-scale simulation model is developed by considering the results of laboratory experiments, scaling group analysis, and core-scale history match, and hydraulic fracturing modeling. Two adjacent hydraulic fracture stages out of 30 fracture stages were randomly picked to construct the field-scale model, as shown in **Fig. 14**. The dimensions of the field-scale model are 600 ft in length by 2,000 ft in width by 200 ft in thickness with a mixed gridding structure to save computational time while still ensure simulation accuracy. Each stage has five clusters, in which two or three hydraulic fractures are suppressed by stress shadow effect that is consistent with reality. The field-scale model is a dual-porosity composition reservoir model to capture the impact of natural fractures that are commonly found in the Wolfcamp formation.

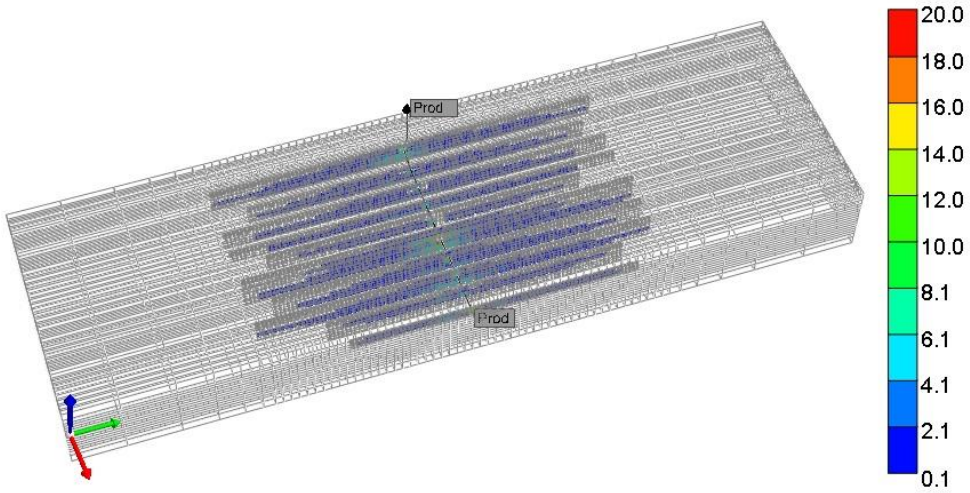

Figure 14 – Gridding structure and permeability distribution of the field-scale. Reprinted with permission from Zhang et al. (2019c).

Despite the lengthy process of incorporating multiple analyses to provide the required data for the field-scale model, several critical variables were still not determined. For instance, the permeability, porosity, and fracture spacing of the natural fracture system are three of the unknown variables. Another history match process was performed to determine all the reservoir properties in the simulation model. Actual production data of the corresponding well was retrieved and applied as the objective of the history match process. Cumulative oil and water production were matched to actual production data by modifying undetermined variables on the field-scale model. The best-matched scenario is plotted in **Fig. 15** and the reservoir properties of the large reservoir model are presented in **Table 4**.

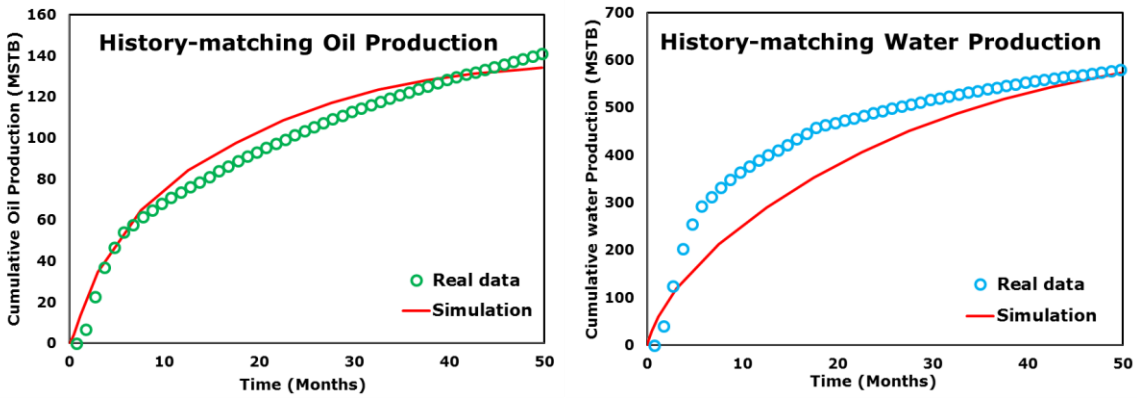

Figure 15 –The history-matching results of the field-scale model to actual oil (left) and water (right) production data. Reprinted with permission from Zhang et al. (2019c).

Results of the best history match case have a decent agreement with actual production data. Therefore, the reservoir model can be utilized to describe the reservoir

conditions and provide accurate production prediction for chemical EOR applications in unconventional liquid reservoirs (Zhang et al. 2019c).

Table 4 – Reservoir properties of the large reservoir model. Reprinted with permission from Zhang et al. (2019c).

Reservoir Property	Value	Reservoir Property	Value
Thickness (ft)	200	Hydraulic fracture half-length (ft)	500
Matrix porosity	5%	Fracture spacing (ft)	0.5
Fracture porosity	0.05%	Water saturation	0.45
Matrix permeability (nd)	150	Initial pressure (psi)	5,500
Fracture permeability (md)	0.04	Temperature (°F)	155

Chemical EOR Applications in ULR

Three schemes of chemical EOR applications were investigated using numerical simulation, which is chemical EOR in completion process, chemical injection EOR, and multi-cycle chemical injection process. In addition, the recovery performance of the water injection (without surfactant) process was also studied to reveal the actual efficiency of chemical injection EOR in ULR.

Chemical EOR in Completion Process

The first chemical EOR application to be explored is the application of surfactant as a part of completion design. The integration of chemical EOR in the completion design

is completed by adding a properly selected surfactant with effective concentration into the fracturing fluids. Interaction between surfactants and shale rock observed in the laboratory experiment is capable of improving the oil production of the well compared to the well without surfactant added into the completion fluids. This chemical EOR method is investigated by the trial of four surfactant concentrations with two types of surfactants. The efficiency of this chemical EOR scheme is estimated by comparing the results to primary depletion. In addition, soak time was also studied to evaluate its effect on improving oil recovery. Both oil rate and cumulative oil production were utilized to evaluate the performance of this EOR method and the impact of all tested variables.

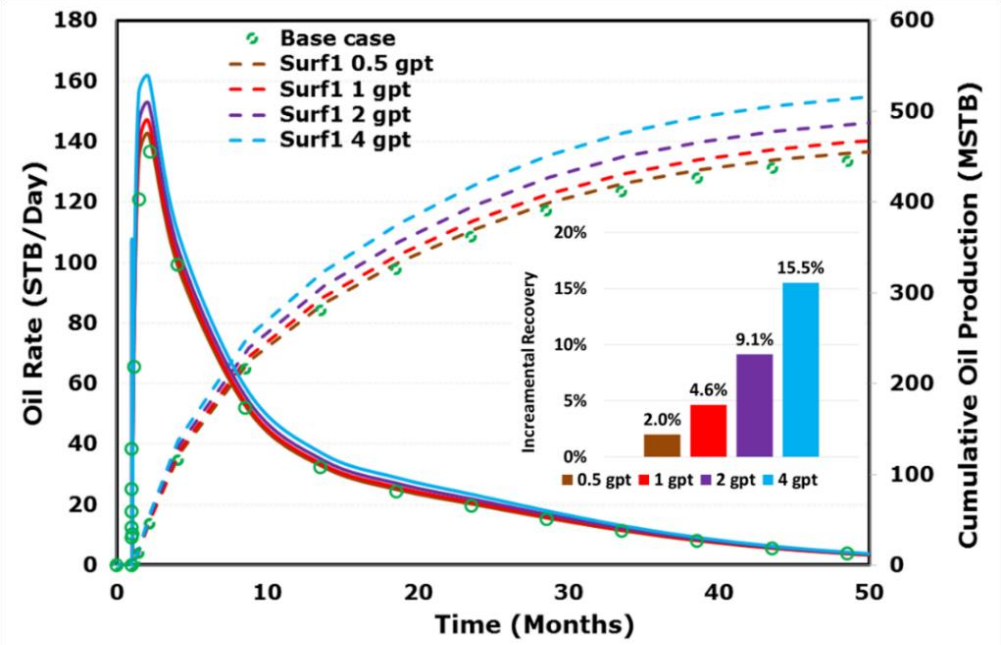

Figure 16 – Simulation results of cumulative oil production, recovery incremental, and oil rate for different concentrations of Surf1 in the completion fluid. Reprinted with permission from Zhang et al. (2019c).

The addition of surfactant to the completion fluid resulted in the improvement of oil recovery in both peak oil rate and cumulative production in ULR. Results of reservoir simulation for chemical EOR in the completion process using Surf1 and Surf2 are presented in **Fig. 16** and **Fig. 17**. Four surfactant concentrations (0.5, 1, 2, and 4 gpt) were tested using both types of surfactants. Surf1 has better performance of improving oil recovery in the Wolfcamp reservoir than Surf2, which is consistent with laboratory observations. The production improvement associated with surfactant concentration was analyzed. Although the continuous increase in surfactant concentration in the completion fluid results in higher recovery, the incremental oil recovery does not follow a linear trend. It is essential to combine economic analysis with reservoir simulation to optimal surfactant concentration for the proper design of surfactant applications in the completion fluid.

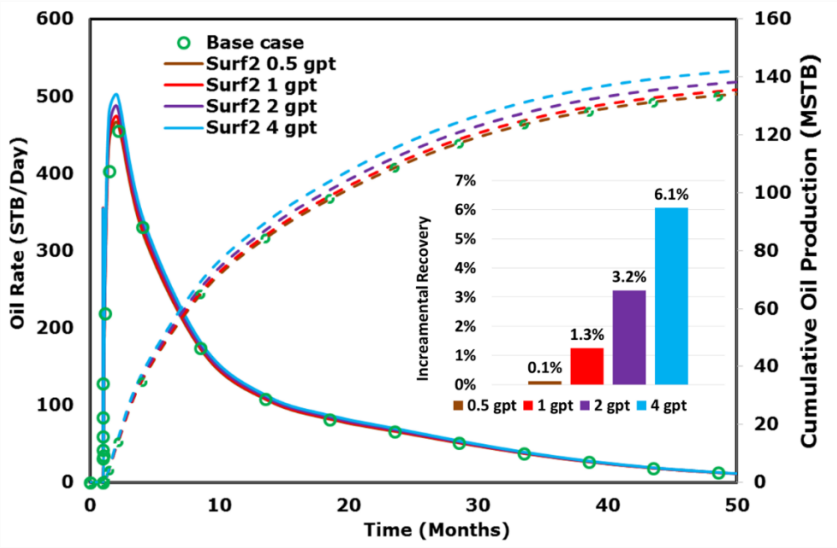

Figure 17 – Simulation results of cumulative oil production, recovery incremental, and oil rate for different concentrations of Surf2 in the completion fluid. Reprinted with permission from Zhang et al. (2019c).

The impact of soak time for the efficiency of chemical EOR in the completion process is then investigated, and the results are depicted in **Fig. 18**. Soak time is defined as the time between the end of completion and the start of production when the well is under shut-in condition. During the soak period, surfactants penetrate into the matrix and alter the wettability from oil-wet to water-wet, and consequently improve oil recovery in ULR. It indicates a long enough soak time is required to trigger the surfactant effect entirely. Different soak times are tested in this study: 5 days, 15 days, 1 month, and 2 months. The concentration of surfactants is kept constant at 2 gpt for all cases. A positive correlation between oil recovery and soak time is observed from simulation results. However, increasing the soak time does not result in significant oil production increase, especially when the soak time is beyond 1 month.

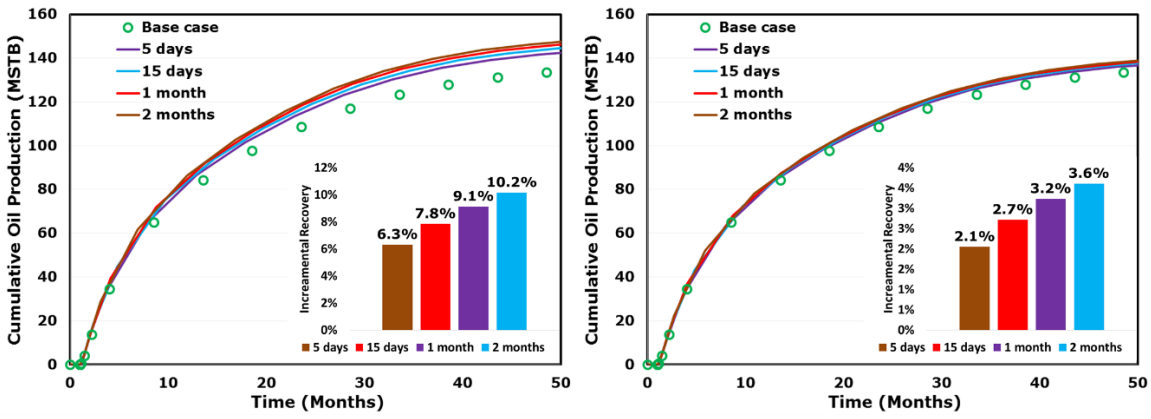

Figure 18 – Simulation results of cumulative oil production and incremental recovery for different soak time using Surf1 (left) and Surf2 (right). Reprinted with permission from Zhang et al. (2019c).

Simulation results indicate that the addition of surfactants into completion fluid displays the potential of enhancing oil recovery in ULR. The surfactant also improves fluid transport by increasing oil relative permeability in the fracture and matrix, which also leads to improved oil recovery. Surfactant concentration and soak time determine the efficacy of this EOR method that higher concentration and a longer soak time correlate to better well performance. In this high initial water saturation reservoir, the surfactant concentration should be higher than 2 gpt to achieve an economical oil production improvement. The initial water saturation contained in the reservoir may dilute the surfactant concentration immediately, which decreases the impact of surfactant on oil recovery in ULR. In addition, a minimum soak period of 15 days is recommended for chemical EOR in the completion process.

Water Injection after Primary Depletion

In order to evaluate the effect of surfactant on improving oil recovery through the injection process, water injection after primary depletion is investigated to quantify the impact of pressure maintenance. The primary mechanism of this method is pressure support through water injection. As mentioned previously, the primary drive mechanism is oil expansion from pressure drawdown during primary depletion. Shale reservoirs are characterized by ultra-low permeability and relatively weak fluid transport capability. During primary depletion, the pressure of the matrix close to the hydraulic fractures decreases to the wellbore's pressure in a short period. However, the source rock far from

the hydraulic fractures maintains a high pressure (close to initial reservoir pressure). Water injection was investigated to test whether re-energizing the depleted shale oil reservoir could result in any incremental recovery. Water injection for depleted wells could have a significant impact on improving oil production by re-pressurizing the reservoirs.

The preliminary results of this water injection scheme showed a promising potential for improving oil recovery in ULR. Therefore, a set of sensitivity analyses was conducted to understand this method better. The impacts of injection pressure and injection time were investigated to understand the potential of water re-energizing method on oil production improvement using the field-scale model. The water injection process started after 30 months of oil production. Four different pressures ranging from 5,500 to 7,000 psi in 500 psi increments were tested to evaluate the impact of injection pressure. In a sensitivity study regarding injection time, a constant injection pressure of 5,500 psi was applied to five different injection times from 1 month to up to 12 months.

The impact of pressure variation on the incremental recovery is presented in **Fig. 19**. In this study, incremental recovery is cumulative oil production increment which was calculated by comparing to the cumulative oil production from primary depletion. Four different injection pressures were investigated with a constant injection time of 6 months for all cases. The highest injection pressure used in the simulation was still lower than the fracture pressure gradient of the formation. The recovery mechanism of water injection is pressure maintenance. As expected, higher injection pressure resulted in both higher incremental of oil production and higher oil production rate after water injection. The cumulative oil increment from water injection varied from 22.5% to 54.4% as the injection

pressure increased from 5,500 psi to 7,000 psi. Higher water injection pressure resulted in higher average reservoir pressure, which in the end leading to more oil production after the injection period.

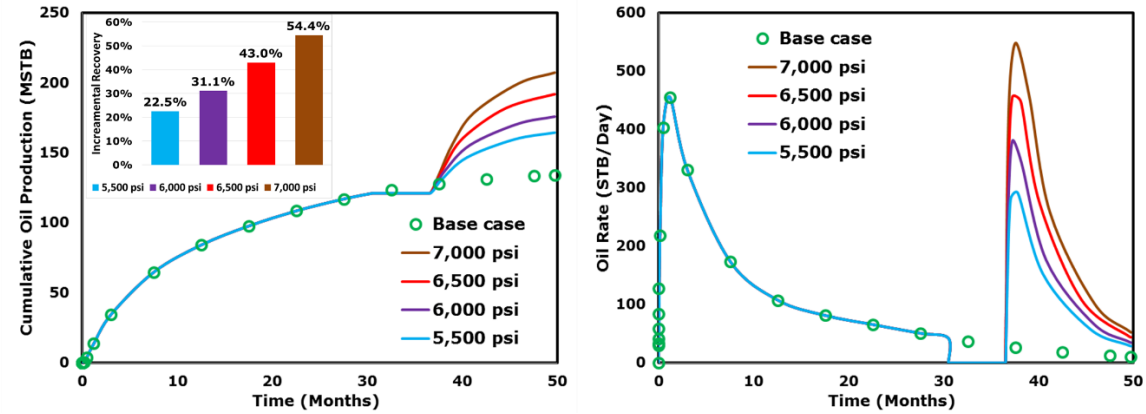

Figure 19 – Simulation results of cumulative oil production, recovery incremental, and oil rate (right) for different water-injection pressure. Reprinted with permission from Zhang et al. (2019c).

The results of water injection using various injection time are presented in **Fig. 20**. Increasing water injection duration improved recovery increment from 7.8% (1-month injection time) to 22.6% incremental of 12 months case. The longer injection time also resulted in higher cumulative oil production and oil rate. However, the injection periods of 6 and 12 months had similar oil production over the 4-years oil production. A water-injection period between 6 to 12 months provides an optimum enhancement in oil production for this well.

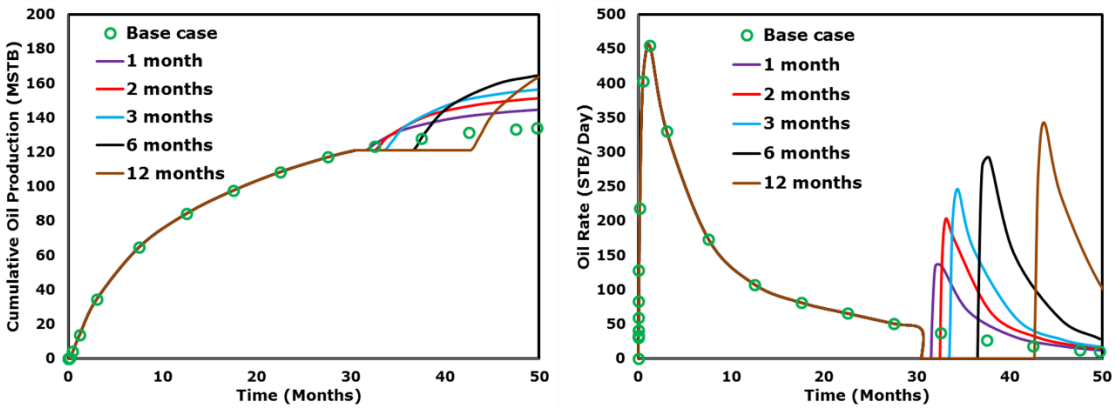

Figure 20 – Simulation results of cumulative oil production, recovery incremental, and oil rate (right) for different water-injection periods. Reprinted with permission from Zhang et al. (2019c).

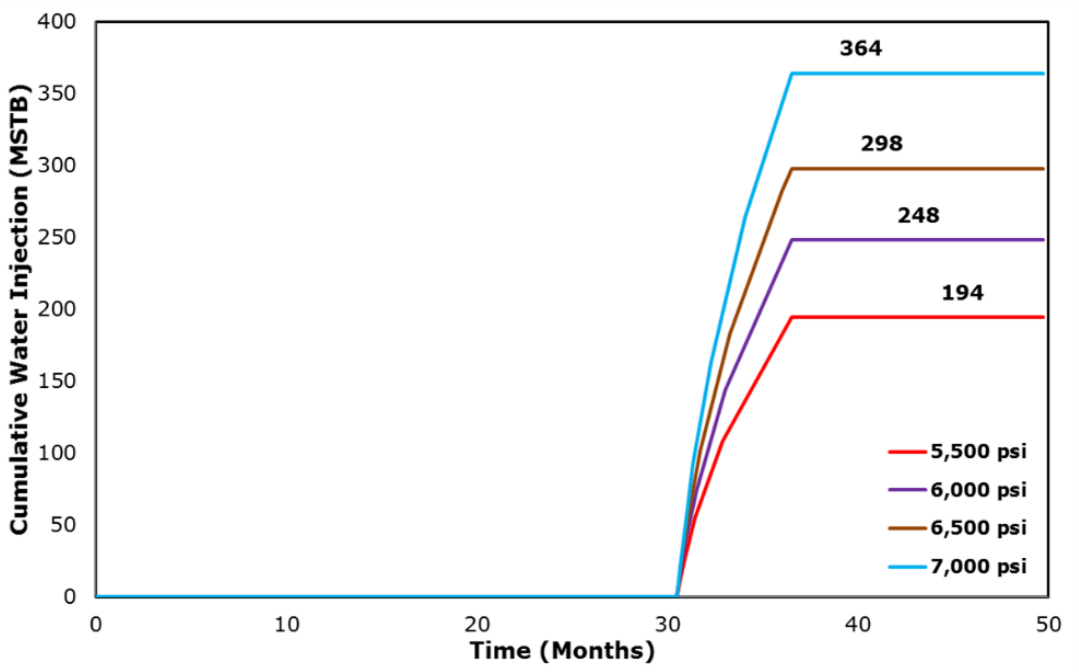

Figure 21 – Cumulative water for different injection pressure. Reprinted with permission from Zhang et al. (2019c).

It is logical to analyze the volume of water injected into the reservoir in this water injection study. The water injection process could come with a high economic requirement

when the water source is limited. However, water injection in the Wolfcamp formation can be highly beneficial as a sufficient volume of water was also produced from each producing well in the formation. **Fig. 21** depicts the information of injected water volume on the cases tested in **Fig. 19**. The cumulative water injection increases with the increase of the injection pressure, resulting in a higher reservoir pressure build-up and a higher oil production. Due to ultra-low permeability, water cannot be injected into the reservoir that the water saturation of the matrix is almost constant during the water injection process. The simulation results also prove that the primary production mechanism of the water injection process is the reservoir presses maintenance. Although the average cumulative water production of wells after 30 months of production in the area is twice the maximum amount of water injected, this method could still provide a significant solution for the produced water problem (Zhang et al. 2019c).

The simulation results of water-injection after primary depletion indicate that this method has significant potential in improving oil production in ULR. Water injection could be a feasible and economical technique in enhancing oil recovery in ULR.

Chemical Injection after Primary Depletion

In this section, the application of chemical injection in unconventional liquid reservoirs is investigated. The two types of surfactants, Surf1 and Surf2, are applied to the injection fluid. Capillary pressure and relative permeability curves, and surfactant

adsorption isotherms are the same as used in the section - Chemical EOR in completion process.

The simulation results of the previous section indicate that water injection has a significant potential for enhancing oil recovery in the Wolfcamp reservoir. Adding surfactants to injection fluid should lead to an even better performance in ULR. As surfactant solutions injected into the reservoir, the capillary pressure and relative permeability curves switched to the set of curves for the water-wet condition. The degree of alteration of the two curves was controlled by the amount of surfactant adsorbed in each grid block.

The potential of chemical injection EOR with various surfactant types and concentrations are investigated using the field-scale reservoir simulation. The injection pressure of all the chemical injection schemes is 5,500 psi with a 6 month injection period. Both types of surfactants were tested at four different concentrations, which are 0.5, 1, 2, and 4 gpt. The simulation results of the cumulative oil production and the oil rate for different cases are depicted in **Fig. 22** and **Fig. 23**.

The two types of surfactants, Surf1 and Surf2, used in this method are the same surfactant formulations that were studied in the laboratory experiments (Zhang et al. 2019c). Surf1 had a better performance on oil production enhancement for the Wolfcamp core plugs compared to Surf2. Similar results were observed in this chemical injection method, where the injection of Surf1 resulted in higher incremental recovery compared to the injection of Surf2.

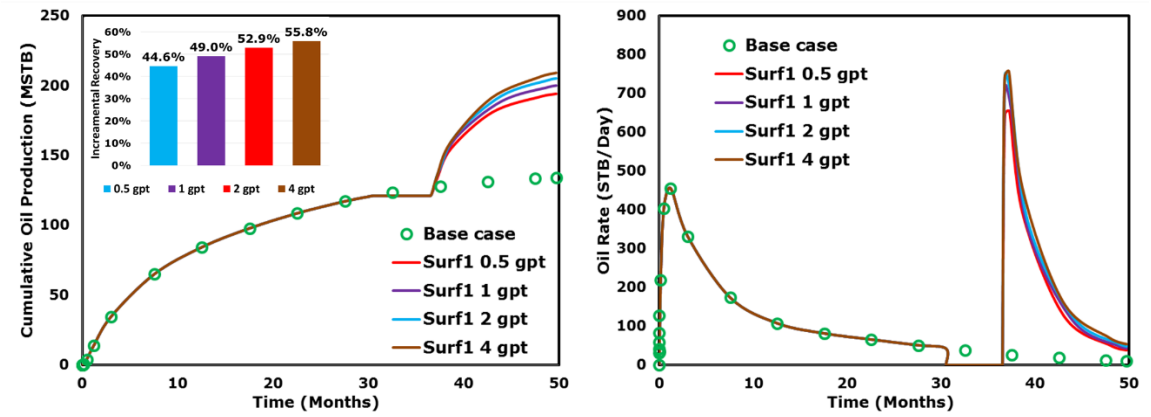

Figure 22 – Simulation results of cumulative oil production, recovery incremental, and oil rate (right) for different surfactant concentrations of chemical injection EOR using Surf1. Reprinted with permission from Zhang et al. (2019c).

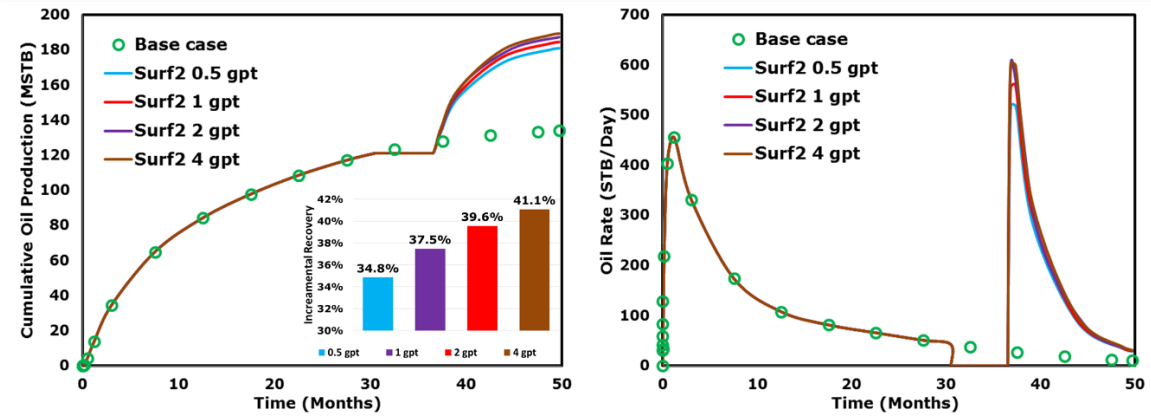

Figure 23 – Simulation results of cumulative oil production, recovery incremental, and oil rate (right) for different surfactant concentrations of chemical injection EOR using Surf2. Reprinted with permission from Zhang et al. (2019c).

The incremental oil production shows a positive trend with surfactant concentration for both surfactant types. However, increasing the surfactant concentration does not result in significant oil production enhancement, especially when the surfactant concentration is above 2 gpt. In **Fig. 24**, as surfactant concentration increases from 2 gpt to 4 gpt (doubled surfactant volume), the cumulative oil production increment increases

from 39.6% to 41.5%. Considering the cost of surfactant, the economic concentration for this chemical injection process is not over than 2 gpt. Surf1 performs better than Surf2 due to it alters the wettability of rock to more water-wet and shifts oil relative permeability higher.

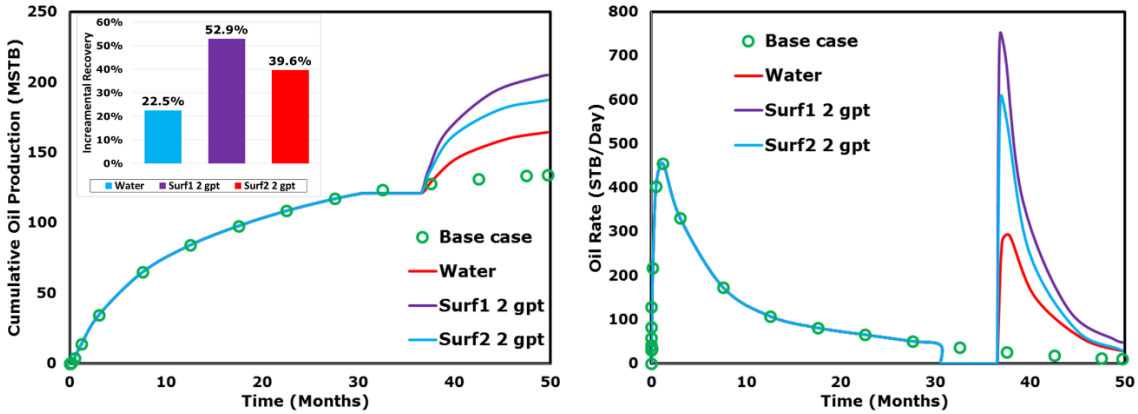

Figure 24 – Comparision of chemical injection EOR using the two surfactants and water-injection case. Reprinted with permission from Zhang et al. (2019c).

The mechanisms of this injection EOR process are wettability alteration, IFT reduction, and pressure support. Therefore, it is essential to investigate the dominant mechanism of the chemical injection EOR technique and determine production improvement caused by the addition of surfactants or pressure build-up. The comparison results of investigating this issue are shown in **Fig. 24**.

The comparison of production increment using water without surfactants, Surf1, and Surf2 at 5,500 psi injection cases is presented in **Fig. 24**. The results indicate that adding surfactant into the injection fluids improved the efficiency of the injection process with incremental recovery improved from 22.5% for the water case to 53% for the case

using 2 gpt of Surf1. However, the incremental recovery of the case using 2 gpt of Surf2 is 39.6%, which is less than using Surf1. A proper type of surfactant could have a significant impact on incremental production when injected after the primary recovery in ULR.

Both surfactants increase oil recovery from the matrix compared to the water injection base case. Chemical injection EOR not only improves oil recovery but also increases the oil rate when the well goes back to production. In the chemical injection process, 195 MSTB of surfactant solution was injected into the reservoir, and the total cost of surfactants is estimated at around $ 100,000. An additional 27 MSTB of oil that worth 1.2 million USD (assumed 45 USD/bbl) was produced after chemical injection treatment, compared to the water injection base case. Therefore, the addition of surfactant into both the completion and the injection fluids could result in higher recovery and attractive economics.

To emphasize the effect of surfactant additives, **Fig. 25** depicts three water injection cases with various pressure, as well as two chemical injection cases using 2 gpt Surf1 and Surf2 with 5,500 psi injection pressure. Surprisingly, the cumulative oil production of surfactant injection using Surf1 at 5,500 psi is similar to the oil production of water-injection at 7,000 psi. Chemical injection EOR scheme is a more suitable method than the water injection because additional oil is recovered by adding surfactant. Chemical injection EOR method should be taken into consideration if the surfactant price is moderate or the fracture pressure of the formation is low.

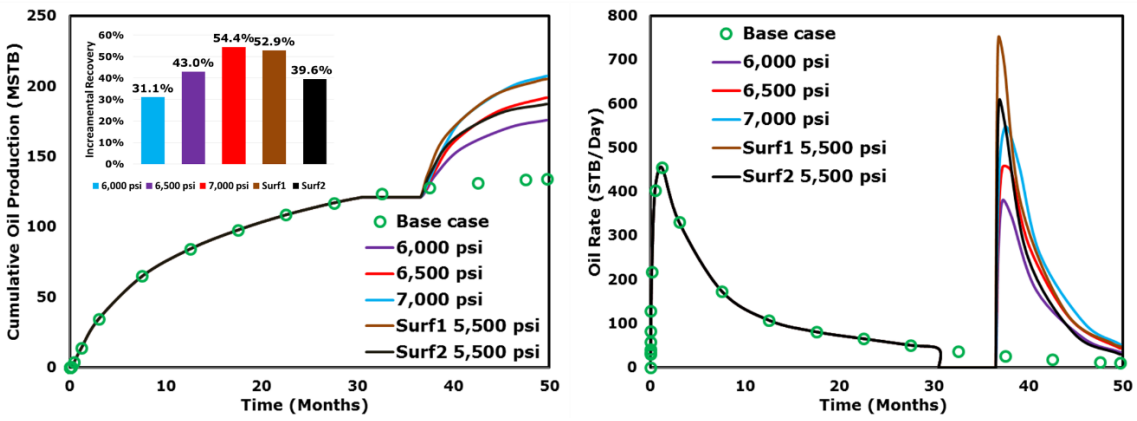

Figure 25 – Comparision of chemical injection EOR and water-injection with different pressure. Reprinted with permission from Zhang et al. (2019c).

Chemical injection EOR technique results in better oil enhancement for this Wolfcamp well compared to both chemical EOR in completion process and water injection method. The economic surfactant concentration of the chemical injection process is 2 gpt. Chemical injection EOR technique opens a substantial possibility to recover significant volumes of hydrocarbons from depleted wells and extend economic drilling locations in ULR.

Multi-Cycle Chemical Injection after Primary Depletion

In this section, a more complex EOR method was developed, which includes multiple cycles of injection and production period in consecutive order. The production period was extended to 7 years to investigate the effectiveness of multi-cycles surfactant injection and water-injection over a more extended production period. In each injection/production cycle, the injection time was six months at 5,500 psi, and the

production period is 12 months. The multi-cycle injection treatment started after 30 months of production. Surfactants were only added to injection fluids in the first injection cycle with 2 gpt concentrations for the multi-cycle chemical injection process. In contrast, in the following two cycles, only water was injected without any surfactant. Three cases are studied utilizing the two types of surfactants and water for three injection cycles after primary depletion. The simulation results including cumulative oil production, oil rate, and incremental recovery are presented in **Fig. 26**. In addition, a summary of all the simulation cases for chemical EOR in completion is presented in **Table 5**, and the simulation cases related to the injection process, including water injection, chemical injection, and multi-cycle chemical injection, are summarized in **Table 6**.

Table 5 – Summary of all simulation cases for chemical EOR in completion process.

Surfactant Concentration (gpt)	Surfactant Type	Soak Time	Recovery Incremental (%)
2	Surf1	5 days	6.3
2	Surf1	15 days	7.8
0.5	Surf1	1 month	2.0
1	Surf1	1 month	4.6
2	Surf1	1 month	9.1
4	Surf1	1 month	15.5
2	Surf1	2 months	10.2
2	Surf2	5 days	2.1
2	Surf2	15 days	2.7
0.5	Surf2	1 month	0.1
1	Surf2	1 month	1.3
2	Surf2	1 month	3.2
4	Surf2	1 month	6.1
2	Surf2	2 months	3.6

Table 6 – Summary of all simulation cases for chemical and water injection process.

Injection Cycle	Surfactant Conc. (gpt)	Injected Fluid	Injection Time (months)	Injection Pressure (psi)	Recovery Incremental (%)
1	N/A	Water	1	5,500	7.8
1	N/A	Water	2	5,500	12.7
1	N/A	Water	3	5,500	16.5
1	N/A	Water	6	5,500	22.5
1	N/A	Water	6	6,000	31.1
1	N/A	Water	6	6,500	43.0
1	N/A	Water	6	7,000	54.4
1	N/A	Water	12	5,500	22.6
1	0.5	Surf1	6	5,500	44.6
1	1	Surf1	6	5,500	49.0
1	2	Surf1	6	5,500	52.9
1	4	Surf1	6	5,500	55.8
1	0.5	Surf2	6	5,500	34.8
1	1	Surf2	6	5,500	37.5
1	2	Surf2	6	5,500	39.6
1	4	Surf2	6	5,500	41.1
3	N/A	Water	6	5,500	43.5
3	2	Surf1	6	5,500	112.4
3	2	Surf2	6	5,500	81.4

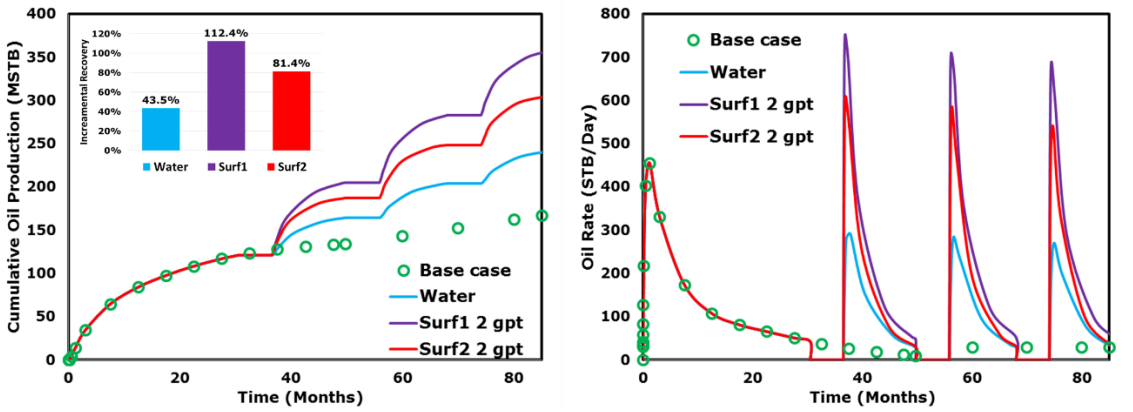

Figure 26 – Comparision of multi-cycle chemical EOR using the two surfactants and corresponding water injection method. Reprinted with permission from Zhang et al. (2019c).

Water injection without surfactant additives on this multi-cycle injection study improved the cumulative oil production by 43%. The addition of surfactant into injection fluid using a multi-cycle injection protocol increases oil production. Compared to the multi-cycle water injection case, surfactant additive results in additional recovery up to 70% additional incremental recovery for the 7-year period compared to primary depletion. Since surfactants were only added into injection fluids in the first cycle, the cost of surfactant was estimated as 100,000 USD per well. The cumulative production and oil rates were similar for all three cycles with a minor decrease trend. Therefore, the multi-cycle chemical injection EOR technique could extend the wells' economic production life and enhance oil production in ULR under certain conditions (Zhang et al. 2019c).

CHAPTER V

GAS INJECTION EOR IN UNCONVENTIONAL RESERVOIRS [*]

In this chapter, laboratory experiments results, ternary diagram analysis, core-scale history match, and field-scale simulation results are presented and discussed to reveal the dominant mechanism of gas injection in unconventional liquid reservoirs. Gas injection Huff-n-Puff experiments are performed at a reservoir temperature of 170 ^{o}F at various pressures. Then, a ternary diagram analysis of the multi-contact miscibility process is conducted to explain the primary mechanism of gas injection EOR. Finally, the recovery performance of the gas injection method in ULR is investigated using numerical simulation. The reservoir model is developed considering the results of laboratory experiments, core-scale history matches, and hydraulic fracturing simulation.

---

[*] Parts of the methodology presented in this chapter have been reprinted from:

"Enhanced Oil Recovery in Unconventional Liquid Reservoir Using a Combination of CO_2 Huff-N-Puff and Surfactant-Assisted Spontaneous Imbibition" by Fan Zhang, I.A. Adel, K.H. Park, I. W. R. Saputra, and D.S. Schechter. SPE Paper 191502. Copyright 2018 by the Society of Petroleum Engineers (SPE). Reproduced with permission of SPE. Further reproduction prohibited without permission.

"Numerical Investigation to Understand the Mechanisms of CO_2 EOR in Unconventional Liquid Reservoirs" by Fan Zhang, I.A. Adel, I. W. R. Saputra, W. Chen and D.S. Schechter. SPE Paper 196019. Copyright 2019 by the Society of Petroleum Engineers (SPE). Reproduced with permission of SPE. Further reproduction prohibited without permission.

"The Impact of MMP on Recovery Factor During CO2 – EOR in Unconventional Liquid Reservoirs" by Imad A. Adel, Francisco D. Tovar, Fan Zhang, and David S. Schechter. SPE Paper 191752. Copyright 2018 by the Society of Petroleum Engineers (SPE). Reproduced with permission of SPE. Further reproduction prohibited without permission.

Laboratory Experimental Results

Five Huff-n-Puff experiments using saturated Eagle Ford cores were performed at different pressures with CO_2. All gas injection experiments were performed inside the CT scanner to obtain time lapse CT images at the same position/slice. Soak and production time for each cycle are constant, which is 10 hours and 3 hours, respectively. In addition, the MMP of CO_2 – Eagle Ford oil was determined using the slim tube method.

MMP Determination

The MMP is a critical parameter for gas injection EOR design, especially in unconventional reservoirs. The MMP was determined using the slim-tube method, which is the most accurate method to measure the MMP. The MMP was 2,130 psi for this light Eagle Ford oil, as shown in **Fig. 27**.

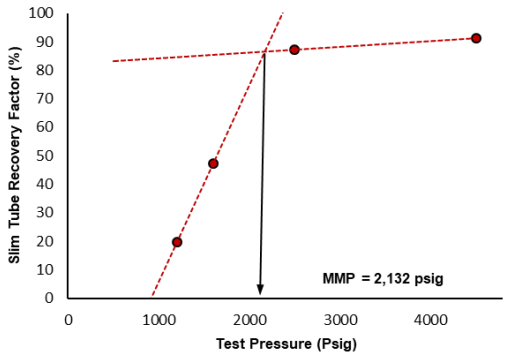

Figure 27 – MMP plot showing the recovery vs. pressure for the Eagle Ford oil. Reprinted from (Adel et al. 2018a).

Gas Huff-n-Puff Experiment

Five CO_2 Huff-n-Puff experiments were performed at the reservoir temperature of 170 ^{o}F using saturated Eagle Ford core plugs, and the information of cores is presented in **Table 7**. The experimental pressures were selected based on the MMP value, two injection pressures are below the MMP, and the other pressures are above the MMP. The oil recovery curves for all gas injection experiments are presented in **Fig. 28,** and a summary of the experimental results are plotted in **Fig. 29**. In each sub-figure, soak and production periods are marked for each of the Huff-n-Puff cycles. Oil recoveries of the gas injection experiments performed above the MMP are significantly higher than those from tests conducted below the MMP. A positive correlation is observed between the recovery factor and pressure. Increasing injection pressure results in high oil recovery, even the experimental pressure above the MMP. The highest recovery factor is 49%, which was achieved from the gas injection experiments at 3,500 psi. However, the ultimate recovery factors decrease to less than 5% when the pressure below the MMP (Zhang et al. 2018a).

Table 7 – Core plugs injected volume and experimental pressure. Modified with permission from (Zhang et al. 2018a).

Core ID	Saturated Oil Volume (ml)	Experimental Pressure (psi)
Core 1	2.900	2,500
Core 2	1.785	3,000
Core 3	1.744	3,500
Core 4	1.129	1,400
Core 5	2.361	1,800

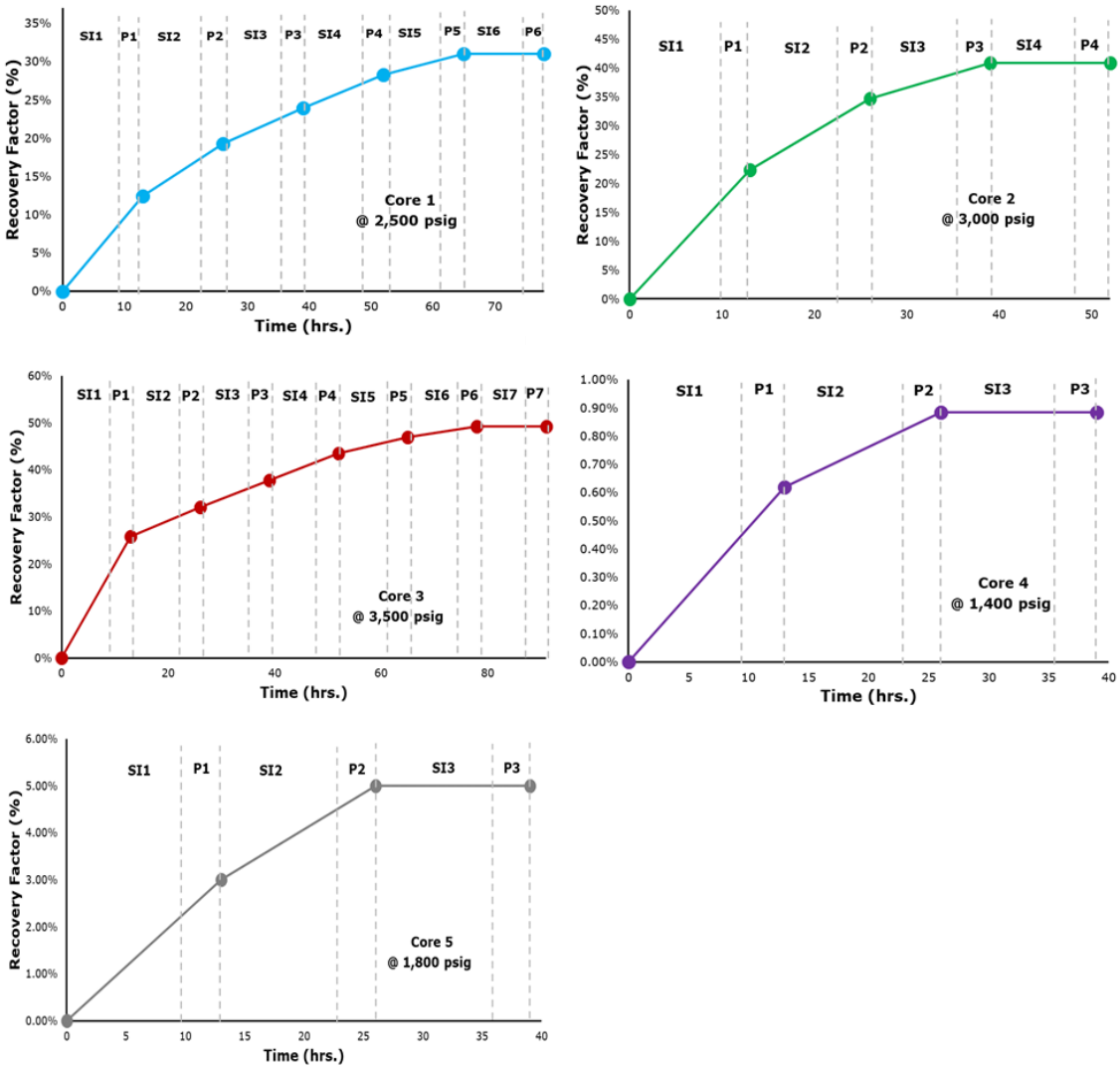

Figure 28 – Recovery factors for gas injection experiments at different pressures. Modified with permission from (Zhang et al. 2018a).

Fig. 29 depicts that about 50% of the ultimate recovery is produced from the first Huff-n-Puff cycle which composed of a soaking interval (SI1) and a production interval (P1). The oil recovery from each cycle decreases after the first cycle until it levels off by reaching the maximum recovery.

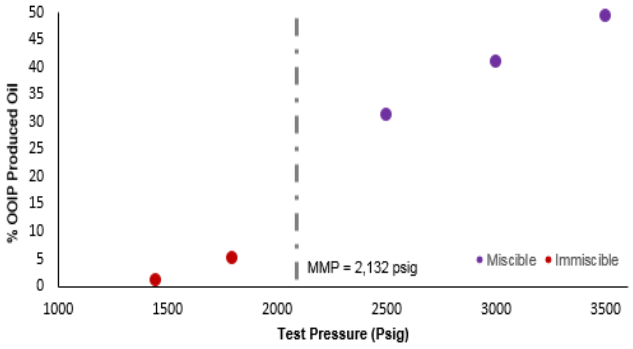

Miscibility Status	Test Pressure (psig)	Oil Recovery (% of OOIP)
Miscible	3500	49.31
	3000	40.9
	2500	31.03
Immiscible	1800	5.00
	1450	1.00

Res Temp (°F)	170
MMP (psig)	2,132

Figure 29 – Ultimate recovery factors for gas injection experiments at different pressure. Reprinted with permission from (Zhang et al. 2018a).

The oil recovery curves of the CO_2 injection experiments conducted above MMP pressure have a similar performance that the curves comprised of three parts. A significant amount of oil is recovered at the beginning of the experiment because the lighter components of the oil are easily vaporized into the gas phase from the fully saturated core plug. In the second part, oil is recovered from the core sample at a constant rate. As the 'easy' produced oil recovered from the first part, the oil recovery rate is limited by the rate of CO_2 penetration into the core plug. By the time of the last part, CO_2 has already penetrated to the center of the core plug causing the oil recovery rate decreases to zero (Zhang et al. 2018a).

The highest recovery factor of gas injection experiments using the Eagle Ford core samples was 49.31% at 3,500 psi, which is higher than the maximum of 40% OOIP previously observed in the Wolfcamp (Adel et al. 2018a). Oil produced from the Eagle Ford reservoirs varied from light oil to heavy oil, and reservoir properties of different areas are also changing in a broad range. This observation indicates that it is essential to evaluate the efficiency of gas injection EOR using oil and core samples from the target reservoir.

Increasing pressure always results in higher ultimate oil recovery, especially when the pressure is beyond the MMP. However, in conventional reservoirs, reaching the MMP is enough to attain the highest recovery factors. These results challenge the paradigm that operating slightly above the MMP is the optimum injection pressure for EOR designs. Increasing the injection pressure leads to better oil production enhancement in the unconventional liquid reservoirs (Zhang et al. 2019a).

In addition, the performance of gas injection EOR using hydrocarbon gases is also included in this research. The results of the gas Huff-n-Puff experiment using methane, natural gas (85% CH_4 - 15% C_2H_6), and enriched gas (50% CH_4 - 50% C_2H_6) are presented in Chapter VII.

Ternary Diagram Analysis

Ternary diagrams are utilized to analyze the mechanisms of gas injection EOR during the injection process. A pseudo-ternary diagram was constructed to represent the oil used in this study. The composition of the Eagle Ford oil sample was determined using high-resolution Gas Chromatography (GC). Two pseudo-component groups of intermediate components and heavy components were lumped based on the composition of the oil. Equations of state (EOS) was applied to calculate the Pressure-Volume-Temperature (PVT) of the gas/liquid equilibrium system (Rathmell et al. 1971).

The pseudo-ternary diagram of the CO_2 – Eagle Ford oil system was generated using Peng-Robinson EOS. The workflow of the pseudo-ternary diagram construction is

presented in **Fig. 30**. Properties of the pseudo-components were determined by grouping the original composition of the oil sample.

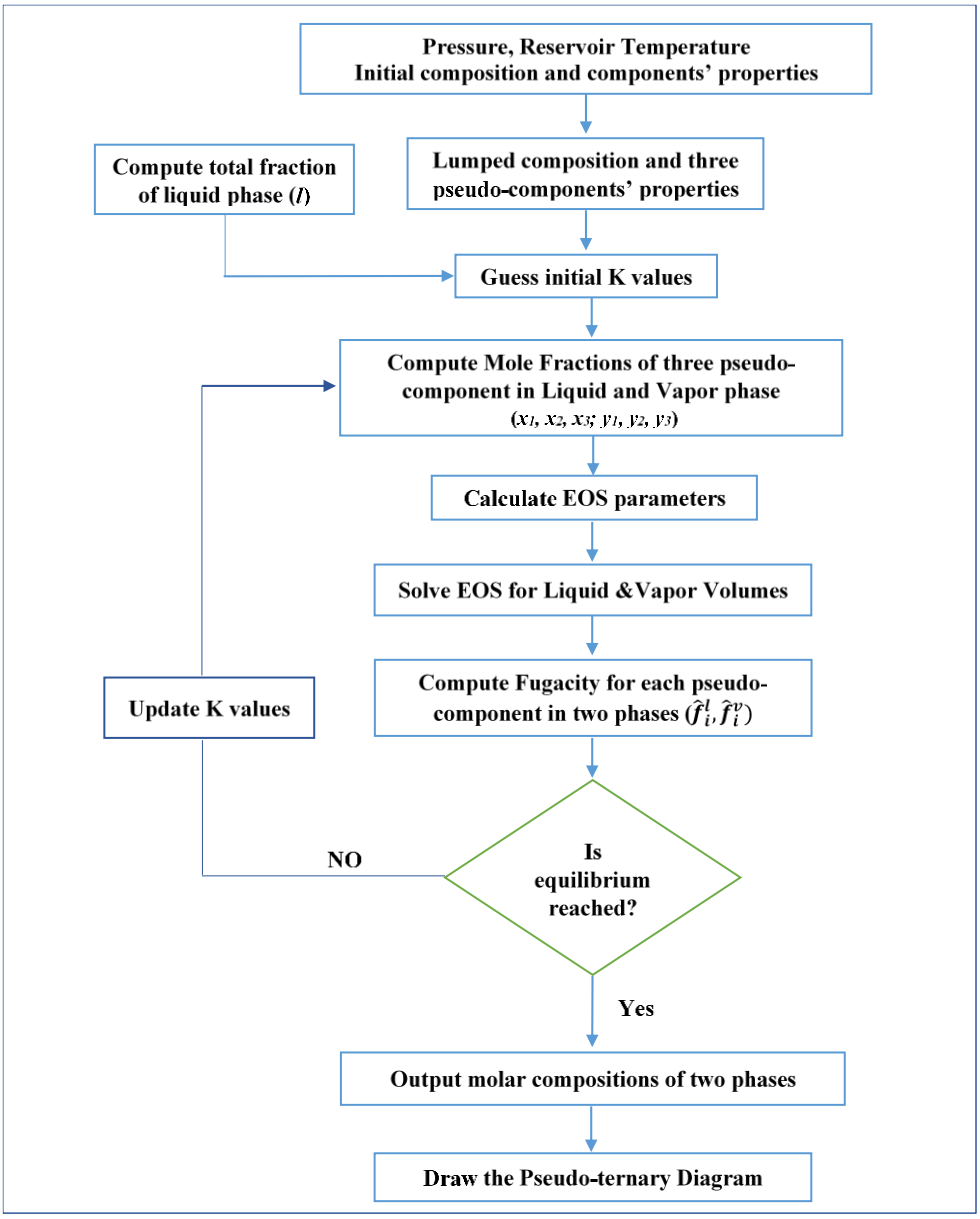

Figure 30 – Workflow for the construction of the Pseudo-ternary Diagram. Reprinted with permission from Zhang et al. (2019a).

The binary interaction parameter for each component pairs is estimated using empirical equation **Eq. 6**, where V_{ci} and V_{cj} are critical molar volumes for component i and j, and θ is the exponential coefficient that is selected from **Eq. 8** (Barragan et al. 2002).

$$k_{ij} = 1 - \left(\frac{2*(V_{ci}*V_{cj})^{\frac{1}{6}}}{V_{ci}^{\frac{1}{3}}+V_{cj}^{\frac{1}{3}}} \right)^{\theta} \quad \text{..... (6)}$$

The initial K-values for EOS calculations are estimated from Wilson's Equation (Wilson 1969), as shown in **Eq. 7**. The K-value is a critical indicator of the solubility of CO_2 in oil.

$$K_i = \frac{y_i}{x_i} = \frac{P_{ci}}{P} \exp\left[5.37\,(1+w_i)\left(1-\frac{T_{ci}}{T}\right)\right] \quad \text{..... (7)}$$

Where, x_i and y_i are the liquid and gaseous mole fractions of a component with index i. P_{ci} and T_{ci} are the critical pressure and temperature of component i. w_i is the acentric factor of the component.

The mixture is then flashed to obtain vapor and liquid compositions. Fugacity coefficients for each component were calculated using EOS when the liquid and vapor volumes were determined. The system equilibrium was determined by the convergence of liquid and vapor fugacity. For each time step, a new K value can be calculated using **Eq.8**.

$$(K_i)^{k+1} = (\frac{\hat{f}_i^{\,l}}{\hat{f}_i^{\,v}} K_i)^k \quad (8)$$

Where, $\hat{f}_i^{\,l}$ and $\hat{f}_i^{\,v}$ are liquid and vapor fugacity of component i. k is the number of iteration steps.

The ternary diagram is commonly used to describe the miscibility process, which is a dynamic fluid mixing and component exchange process. Miscibility is reached through the multi-contact process in most gas injection applications. In this study, the multi-contact miscibility process in gas injection was illustrated using a ternary diagram, then the effect of pressure on the miscibility process was analyzed to explain the mechanism of gas injection EOR in ULR. Finally, the correlation between pressure and recovery factor from Huff-n-Puff experiments is discussed based on ternary diagram analysis.

The ternary diagram of analyzing miscibility and production processes during gas injection is presented in **Fig. 31**. As gas is injected into a cylinder and interacted with oil, the mixture of the gas and crude oil is located in the two-phase area. The location of the mixture is determined by the volume proportion of oil and gas, which is shown as O_1 and G_1. Then, the gas continues contacting with reservoir oil and mixed into the oil phase. The new mixture point moves to M_2, O_2, and G_2 which are the corresponding oil and gas fractions at M_2 state. This process repeatedly occurs until reaching the critical point where the gas and oil are miscible (Zhang et al. 2019a).

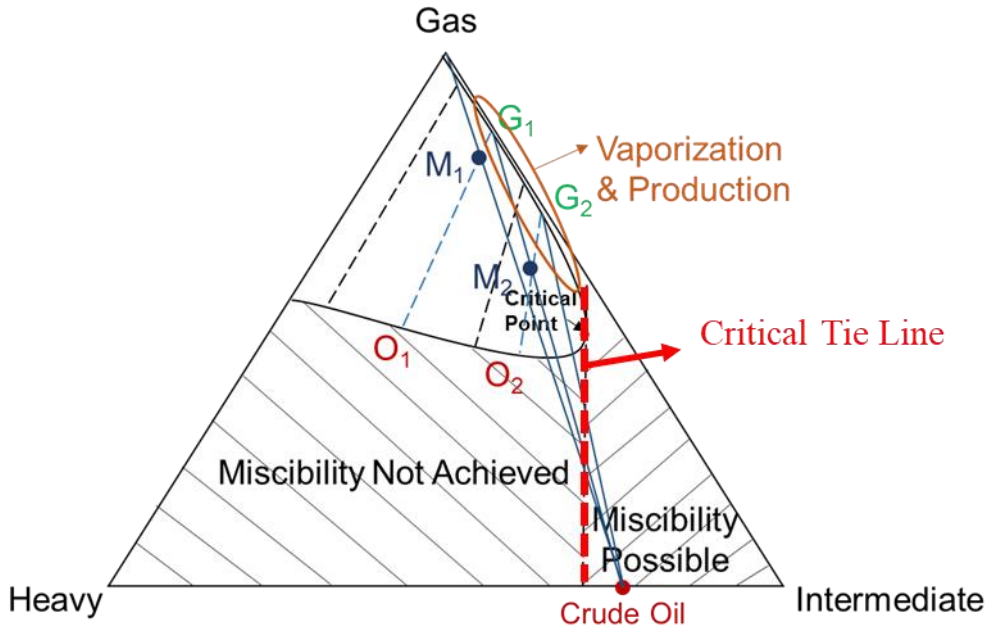

Figure 31 – Schematic of the ternary diagram for the determination of miscibility and production processes during the gas injection experiment. Reprinted with permission from Zhang et al. (2019a).

Only the original oil composition located in the 'miscibility possible' zone (shown in **Fig. 31**) could move to the critical point in the end. Therefore, miscibility is achieved through the multi-contact process. Otherwise, if the original oil composition is located in the 'miscibility not achieved' zone and the extension of a tie line (such as the G_2-O_2 line) passes through the oil, the multi-contact process is suspended at this point and the miscibility state cannot be reached.

As pressure increases, the two-phase area shrinks, and the critical tie line moves towards the gas-heavy components side (shown in **Fig. 32**). According to the MMP definition, minimum miscibility pressure occurs when the critical tie line first intersects the crude oil point in the ternary diagram. The MMP is estimated numerically using ternary

diagrams, but this method needs to be validated by slim tube laboratory data. In the multi-contact process, intermediate components of the oil phase vaporize into the gas phase, and gas dissolves into the oil phase. This dynamic process primarily occurs in the soak period in the gas injection experiment. The vaporized oil, along with gas, is produced during the production period and condenses back to the liquid phase at room pressure and temperature (Zhang et al. 2019a).

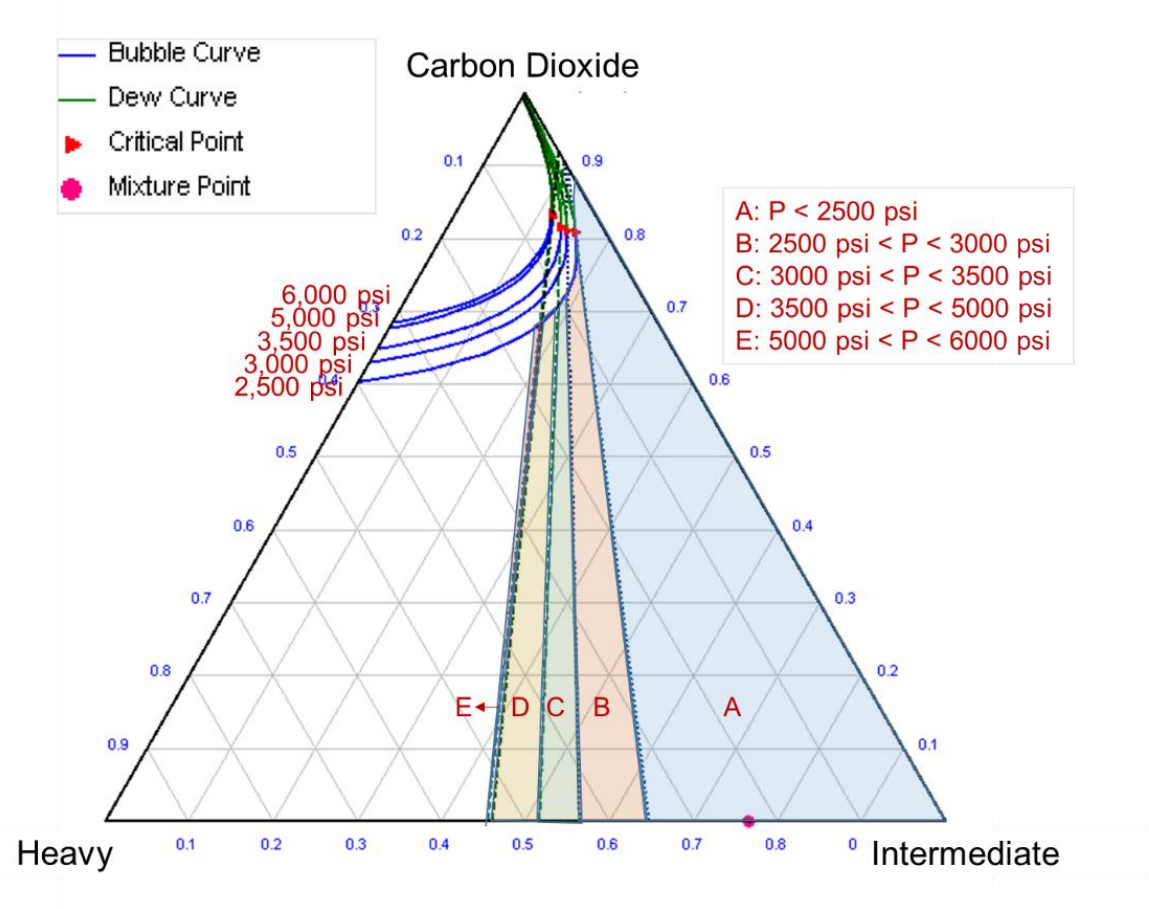

Figure 32 – Ternary diagram for Eagle Ford oil sample at different pressure. Reprinted with permission from Zhang et al. (2019a).

The heterogeneity nature of unconventional reservoir rock results in a widespread pore size distribution. The heavier components of the oil tend to gather in small radius pores (Luo et al. 2018), resulting in different MMP of the oil in the smaller pores and larger pores. The MMP determined from slim tube measurement is the miscibility pressure for the general composition of oil with gas. The oil within the small pores possesses a higher MMP compared to the MMP determined from laboratory measurement. The MMP for the specific pore radius could be varied from 2,000 psi to 5,000 psi size in shale rock.

During Huff-n-Puff experiments, increasing pressure results in a higher oil recovery because heavier components of oil in the smaller pore reach miscibility. The color of produced oil changes to darker as pressure increases. This observation explains that a further increase in pressure beyond the MMP leads to more oil production enhancement. However, there is an optimum injection pressure for gas injection EOR. In Chapter VII, CO_2 injection experiments were performed at 5,000 psi, and the recovery factor of the test was less than the recovery factor of the CO_2 injection experiment conducted at 3,500 psi. More discussion is available in Chapter VII.

Core-Scale History Match

In order to reveal the mechanisms of gas injection EOR and upscale the experimental data to the field scale, the parameters governing the gas injection EOR process is determined from core-scale simulation results. A slim tube model was constructed to validate the PVT table used in the simulation model by history match with

the MMP data. Then, the core-scale model was developed by combining CT-scan images, laboratory data, and validated PVT table. Finally, the diffusion coefficient of CO_2 was determined from the core-scale history match, and the primary mechanism of gas injection EOR was concluded based on the simulation results.

Slim Tube Model

A correct PVT table is critical to accurate history match the gas injection experiment results and to estimate the diffusion coefficient of gas. In this study, the PVT table was validated by considering the results of the history match to the slim tube MMP data and the Gas Chromatography (GC) data, as shown in **Fig. 33**.

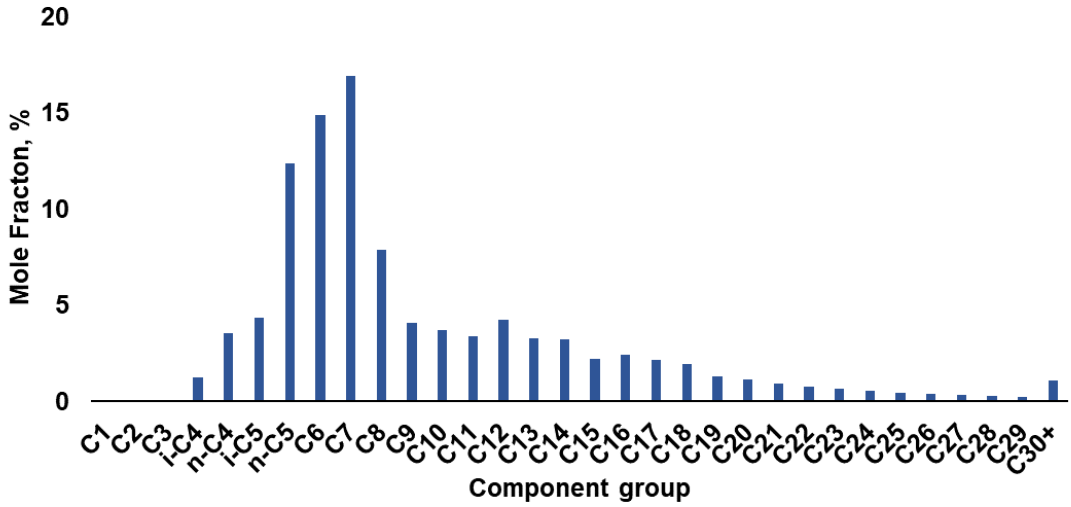

Figure 33 – Oil composition of the Eagle Ford oil determined by GC.

The majority of the composition of the Eagle Ford oil is in the lighter and intermediate components, especially C_5 to C_7. The slim tube model was constructed using the geometries and properties of the slim tube in the laboratory to simulate the 1D oil displacement by injected gas. The injection rate and pressure were also the same as the MMP experiment. The phase behavior of each component in the oil composition is mainly controlled by its k-value in the PVT table. The K-value table was adjusted to match MMP experimental results. The history match results of the MMP measurement are presented in **Fig. 34**.

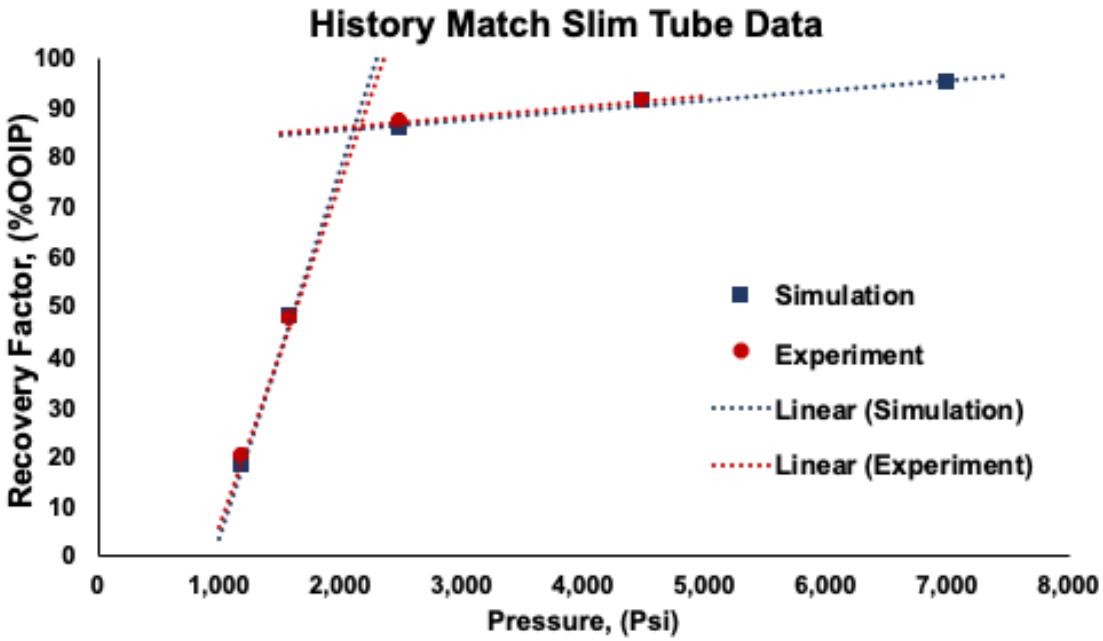

Figure 34 – History match of slim tube MMP data. Reprinted with permission from (Zhang et al. 2019a).

In **Fig. 34,** the simulation results agree with the MMP experimental data. The consistency of simulation results with experimental results indicates the PVT table is

reliable to describe the Eagle Ford oil used in the MMP and gas injection tests. This PVT table was implemented in the core-scale simulation model to determine the diffusion coefficient of CO_2 and also utilized in the reservoir model to evaluate the potential of gas injection on enhancing oil recovery in unconventional liquid reservoirs.

Core-Scale Modeling

The core-scale model was developed using CT scan technology to represent the heterogeneity of the core plugs. A comparison of actual core images from CT - scan and converted core-scale structures is presented in **Fig. 35**. Multiple unique features (such as bedding planes) of core plugs observed from CT images are accurately implemented in the core-scale model.

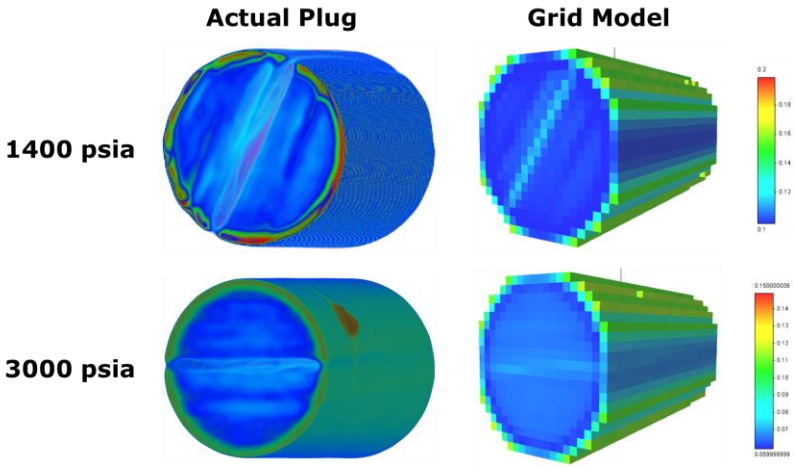

Figure 35 – Comparison of the 3D CT-scan image (left) and core-scale model (right). Reprinted with permission from Zhang et al. (2019a).

Fig. 35 shows the grid models of core plugs used in the gas injection experiments at 1,400 psi and 3,000 psi, indicating the core-scale model captured the heterogeneity of the core plugs, especially the bedding planes of the core plugs. Due to the high heterogeneity nature of the shale cores, it is essential to integrate heterogeneity into the core model to ensure the accuracy of estimating the diffusion coefficient at different pressures from the numerical simulation.

History Match Results

The initial condition of the core-scale model was established to simulate the laboratory conditions. The core plug grid model was located in the center of the core-scale model and surrounded by a high permeability region representing the glass beads. The initial pressure, the soak time, the production time, and the number of cycles were all the same as the gas injection experiments. Validated PVT table for the Eagle Ford oil was applied to the core-scale model. The history match results of gas injection experiments using the core-scale model are presented in **Fig. 36**, and the oil volume in the figure is the oil produced from the outlet during the production period. Therefore, there is no oil volume change during the soak period.

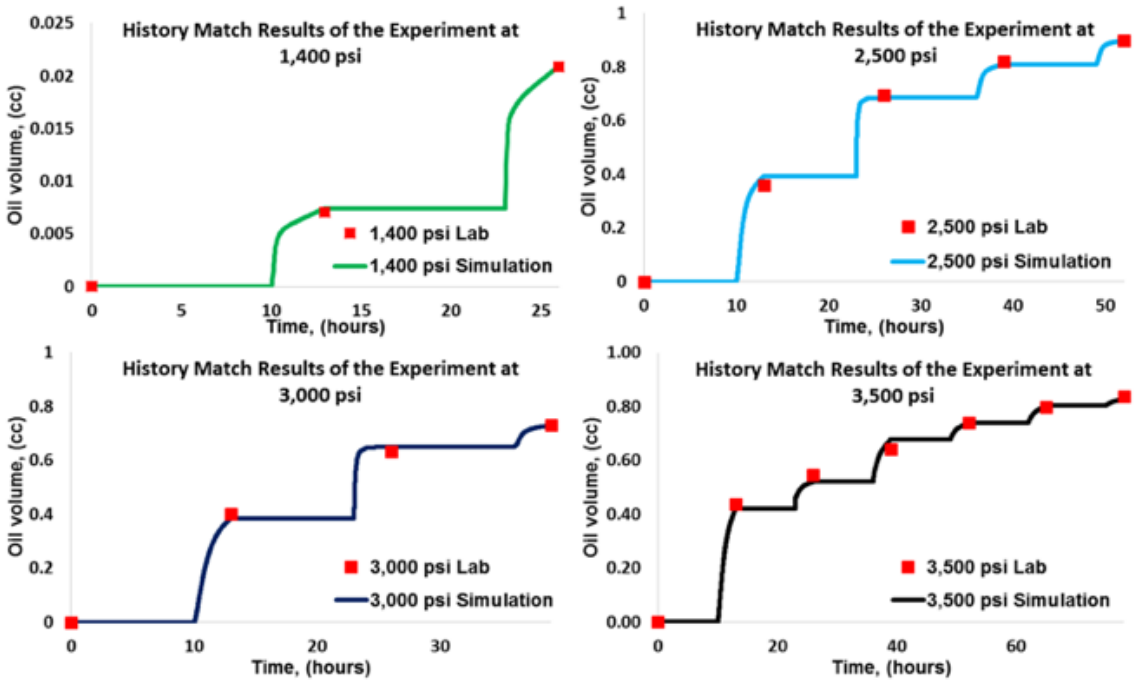

Figure 36 – The history-matching results of gas injection experiments at different pressure. Reprinted with permission from Zhang et al. (2019a).

History match results have a decent agreement with the oil recovery curves of all gas injection experiments. The consistency of simulation results with experimental results demonstrates the diffusion coefficient obtained from the history match is reliable for representing the effect of the gas injection EOR technique. However, the diffusion coefficient is the only tuning parameter that controls the effect of gas injection EOR in the simulator. It may include the effect of multi-contact miscibility. In order to reveal the actual meaning of the diffusion coefficient from simulation, the diffusion coefficients of CO_2 at different pressure achieved from the history match were plotted in **Fig. 37** and analyzed the actual effect of diffusion.

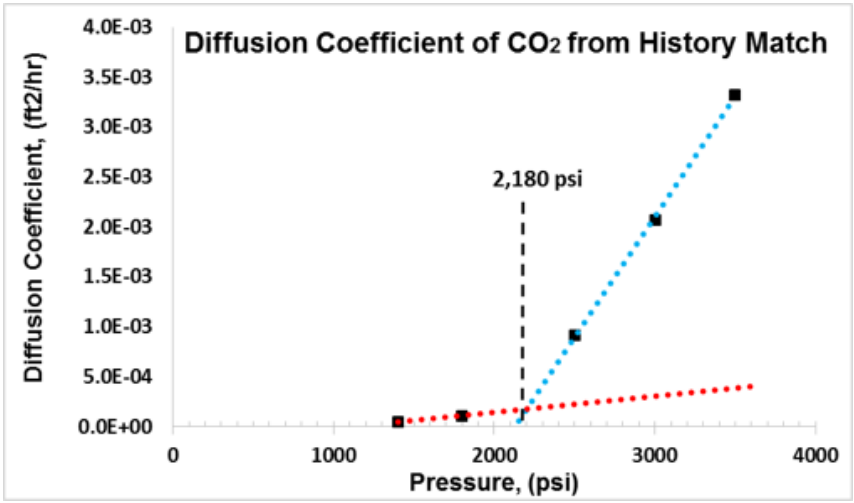

Figure 37 – The diffusion coefficient of CO_2 from history matching results. Reprinted with permission from Zhang et al. (2019a).

The diffusion coefficient obtained from history matching results separates into two groups, which are high pressure group (beyond the MMP) and low-pressure group (below the MMP). The diffusion coefficient in each group has a linear correlation with pressure, and the intersection of these two trend lines is at 2,180 psi, which is close to the measured MMP of 2,132 psi. The diffusion coefficient of CO_2 from history match results of the experiments performed below the MMP is much smaller than the diffusion coefficient for the tests beyond the MMP. The diffusion coefficient of the group above the MMP is two orders of magnitude larger than the group below the MMP.

However, the laboratory-measured diffusion coefficient of CO_2 has a linear trend with pressure (Shu et al. 2017), and the diffusion coefficient of the group below the MMP has the same order of magnitude to the laboratory-measured diffusion coefficient of CO_2. The diffusion coefficient from history match results includes not only the effect of diffusion as defined by Fick's law (Fick 1855) but also the effect of the multi-contact

miscibility. Therefore, the actual effect of diffusion for gas injection EOR is along the red line, contributing a minor impact in gas injection EOR. The difference between the blue and red line is the effect of the multi-contact miscibility in the gas injection process. Because the diffusion coefficient is the only tuning parameter in the simulator, the diffusion coefficients from history match results combine the effect of miscibility and diffusion. The observations of the simulation results and ternary diagram analysis indicate the actual dominant mechanism of gas injection EOR is the multi-contact miscibility.

Additional laboratory observations are also evidence that diffusion is a minor effect compared to multi-contact miscibility. Tovar et al. (2018) performed gas injection experiments using N_2, following the same gas injection experiment workflow presented in this research. No oil was produced from the shale cores during N_2 injection experiments, even when the pressure was increased to 5,000 psi. The diffusion coefficient of N_2 at 5,000 psi is the same order of magnitude as the diffusion coefficient of CO_2. However, the multi-contact miscibility effect on improving oil recovery cannot be triggered using N_2 at 5,000 psi due to the MMP of oil-N_2 is higher than 5,000 psi. Therefore, the primary mechanism of gas injection EOR in ULR is multi-contact miscibility, and diffusion has a minor effect on improving oil recovery in unconventional liquid reservoirs.

Field-Scale Model

In order to upscale gas injection experiments data to a large reservoir scale, numerical simulation method is used to investigate the recovery performance of the gas

injection process in ULR. The field-scale simulation model is developed by considering the results of laboratory experiments, core-scale history match, and hydraulic fracturing modeling. Diffusion coefficients achieved from core-scale history matches are implemented into the field model to represent the effect of gas injection EOR. This modeling algorithm was believed to be the most accurate method to depict the recovery mechanism of gas injection in ULR.

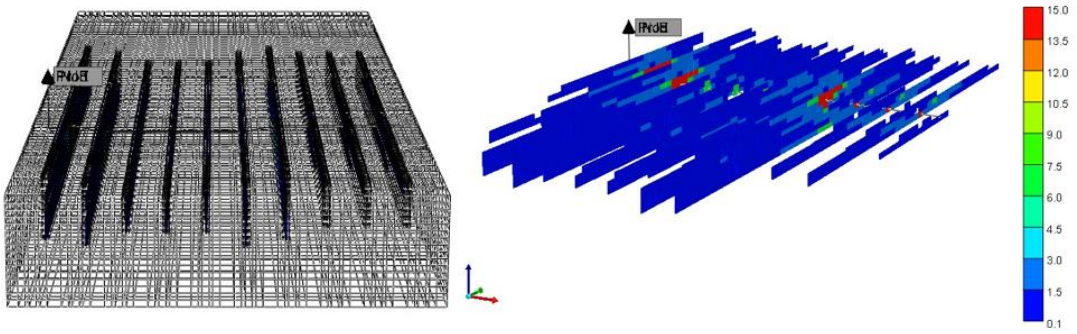

Figure 38 – Gridding structure (left) and permeability distribution in hydraulic fractures of the field-scale. Reprinted with permission from Zhang et al. (2019a).

Two adjacent hydraulic fractures stages were randomly selected to construct the field-scale model (shown in **Fig. 38)**. The dimensions of the field-scale model were 600 ft, 1,600 ft, and 100 ft with a mixed gridding structure to ensure the accuracy of simulation results and to decrease the simulation time. Five hydraulic fracture clusters were included in each stage, in which two or three hydraulic fracture clusters were suppressed by the pressure shadow effect from adjacent clusters and stages. In reality, this stress shadowing effect was also observed in the field as some of the clusters grow short and narrow. Due to the large number of natural fractures existing in unconventional liquid reservoirs and

the fact that the permeability of the matrix is ultra-low, the reservoir simulation model was developed using a dual-porosity system (Zhang et al. 2019a).

The field-scale model was developed and validated by matching the actual production data of Eagle Ford well. Reservoir properties were modified to history match the well production data. The best history match results and actual production data of cumulative oil and water production are presented in **Fig. 39**. Then, all reservoir properties were determined from the best history match results.

Both cumulative oil and water production of field-scale history match agree with the actual well production data. The error of history match in the cumulative oil and water production was less than 1%, indicating that the field-scale model was reliable to describe the actual reservoir conditions. The gas injection reservoir model could provide convincing simulation results for understanding the efficiency of different gas injection EOR schemes.

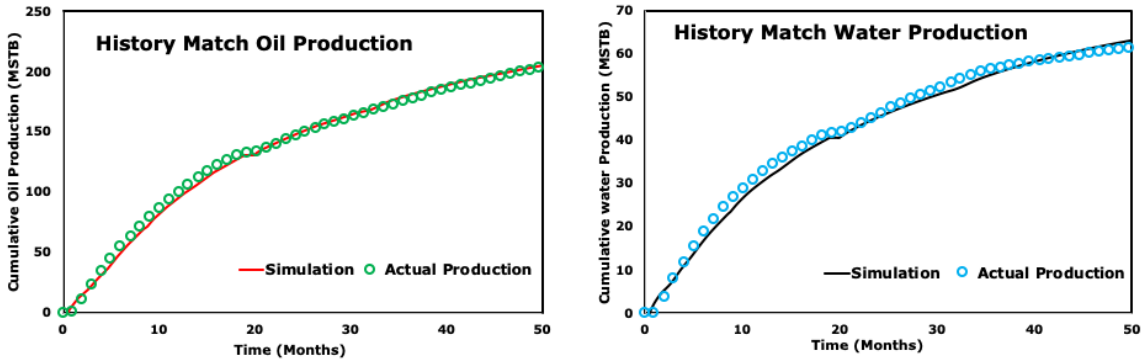

Figure 39 – The history match results of the field-scale model to the actual oil (left) and water (right) production data. Reprinted with permission from Zhang et al. (2019a).

The results of the gas injection experiments proved the potential of gas injection as an effective EOR method in improving oil production in ULR. In order to evaluate the effectiveness of gas injection EOR in the Eagle Ford reservoir, oil production enhancement from the gas injection process was investigated through reservoir simulation using the validated field-scale model. The diffusion coefficients from the core-scale history match were also implemented in the field-scale model. In this study, the effects of injection pressure and start time of gas injection treatment on improving oil recovery were evaluated and compared to primary depletion cases. Cumulative oil production was selected as the evaluation factor to describe the performance of the gas injection EOR in the Eagle Ford reservoir. The incremental recovery was calculated using **Eq. 9**.

$$\text{Incremental recovery} = \frac{\text{cum. oil (gas injection)} - \text{cum. oil (base)}}{\text{cumulative oil production of the base case}} \quad \text{(9)}$$

Two injection pressures of 4,000 psi and 4,500 psi were studied to demonstrate the effect of injection pressure on improving oil production in ULR. The cumulative oil production and incremental recovery of both cases are presented in **Fig. 40**. The gas injection process results in add up to 9% of oil production incremental by one injection cycle. In addition, higher the injection pressure leads to higher cumulative oil production in this Eagle Ford reservoir, and this trend was also observed in the laboratory results. Higher injection pressure causes heavier components of oil to reach a miscible state and further increases the average pressure of the reservoir. The pressure difference determines

the oil production rate of a well during primary depletion. Hence, re-energizing the reservoir to a higher pressure could improve oil production after the gas injection process.

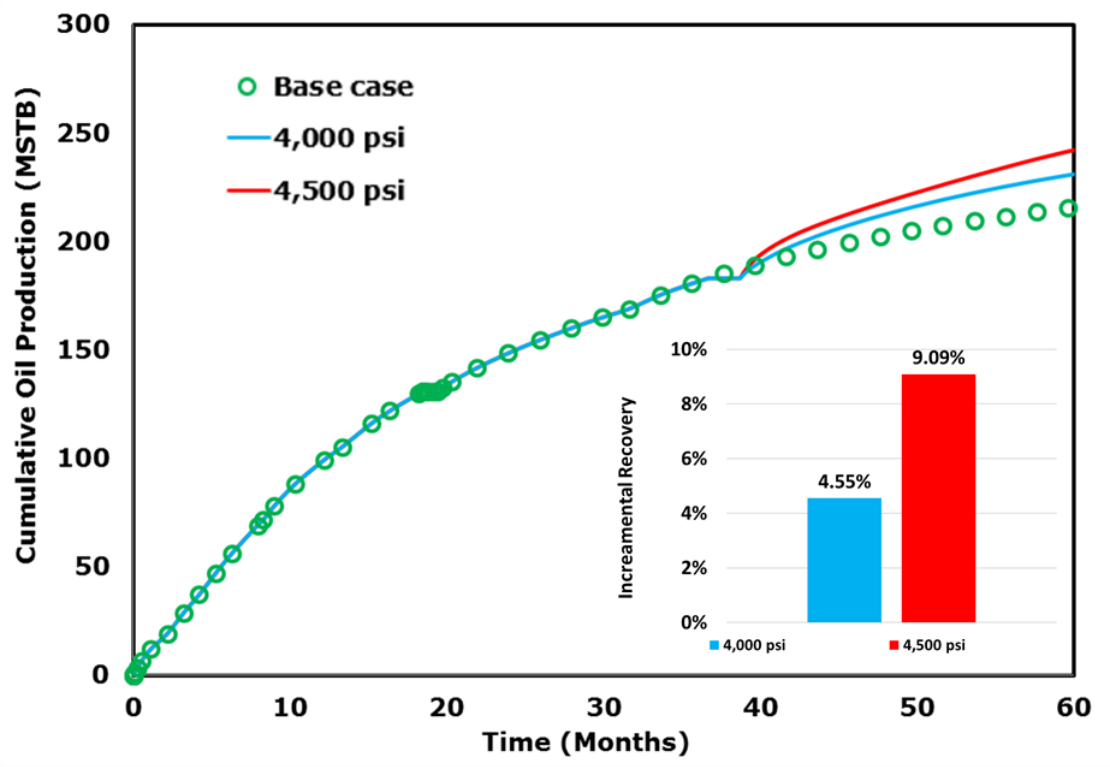

Figure 40 – Simulation results of cumulative oil production and recovery incremental for different injection pressure. Reprinted with permission from Zhang et al. (2019a).

The impact of the starting time of the gas injection process is also investigated, and the simulation results of different starting times are depicted in **Fig. 41**. In addition, a summary of gas injection simulation cases is presented in **Table 8**. Two gas injection starting times (after three and four years of oil production) were tested, and the pressure of the gas injection process was 4,500 psi. The gas injection start time does not show a substantial effect on oil production enhancement in the Eagle Ford well compared to the

result of injection pressure. Gas is injected through well-bore after three years of oil production, leading to a slightly better performance than the four-year case. Also, the starting time of gas injection should not be less than two years, because it is difficult to inject enough gas volume into the reservoir to economically improve oil production in unconventional liquid reservoirs. In this study, three years was found to be the optimum gas injection starting time for this Eagle Ford well.

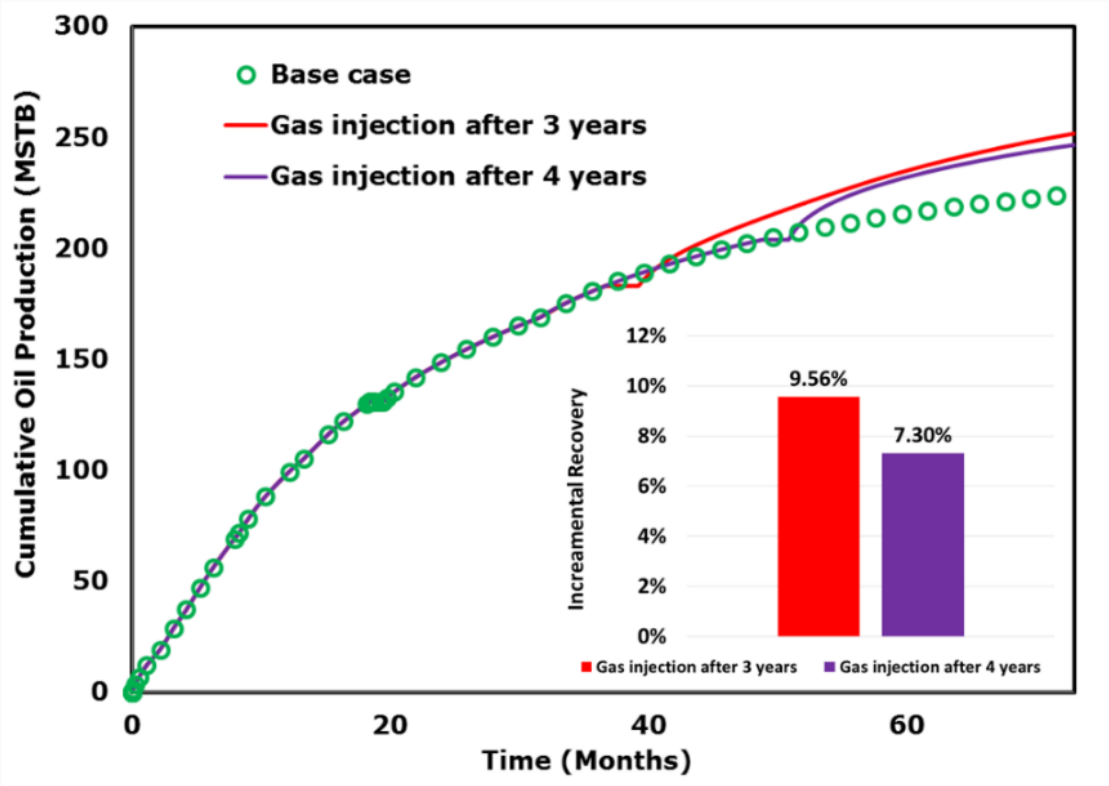

Figure 41 – Simulation results of cumulative oil production and recovery incremental for the different gas injection start time. Reprinted with permission from Zhang et al. (2019a).

Table 8 – Summary of gas injection simulation cases

Injection Start time	Injection Pressure (psi)	Injection Time	Recovery Incremental (%)
After 3 years of depletion	4,000	1 month	4.6
After 3 years of depletion	4,500	1 month	9.1
After 3 years of depletion	4,500	2 months	9.6
After 4 years of depletion	4,500	2 months	7.3

CHAPTER VI

HYBRID EOR IN UNCONVENTIONAL RESERVOIRS *

As demonstrated in the previous chapters, chemical and gas injection EOR techniques have potential for improving oil recovery in unconventional liquid reservoirs. It is a natural step to investigate whether a hybrid EOR technique, which is a combination of chemical and gas injection EOR methods, could further improve oil recovery in unconventional liquid reservoirs.

In this chapter, a novel hybrid EOR method is utilized to study the feasibility of this method and the efficiency of oil production improvement in ULR through experiments and numerical simulation. Spontaneous imbibition experiments and gas injection experiments were performed to assess the capability of the hybrid EOR method on improving oil recovery in ULR and gathered required data for upscaling the experimental results to the reservoir scale. Then, the core-scale model was constructed to match the experimental data. Capillary pressure curves, relative permeability curves, and diffusion coefficients are determined from history match results using the core-scale models. All

---

* Parts of the methodology presented in this chapter have been reprinted from:

"Enhanced Oil Recovery in Unconventional Liquid Reservoir Using a Combination of CO_2 Huff-N-Puff and Surfactant-Assisted Spontaneous Imbibition" by Fan Zhang, I.A. Adel, K.H. Park, I. W. R. Saputra, and D.S. Schechter. SPE Paper 191502. Copyright 2018 by the Society of Petroleum Engineers (SPE). Reproduced with permission of SPE. Further reproduction prohibited without permission.

"Numerical Investigation of EOR Applications in Unconventional Liquid Reservoirs through Surfactant-Assisted Spontaneous Imbibition (SASI) and Gas Injection Following Primary Depletion" by Fan Zhang, I.A. Adel, I. W. R. Saputra, and D.S. Schechter. SPE Paper 196055. Copyright 2019 by the Society of Petroleum Engineers (SPE). Reproduced with permission of SPE. Further reproduction prohibited without permission.

parameters determined from the core-scale history match were implemented in the reservoir model to describe the recovery performance of this hybrid EOR technique in shale reservoirs. Finally, the field-scale model was developed and validated by history matched well production data, and then predict oil production increment of hybrid EOR applications in the Eagle Ford reservoir.

Experimental Observations

Gas Huff-n-Puff experiments, along with surfactant imbibition tests, were performed at the reservoir temperature of 170 ^{o}F using saturated side-wall shale core plugs from the Eagle Ford formation. To observe the effectiveness of combining gas and surfactant EOR techniques to recover additional oil, core plugs used on the spontaneous imbibition experiments went through the gas injection tests. The core plug was retrieved and directly placed in the modified Amott Cell set-up after the last cycle on the gas injection experiment. These tests were performed following the experimental procedures of spontaneous imbibition and gas injection experiments, which were described in the previous sections. In addition, CT images of the cores during experiments are used to monitor fluid movement in the cores and investigated invasion distance of each technique. The color of produced oil is also analyzed and discussed to understand the mechanisms of this hybrid EOR in ULR.

Gas Injection Experiment

The recovery factors of gas injection experiments and the oil recovery curve of the maximum oil recovery case are presented in **Fig. 29**. The maximum recovery factor of gas injection experiments is 50% OOIP when experimental pressure at 3,500 psi. Around half of the total oil production was recovered during the first cycle, indicating the gas injection process to improve oil recovery during a short period in shale reservoirs. Increasing injection pressure results in a larger recovery factor, especially the pressure above the MMP. However, the recovery factors of the gas injection experiment are less than 5% of the OOIP when the injection pressure below the MMP. Since the primary mechanism of gas injection is the multi-contact miscibility, the oil production enhancement effect from the gas injection process could be activated when the injection pressure above the MMP.

Chemical EOR Related Experiments

In order to evaluate the possibility of combining gas injection and chemical EOR methods, surfactant imbibition experiments were performed immediately on the same core plugs that were previously utilized on the gas injection experiments. Contact angle, IFT, and surfactant adsorption isotherm data were referencing from (Zhang et al. 2019b). One surfactant formulation was used on hybrid EOR tests to eliminate the effect of improving oil recovery by surfactant types.

Imbibition tests were performed using a modified Amott cell at the reservoir temperature of 170 ^{o}F. The core plugs used for gas injection experiments were immediately submerged into the surfactant solution at 2 gpt concentration. The results of the imbibition tests are presented in **Fig. 42**.

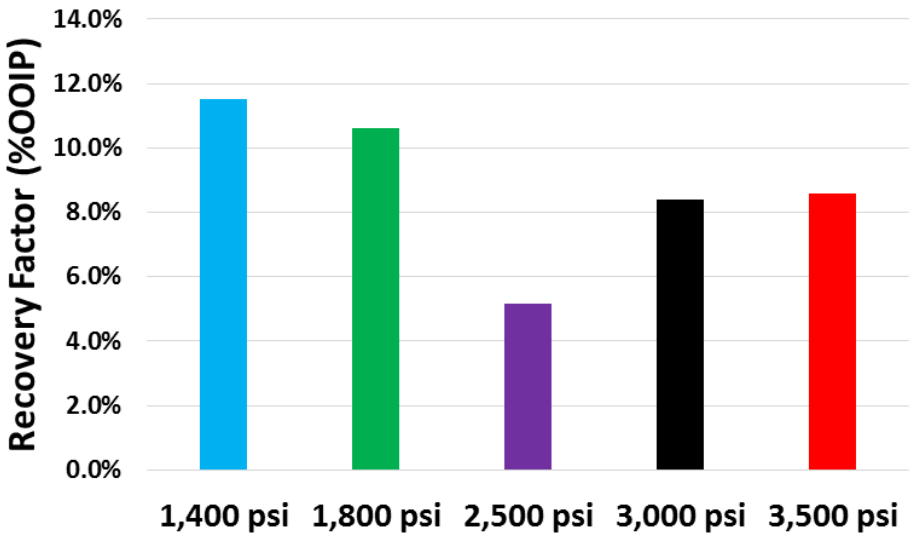

Figure 42 – Results of spontaneous imbibition experiments. Reprinted with permission from (Zhang et al. 2019b).

Although a substantial amount of oil had already recovered from the core sample through gas injection experiments, more oil was produced from those core samples after the spontaneous imbibition experiments. A properly selected surfactant could lead up to an additional 11.5% of OOIP from imbibition experiments after gas injection. Even the core plug that recovered 50% of OOIP from the gas injection experiment was capable of producing about an additional 10% of OOIP using the chemical EOR method. These

laboratory observations indicate the hybrid EOR technique is a feasible method to improve oil recovery in ULR.

Figure 43 – The produced fluid (foam at 12 h and oil at 240 h) inside the graduate cylinder during Surfactant-Assisted Spontaneous Imbibition. Reprinted with permission from Zhang et al. (2018a).

Another fascinating phenomenon was observed in the produced fluid during imbibition tests, as shown in **Fig. 43**. Typically, only oil could be collected at the top graduate cylinder of the modified Amott cell. However, foam was observed inside the graduated cylinder before oil was produced from the core plugs at the beginning of the imbibition experiment. This observation indicates the CO_2 invaded and adsorbed in the shale core plugs during gas Huff-n-Puff experiments. In addition, it also demonstrated that water imbibed into the shale core and displaced adsorbed gas and oil from core plugs by adding surfactant additives.

Summary of Hybrid EOR Experimental Results

The results of gas injection experiments and imbibition tests are gathered to analyze the performance of hybrid EOR in the laboratory-scale. Recovery factors from each production mechanism of the hybrid EOR technique are presented in **Fig. 44**. The production from gas experiments presented as the horizontal pattern and the production from imbibition tests shown as the diagonal pattern. The maximum oil recovery of 57.6% was achieved from the core used in gas injection experiments at 3,500psi, comprising 49% of OOIP from gas Huff-n-Puff experiment and an additional 8.6% oil recovery contributed from spontaneous imbibition experiment. Oil recovery from chemical EOR is not significantly affected by the pressure of gas injection experiments.

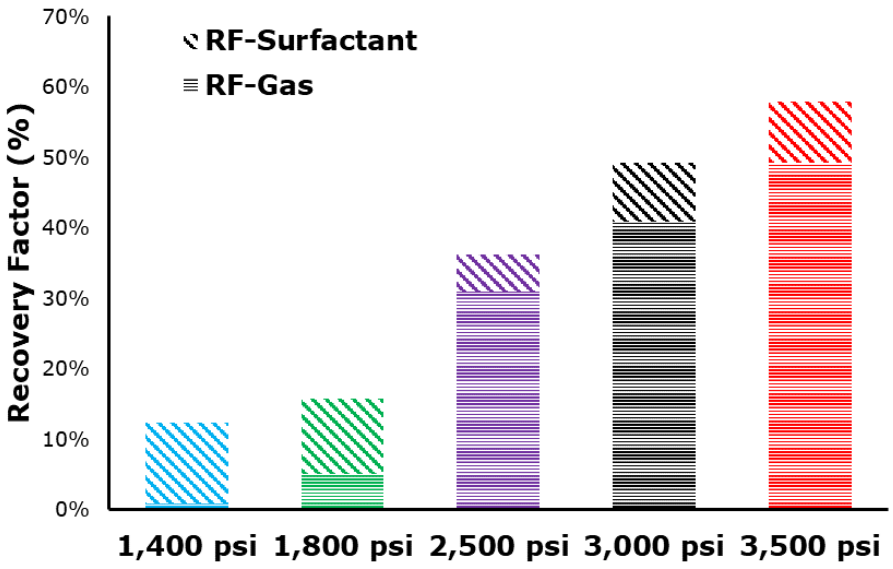

Figure 44 – Summary of oil recovery of combining EOR techniques. Modified with permission from Zhang et al. (2018a).

The time frame (shown in **Fig. 45**) of the entire hybrid EOR tests, including saturation and aging process, gas Huff-n-Puff experiments, and spontaneous imbibition experiments, is investigated to evaluate the efficiency of this hybrid EOR technique in ULR. Typically, the saturation and aging process takes three months to restore the core plugs to original reservoir conditions. The ultimate oil recovery is achieved from gas Huff-n-Puff experiments within four days. Commonly, no more oil can be retrieved from spontaneous imbibition experiments after five days.

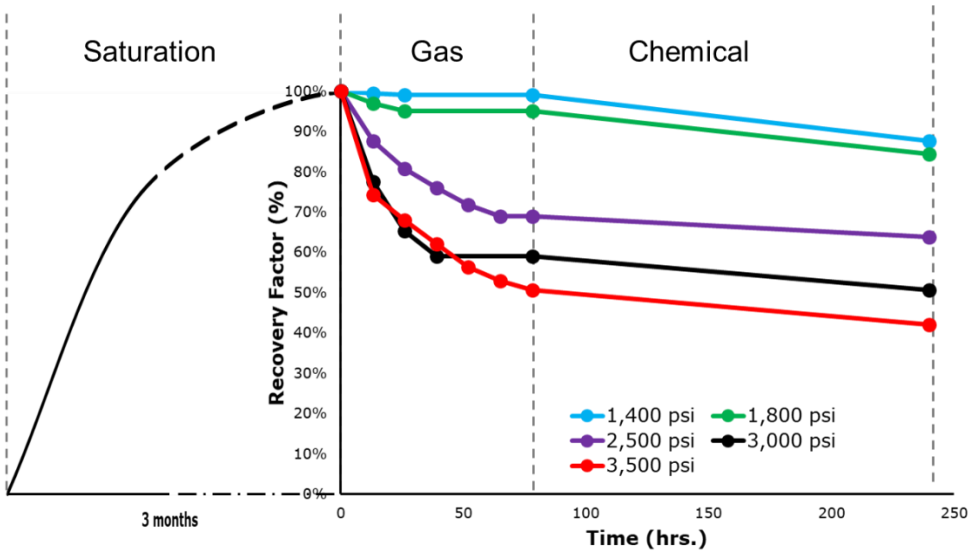

Figure 45 – Oil saturation of the core through the aging process, gas injection experiments, and spontaneous imbibition experiments. Modified with permission from Zhang et al. (2018a).

Fig. 45 depicts the evolution of oil saturation change throughout the entire hybrid EOR evaluation. Three months are required to restore the core plugs to original reservoir conditions. However, up to 60% of OOIP was recovered from the core plug within ten days, which is less than 10% of saturation time. This observation indicates that the hybrid

EOR technique is a feasible and fast method to improve oil recovery in ULR effectively. The remarks from the study open the possibility of utilizing the hybrid EOR technique to achieve optimum oil recovery in shale reservoirs.

CT-Scan Images

CT-scan images were utilized to illustrate the fluid movement inside shale core plugs during hybrid EOR test. The core plugs were scanned periodically throughout the duration of both gas injection experiments and imbibition tests, as shown in **Fig. 46**. Consistent color coding was also applied to all the images to improve the visibility of the scan results. Color corresponds to specific CT number range, such as brighter color correlates to higher CT-number and reddish color relates to higher CT-number. In addition, the legend of the color code is shown on the right side of **Fig. 46**.

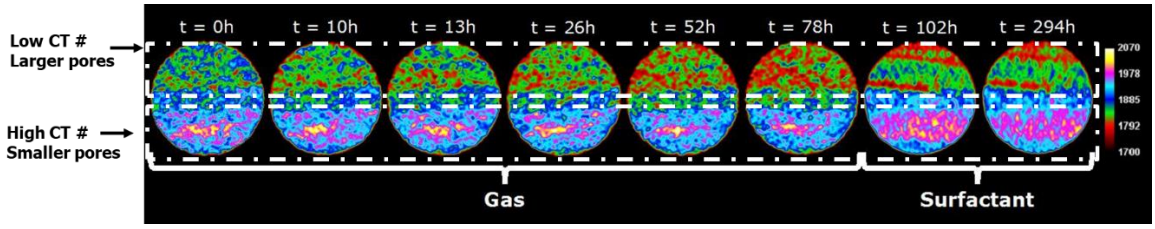

Figure 46 – CT scan images of the gas injection experiment at 3,500 psi and corresponding spontaneous imbibition experiment. Modified with permission from Zhang et al. (2018a).

As marked in **Fig. 46**, the core is highly heterogeneous that the top half of the core possesses relatively low CT numbers, and the bottom half has an average high CT number.

CT number shows a negative correlation with pore size, indicating the top half of the core plug contains larger pores and smaller pores located at the bottom half of the core. Typically, lighter components of oil gathered in the larger pore and smaller pores contain heavier components of the oil. In the CT images of the gas injection experiment, a clear color shift occurs at the top part of the core from greenish color to reddish color. However, a slight color change is observed at the bottom part. This observation indicates that most of the oil recovered from the larger pores of the core plug with lighter components in the gas injection experiment. This also proves the mechanism of gas injection EOR is multi-contact miscibility. In addition, a clear color change is also observed at the center of the core at 10 hours of the experiment, demonstrating that gas is invaded the center of the core within 10 h.

The last two CT images (in **Fig. 46)** depict fluid movement in the surfactant imbibition experiment. Due to the relatively less volume of oil produced from the imbibition test, only the initial and final time steps are shown to provide the best contrast of CT change. A distinct color change from purple to blue is observed at the bottom half of the CT images, indicating the heavier components of the oil are recovered from smaller pores through spontaneous imbibition experiments.

Color Change of Produced Oil from Hybrid EOR Method

An unexpected phenomenon was observed in the color of produced oil obtained from gas injection and spontaneous imbibition experiments. Oil produced from surfactant

imbibition experiments was darker compared to original oil, and the color of produced oil from gas injection experiments is much lighter than the original oil color used in this study. The color of produced oil from gas injection experiments and imbibition experiments is dissimilar due to the different dominant mechanisms of the two techniques. To show the color difference of the oil recovered from the two tests and discuss the mechanism govern each technology, the images of produced oil and the original oil are presented in **Fig. 47**.

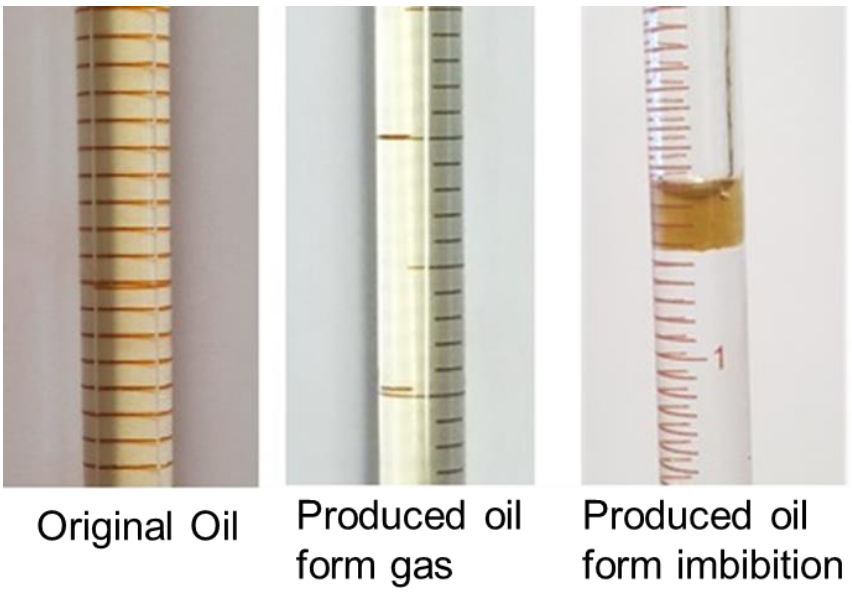

Figure 47 – Color change of oil observed from original oil to produced oil from CO_2 process and oil recovered from surfactant-assisted spontaneous imbibition experiment. Reprint with permission from Zhang et al. (2018a).

The color of produced oil from gas Huff-n-Puff experiments was light yellow, but the color of produced oil from spontaneous imbibition experiments was the darker (brownish) color. Generally, heavier components of oil lead to a darker color, and lighter components of oil show a bright color. The lighter components of the oil vaporized into

the gas phase and consequently were expelled out from the shale core plug when the injection pressure beyond the MMP. The oil produced from the gas injection process consists of lighter components of the oil, resulting in a lighter color.

The primary mechanism of chemical EOR on enhancing oil recovery in ULR is wettability alteration. Capillary pressure is the only governing force in the spontaneous imbibition process and inversely proportional to the radius. Therefore, the capillary pressure in the smaller pores is larger than in the larger pores, resulting in oil is more easily produced from smaller pores in spontaneous imbibition tests. In addition, the heavier components of oil prefer to gather in the smaller pore. The oil produced from spontaneous imbibition experiments contained a significant portion of heavier components of oil with a brownish color.

Core-Scale Modeling

In order to determine the scaling parameters of the hybrid EOR in ULR, a laboratory-scale simulation model is developed to history match experimental results of all related experiments. The core-scale model used in the study is the same as the model developed in the previous chapter. The validated PVT table and diffusion coefficient determined from the history match of gas injection experiments are also applied to the field-scale to investigate the efficiency of the hybrid EOR technique in ULR in this chapter. The history match results of spontaneous imbibition experiments are illustrated next.

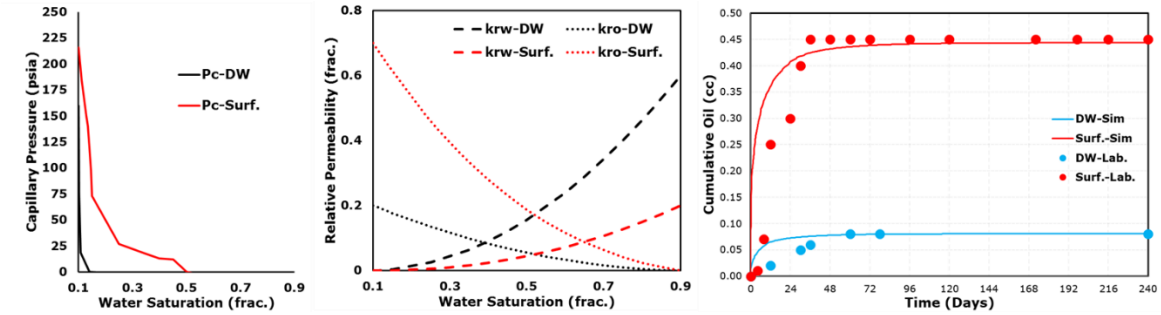

Figure 48 – Capillary pressure curves from scaling group analysis (left), corresponding relative permeability curves (middle), and best history match results (right). Reprint with permission from Zhang et al. (2019b).

Core-scale history match results of the spontaneous imbibition experiment are presented in **Fig. 48**. Capillary pressure of both base and surfactant cases are located on the left figure, the relative permeability curves of both cases in the middle, and the best history match of oil recovery from the experiment on the right figure. Adding the surfactant to aqueous phase results in an increment of the capillary pressure curve due to wettability alteration. In addition, the intersection of capillary pressure and the x-axis is also shifted to the right, allowing for capillary pressure sufficient at a broader range of water saturation. The oil relative permeability of the surfactant case is significantly higher than the base case, while the opposite is displayed on the water relative permeability curve. This phenomenon could be caused by the combined effects of wettability alteration and IFT reduction. As the rock surface is altered to water-wet, the flow of water across the rock is hindered, resulting in a lower water relative permeability. On the contrary, oil relative permeability is improved by wettability alteration. Although IFT reduction leads

to an increase of the relative permeability, the effect of IFT reduction using this surfactant on relative permeability is negligible compared to the impact of wettability alteration.

The diffusion coefficient, validated PVT table, capillary pressure curves, and relative permeability curves achieved from core-scale history matching are implemented into the field-scale model to evaluate the efficiency of different hybrid EOR applications in unconventional liquid reservoirs.

Field-Scale Modeling

The field-scale model used in this chapter is developed following the same numerical simulation workflow as demonstrated in Chapter III. Gridding structure and permeability distribution in hydraulic fractures of the reservoir model are presented in **Fig. 49**. The history match of actual well production data is performed to determine all the undetermined parameters using CMG CMOST. The history match results agree with actual production data with less than 1% overall error. The efficiency of four hybrid EOR scenarios are assessed using the validated field-scale model in this study, including 1. chemical EOR in completion followed by gas injection after primary depletion; 2. gas injection following chemical injection after primary depletion; 3. chemical injection following gas injection after primary depletion; and 4. multi-cycle gas injection and chemical injection after primary depletion.

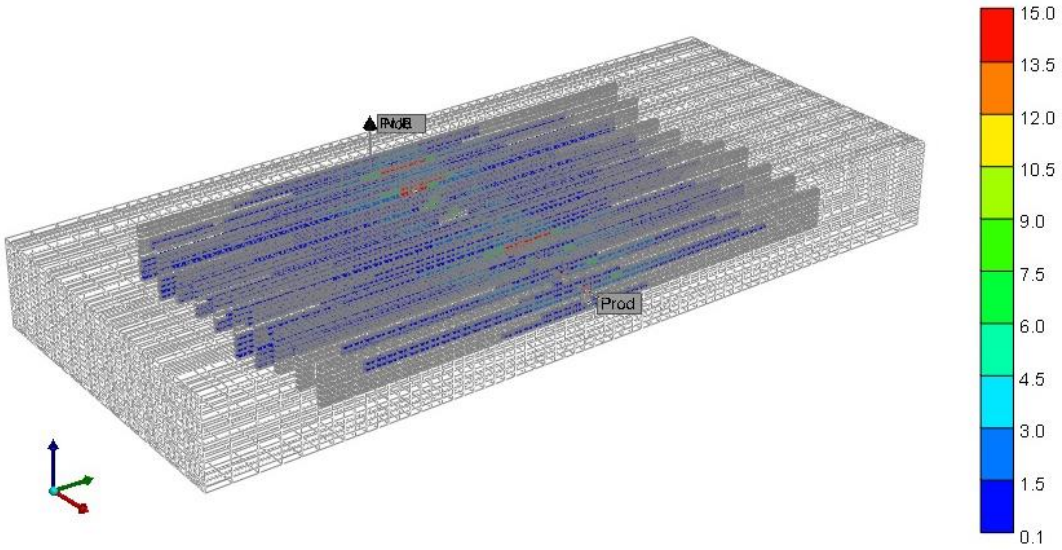

Figure 49 – Gridding structure and permeability distribution in hydraulic fractures of the field-scale. Reprint with permission from Zhang et al. (2019b).

Basic Chemical EOR and Gas Injection EOR Field Applications

In order to provide a comprehensive comparison of the efficiency of the Hybrid EOR techniques in ULR, the standard applications of chemical and gas injection are investigated to show the effect of a single EOR technique on improving oil recovery EOR in the Eagle Ford reservoir. Three cases of standard chemical and gas injection applications in ULR are included in this study, which are chemical EOR in the completion process, chemical injection after primary depletion, and gas injection after primary depletion. For any injection processes applied after the primary depletion, the starting time of injection processes is designed as after three years of oil production.

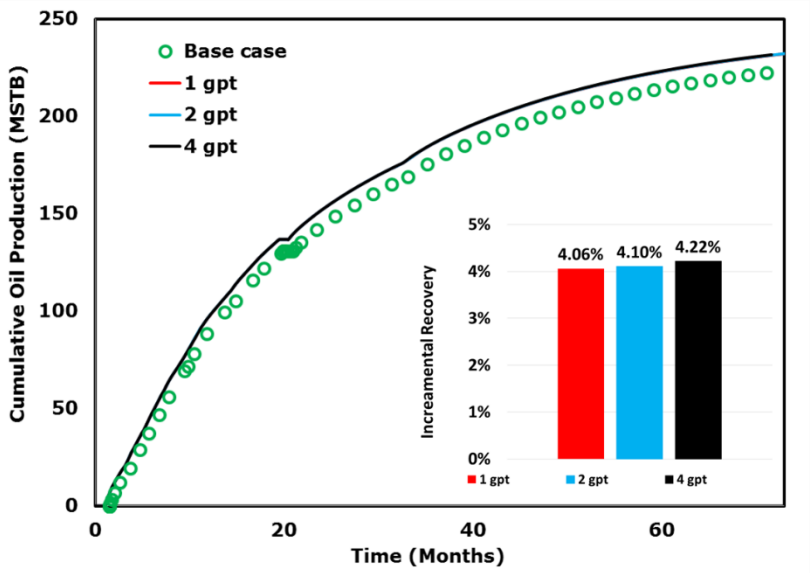

Figure 50 – Results of cumulative oil production and recovery incremental with different surfactant concentrations. Reprint with permission from Zhang et al. (2019b).

The integration of surfactants into the completion process is commonly believed as one method of applying chemical EOR in unconventional liquid reservoirs. The addition of a proper surfactant into the completion fluid results in a significant oil production enhancement from wettability alteration and IFT reduction. In this study, different surfactant concentrations are utilized to observe the effect of surfactant concentration on well performance. The simulation results of cumulative oil production and oil recovery incremental for three different surfactant concentrations of 1, 2, and 4 gpt are presented in **Fig. 50**. The oil recovery incremental is calculated by comparing the cumulative oil production of primary depletion. Applying chemical EOR in the completion process leads to a 4% oil production improvement compared to the base case. Incremental oil recovery increases as surfactant concentration increases, but the surfactant

concentration does not show a strong production enhancement effect on this Eagle Ford reservoir.

The second chemical EOR scheme is the chemical injection after primary depletion. The surfactant is added to injection fluid and implemented to the field after three years of oil production. This chemical EOR application should improve oil recovery further compare to add surfactants into the completion fluid, as the recovery mechanisms include pressure maintenance as well as wettability alteration and IFT reduction. The effect of pressure and surfactant concentrations are investigated for the chemical injection scheme, and the simulation results are shown in **Fig. 51**.

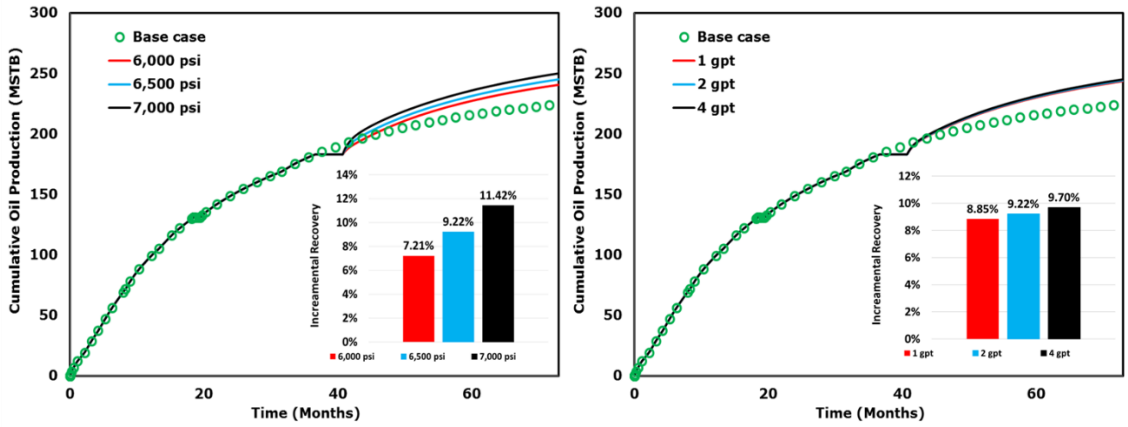

Figure 51 – The results of cumulative oil production and recovery incremental for different injection pressures and surfactant concentrations in the chemical injection process. Reprint with permission from (Zhang et al. 2019b).

Three different injection pressures of 6,000 psi, 6,500 psi, and 7,000 psi with a constant surfactant concentration of 2 gpt were evaluated to reveal the effect of pressure on oil production improvement. A positive correlation was observed between the

cumulative recovery and injection pressure. Higher injection pressure could re-energize the reservoir to higher pressure, leading to better oil production in the post-injection period. However, further increasing the injection pressure could result in a significant operation cost, especially the injection pressure is beyond 8,000 psi. Simulation results of different surfactant concentrations at 6500 psi injection pressure indicate increasing the surfactant concentration leads to slightly higher oil recovery. Similar to chemical EOR in the completion process, surfactant concentration fails to present a significant effect of improving oil recovery for this Eagle Ford well.

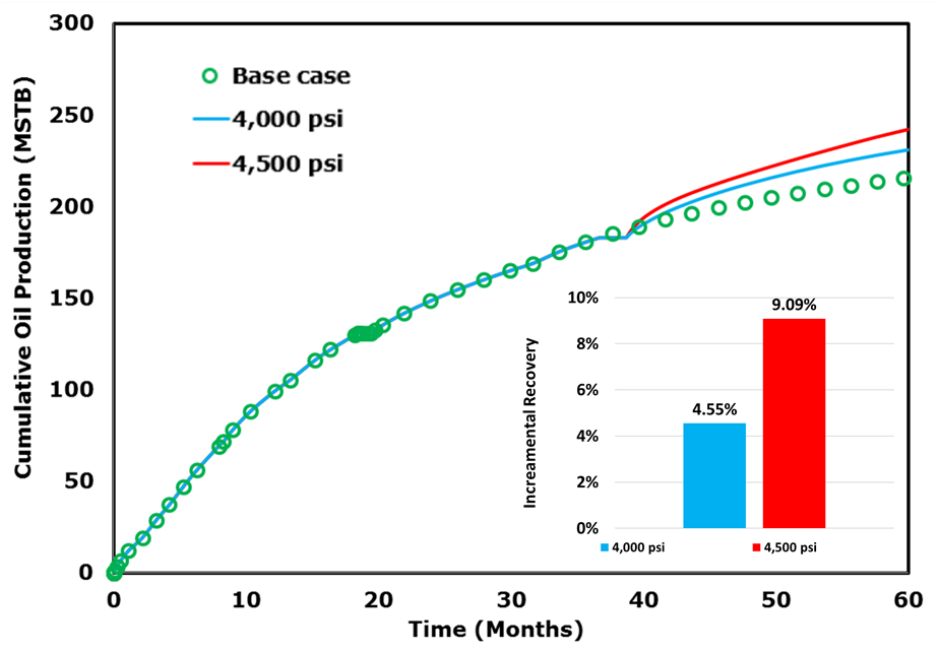

Figure 52 – The results of cumulative oil production and recovery incremental for different gas injection pressures. Reprint with permission from Zhang et al. (2019b).

The third basic EOR application is the gas injection process after primary depletion. Two injection pressures were tested on the reservoir model with the diffusion

coefficient obtained from the core-scale history match. The simulation results of cumulative oil production and recovery incremental for gas injection processes at 4,000 psi and 4,500 psi are presented in **Fig. 52**. The injection pressure has a positive correlation with oil recovery improvement. Up to 9% of oil recovery enhancement is achieved from gas injection at 4,500 psi. Higher injection pressure results in a broader spectrum of oil composition reach the miscible while simultaneously increases the reservoir to higher pressure. Increasing the injection pressure always leads to higher cumulative oil production, and this trend is also observed from the gas injection experiments.

Chemical EOR in Completion Followed by Gas Injection EOR Field Application

In the following sections, the simulation results of four different hybrid EOR methods are demonstrated and discussed to evaluate the efficiency of each hybrid EOR scheme. The first scenario referred to Hybrid EOR 1 is the combination of chemical EOR in the completion process and gas injection after primary depletion. In the Hybrid EOR 1 scenario, 1gpt of surfactant is added into the completion fluids, and then gas is injected at 4,500 psi after three years of oil production. This scheme targets the new drilling wells, or the wells have already implemented surfactants in the completion process. Simulation results of cumulative oil production using the Hybrid EOR 1 method are presented in **Fig. 53**.

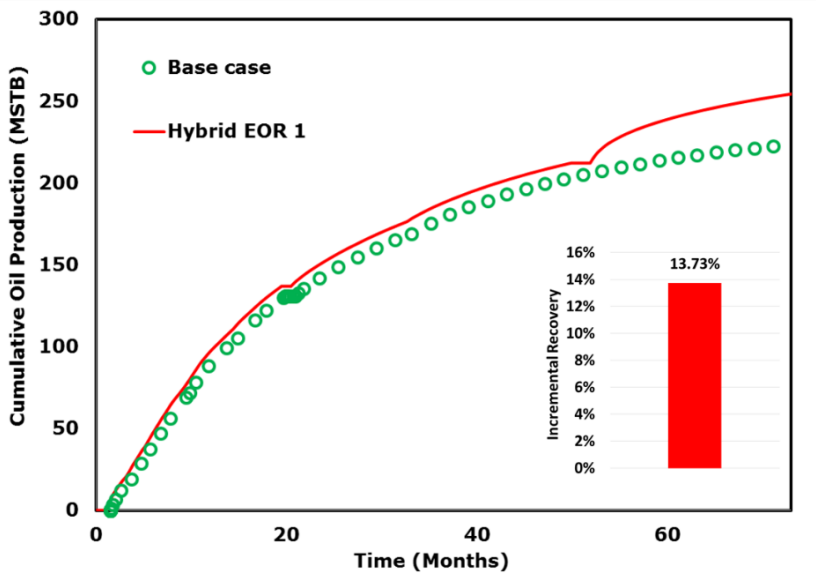

Figure 53 – The results of cumulative oil production and recovery incremental for Hybrid EOR 1.

Implementation of Hybrid EOR 1 into this Eagle Ford well results in an additional 13.7% of oil production compared to cumulative oil production of primary depletion. This combination of chemical and gas injection EOR provides a better incremental recovery than these EOR techniques used alone. The cumulative production increment from Hybrid EOR 1 is similar to the sum of incremental recovery from chemical EOR in the completion process and gas injection process when performed separately. This observation indicates that chemical and gas injection EOR techniques recover two different spectra of the hydrocarbons due to the recovery mechanisms of the two methods are dissimilar. In addition, a similar finding is observed in the laboratory experiments that different colors of oil produced from gas injection Huff-n-Puff and surfactant imbibition experiments. Nevertheless, Hybrid EOR 1 has great potential in enhancing the oil recovery in ULR.

Gas Injection Following Chemical Injection EOR Field Application

Chemical injection after three years of primary depletion and then followed by the gas injection process is the second hybrid EOR scheme referred to as Hybrid EOR 2. Hybrid EOR 2 method targets existing well without chemical EOR treatment in the completion process. After three years of primary depletion, the surfactant is injected into the reservoir with one gpt concentration at 7,000 psi for six months. Then, well goes back to production, and gas injection occurs at 4,500 psi after a one-year post chemical injection. The simulation results of the Hybrid EOR 2 method are shown in **Fig. 54**.

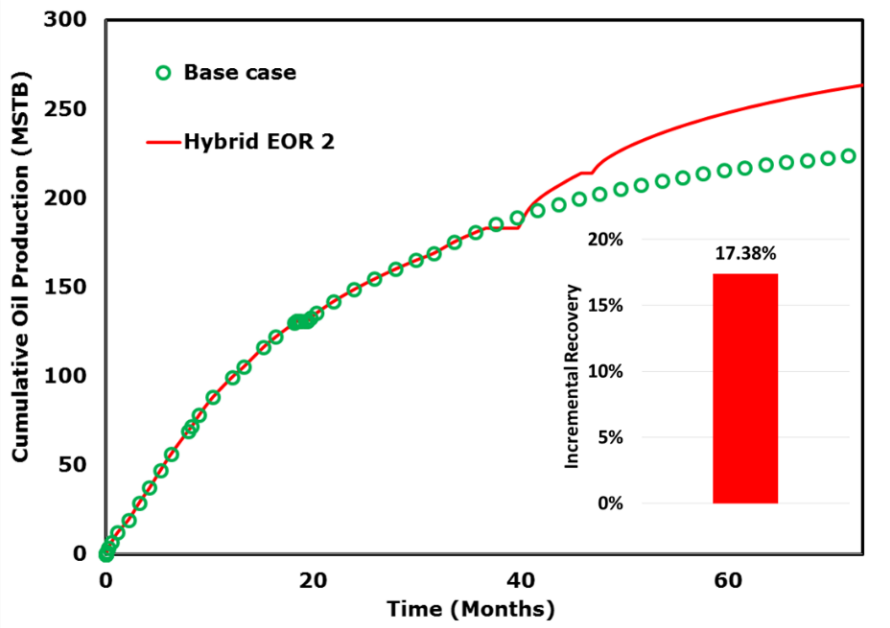

Figure 54 – The results of cumulative oil production and recovery incremental for Hybrid EOR 2. Reprint with permission from Zhang et al. (2019b).

Hybrid EOR 2 method has a better production enhancement than using Hybrid EOR 1, resulting in a 17.4% incremental production. Compared to chemical EOR in the completion process, the chemical injection process is a more suitable method to implement chemical EOR into unconventional reservoirs. However, the injection process increases the cost of applying chemical EOR technique in ULR, the optimal chemical EOR scheme for new drilling wells needs to consider the oil production increment and cost of injection. The simulation results indicate that Hybrid EOR 2 is also a feasible EOR method in improving oil recovery in shale reservoir.

Chemical Injection Following Gas Injection EOR Field Application

The third scenario of the combined EOR technique application denoted as Hybrid EOR 3 is performing the gas injection process after three years of oil production then followed by surfactant injection. Gas is injected into the reservoir at 4,500 psi for one month; then, surfactant injection with one gpt concentration is performed to the reservoir at 7,000 psi after one-year post gas injection treatment. The simulation results of Hybrid EOR 2 provides evidence that the combined injection process possesses the ability to increase oil production in unconventional reservoirs. The effect of the injection sequence on oil production enhancement is investigated next. The oil production and recovery incremental using the Hybrid EOR 3 scheme are presented in **Fig. 55**.

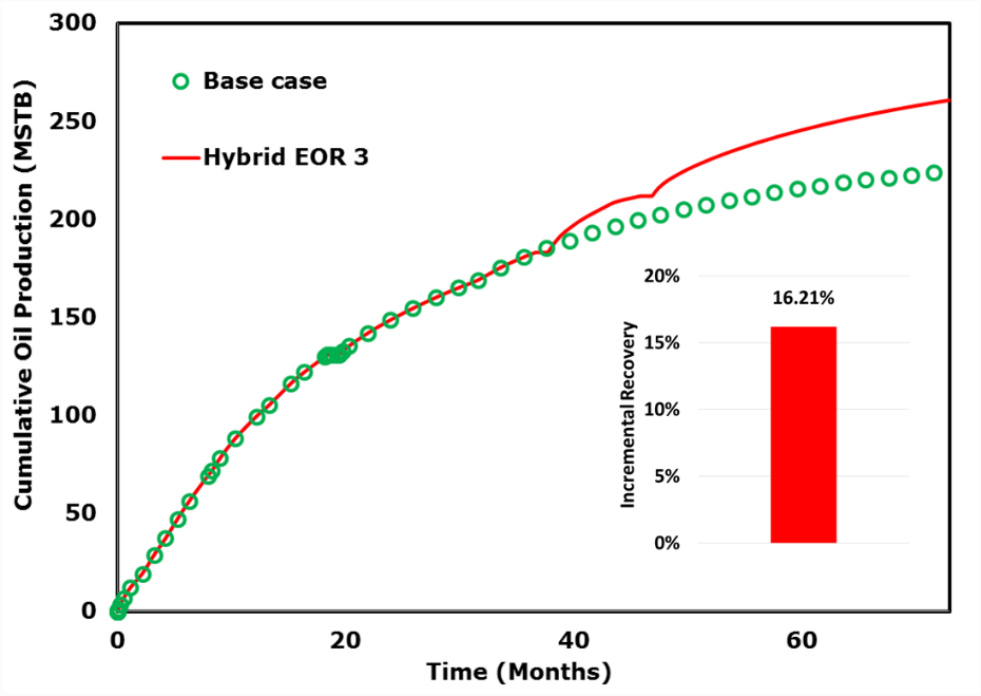

Figure 55 – The results of cumulative oil production and recovery incremental for Hybrid EOR 3. Reprint with permission from Zhang et al. (2019b).

Hybrid EOR 3 scenario also has a great potential for improving oil production in this Eagle Ford reservoir. However, the cumulative oil production from the Hybrid EOR 3 scheme is less than that from Hybrid EOR 2. The only difference between the Hybrid EOR 2 and 3 is the sequence of the injection process. In Hybrid EOR 2, the surfactant is injected into the reservoir earlier than in Hybrid EOR 3. The oil relative permeability of matrix and fractures is improved as the surfactant alters the wettability of rock, resulting in a longer enhanced flow path in Hybrid EOR 2. The efficiency of gas injection EOR is determined by injection volume. In addition, the reservoir pressure at the beginning of gas injection process is lower in the Hybrid EOR 2 scheme compared to Hybrid EOR 3,

indicating more gas is injected in the Hybrid EOR 2. Chemical injection is performed before the gas injection is the optimum Hybrid EOR design for this Eagle Ford reservoir.

Multi-Cycle Gas and Chemical Injection EOR Field Application

Finally, multi-cycle gas injection and chemical injection is tested to evaluate the effect of injection cycles on improving oil recovery in ULR. Three injection/production cycles of chemical and gas are applied to the reservoir after three years of primary depletion. In each injection/production cycle, the injection and production time is one month and one your, respectively. The surfactant of 1 gpt concentration is injected at 7,000 psi in the multi-cycle chemical injection scheme, and gas injection is performed at 4,500 psi using CO_2.

The cumulative oil production and recovery incremental of multi-cycle chemical injection cases are plotted in **Fig. 56**. An additional 15.7% of oil production incremental is observed after three-cycles. However, the oil increment for one cycle of chemical injection is about 11% based on the results of basic chemical injection in the previous section. Increasing the number of the injection/production cycle using surfactant solution does not result in significant improvement in oil production, especially for very low water-cut of Eagle Ford wells. The water saturation in hydraulic fractures increases as water is injected into the reservoir, resulting in oil relative permeability decrease. Increasing chemical injection cycles can significantly increase total liquid production, but oil production is suppressed as water saturation increases. In Chapter III, the multi-cycle

chemical injection technique was observed to significantly improve oil recovery and extend well life for the high water-cut reservoir. Therefore, multi-cycle chemical injection displays the great potential to increase ultimate oil recovery for the reservoir with high water saturation, but may not be the best option for low water-cut reservoirs (Zhang et al. 2019b).

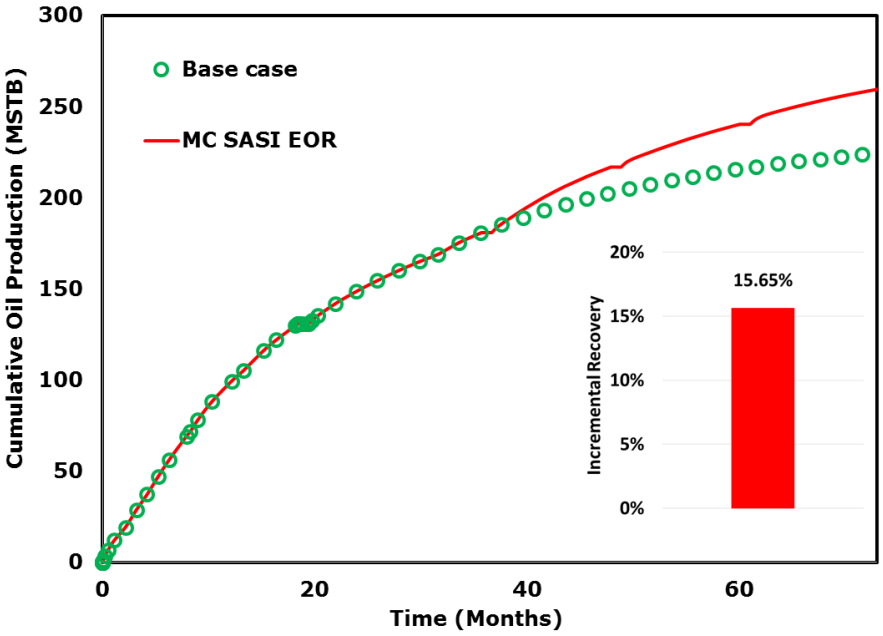

Figure 56 – The results of cumulative oil production and recovery incremental for multi-cycle chemical injection EOR application. Reprint with permission from Zhang et al. (2019b).

Finally, the efficacy of multi-cycle gas injection on enhancing oil recovery is evaluated in the Eagle Ford formation. Injection pressure and injection time are constant for each gas injection process. Simulation results of cumulative oil production and incremental oil recovery are depicted in **Fig. 57**. In addition, all field-scale simulations in

this chapter are summarized in **Table 9**. The multi-cycle gas injection process (cyclic-gas injection) results in the highest six-year oil production compared to all other EOR methods, with a 24% cumulative oil production incremental. The cyclic-gas injection method possesses a significant potential of increasing oil recovery in shale reservoirs, especially when the water saturation of the reservoir is low.

Table 9 – Summary of simulation cases (basic chemical and gas injection EOR, hybrid EOR, and multi-cycle chemical and gas injection) in this chapter.

Chemical EOR in Completion

Surfactant Concentration (gpt)	Recovery Incremental (%)
1	4.06
2	4.10
4	4.22

Chemical Injection EOR

Surfactant Concentration (gpt)	injection Pressure	Recovery Incremental (%)
1	6500	8.9
2	6000	7.2
2	6500	9.2
2	7000	11.4
4	6500	9.7

Gas Injection EOR

Injection Pressure	Injection Time (months)	Recovery Incremental (%)
4,000	1	4.6
4,500	1	9.1

Hybrid and Multi-cycle EOR

	Surfactant Conc.	Gas injection Pressure (psi)	Chemical injection Pressure (psi)	Recovery Increment (%)
Hybrid EOR 1: Chemical EOR in Completion + Gas Injection	1 gpt	4,500	6,500	13.7
Hybrid EOR 2: Gas Injection Following Chemical Injection	1 gpt	4,500	6,500	17.4
Hybrid EOR 3: Chemical Injection following Gas Injection	1 gpt	4,500	6,500	16.2
Multi-Cycle Gas Injection	1 gpt	4,500	6,500	15.7
Multi-Cycle Chemical Injection	1 gpt	4,500	6,500	24.0

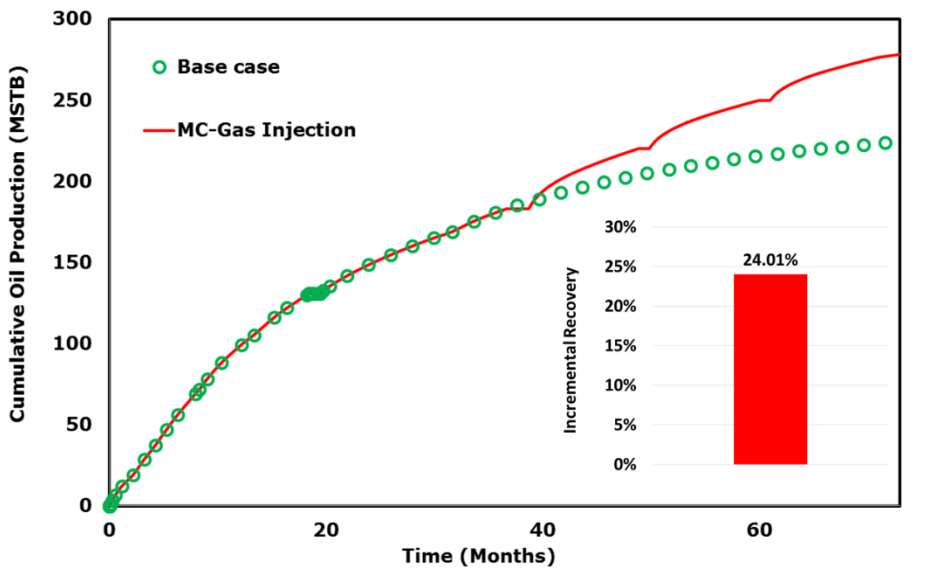

Figure 57 – The results of cumulative oil production and recovery incremental for multi-cycle gas injection EOR application. Reprint with permission from Zhang et al. (2019b).

CHAPTER VII

FOAM INJECTION EOR IN UNCONVENTIONAL RESERVOIRS

As demonstrated in the previous chapters, chemical, gas injection, and the hybrid (sequencing surfactant/gas injection) EOR techniques show the great potential of improving oil recovery in unconventional reservoirs. In addition, the mechanisms and efficiency of these EOR techniques are discussed to provide insights for EOR design in different shale plays.

In this chapter, the other hybrid EOR technique (foam injection) was investigated to the feasibility of this method in improving oil recovery in ULR. To compare the recovery performance of foam injection EOR to other EOR techniques, chemical and gas injection experiments were also performed at the same conditions. A novel foam injection experimental workflow is developed to identify the challenges, risks, potentials, and mechanisms of the foam injection EOR method.

Chemical (surfactant), gas, and foam Huff-n-Puff experiments are performed using sidewall core plugs from the same Wolfcamp A formation at reservoir temperature of 155 ^{o}F and 5,000 psi. CT scan technology is coupled with all experiments to monitor fluid movement inside core samples and examine foam quality in glass beads throughout the experiments. Experimental results are utilized to evaluate and compare the efficiency of each method in improving oil recovery at the same operating and reservoir conditions. Then, the color of the produced oil is analyzed and discussed to reveal the recovery

mechanism of each method. Finally, the core-scale model is developed for all the Huff-n-Puff experiments to achieve scaling parameters from history match experimental data.

Core and Oil Samples

In this chapter, various EOR methods are investigated that targeted in the Wolfcamp formation, which is the most portfolio shale reservoirs in the United States. Core plugs and oil samples used in this study are retrieved from the Wolfcamp A formation in Martin County, TX. 14 ULR cores were cut from the same1-ft interval (as shown in **Fig. 58**), and 9 of these core samples were used in this study. The geometries of the cut ULR cores are 0.965 in diameter and 2 in length. In addition, some rock chips were trimmed from this 1-ft Wolfcamp rock and were used for the contact angle measurements.

Figure 58 – Core Plugs cut from the Wolfcamp A formation in Martin County, TX.

The oil sample used in this study was also obtained from the same Wolfcamp A formation. The density of the oil was 0.797 g/cc, and it was measured at 155 ^{o}F. The composition of the oil was determined by gas chromatography, and it is presented in **Fig.**

59. This is a dead oil that no C_1 to C_3 components were observed in the GC results. The composition of the Wolfcamp oil is in the lighter range, with peaks around C_5 to C_8.

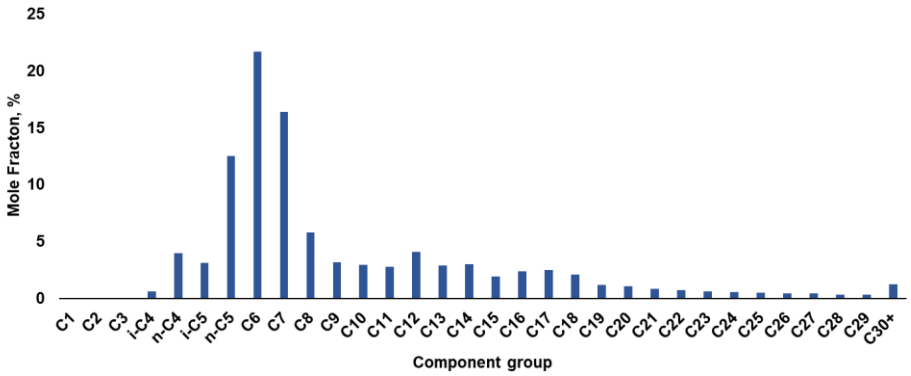

Figure 59 – Oil composition of the Wolfcamp oil determined by GC.

Saturation Process

In order to determine the OOIP for each core plug and accurately calculate the recovery factor of each experiment, the core samples were cleaned using the Dean-Stark method and dried under a vacuum oven. The clean cores were then saturated and aged using reservoir oil from the corresponding well at 10,000 psig and room temperature. This saturation process lasts for more than three months to restore the core samples to original reservoir conditions. CT scan technology is coupled with the entire saturation process to verify oil saturating into the cores. However, it is challenging to identify the supercritical gas phase and the oil phase in the CT image of Huff-n-Puff experiments. Idobenzene with 5% wt. of concentration was added to the oil sample to increase the contrast between supercritical gas and oil in the CT images.

Core samples were weighted, and CT scanned every 1-2 weeks during the saturation/aging process. The saturation process was monitored by recording the change in weight for each core sample, and this process was stopped when the weight of the core sample was constant for two consecutive weeks. **Table 10** presents the core plugs saturation data.

Table 10 – Saturation results of all core plugs used in this research.

Core #	Clean Weight (g)	Saturated Weight (g)	Weight Difference (g)	Oil Volume (cc)
1	64.655	65.806	1.152	1.445
2	64.485	65.818	1.334	1.673
3	64.567	65.578	1.011	1.267
4	66.618	65.380	1.238	1.553
5	66.557	65.218	1.339	1.680
6	66.752	65.641	1.111	1.394
7	65.926	64.457	1.469	1.843
8	66.710	65.463	1.247	1.565
9	63.823	62.668	1.155	1.449

CT Images of Saturation Process

CT-scanning technology was used to track oil saturation changes of core samples in the aging process. **Fig. 60** displays the saturation changes using the CT images for all cores. The first scan at time zero was performed after the cleaning process and before saturation. The last scan shows the final stage of saturation, after three months of the aging process. The CT-number increased at each time step as the oil penetrated into the cores.

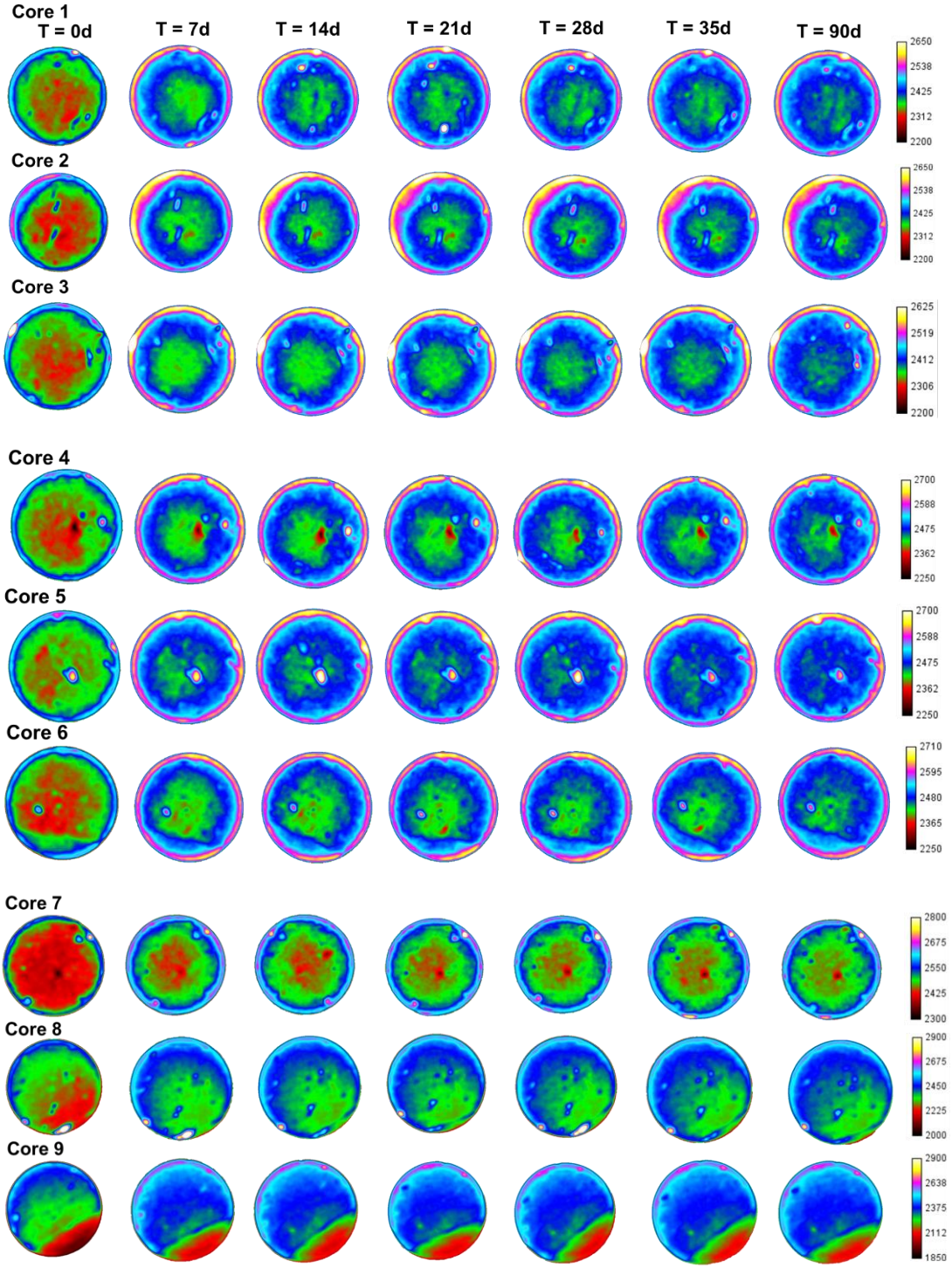

Figure 60 – CT-scan images tracking the changes in saturation over time for Wolfcamp A sidewall cores.

Minimum Miscibility Pressure Determination for Different Gases

MMP is a critical parameter for gas injection projects, and significant oil incremental is observed only if the injection pressure above the MMP. The MMP of the Wolfcamp A oil and four gases (CO_2, CH_4, a mixture of 85% CH_4 and 15% C_2H_6, and enriched gas (50% CH_4 – 50% C_2H_6)) were measured at reservoir temperature of 155 ^oF using the slim tube apparatus described in Chapter III. The MMP of the Wolfcamp oil and all four gases is presented in **Table 11**, and the recovery factors at different pressure for each case are shown in **Fig. 61**.

Table 11 – The MMP determination results of the Wolfcamp oil and different gases.

Gas Composition	Temperature (^oF)	Crude Oil	MMP (psi)
CO_2	155	Wolfcamp A	2,061
CH_4	155	Wolfcamp A	5,715
85% CH_4 15% C_2H_6	155	Wolfcamp A	4,452
50% CH_4 50% C_2H_6	155	Wolfcamp A	2,853

The MMP of the oil sample – CO_2 was determined to be 2,061 psig, which was the lowest MMP value of all four gases. The MMP of the Wolfcamp oil – CH_4 was estimated to be 5,715 psig, it was the highest MMP value among all the tested gases. As demonstrated in the previous chapters, it was shown that increasing injection pressure led to higher oil recoveries, and the best results were obtained when the pressure was above the MMP. Considering the case of Wolfcamp oil – CH_4, in order to effectively enhance oil production in this reservoir, the injection pressure needs to be around 6,000 psi. The

injection cost is directly related to the operating pressure. CH_4 may not be economically feasible for gas injection EOR in this reservoir, because the costs of injection process using CH_4 is very high.

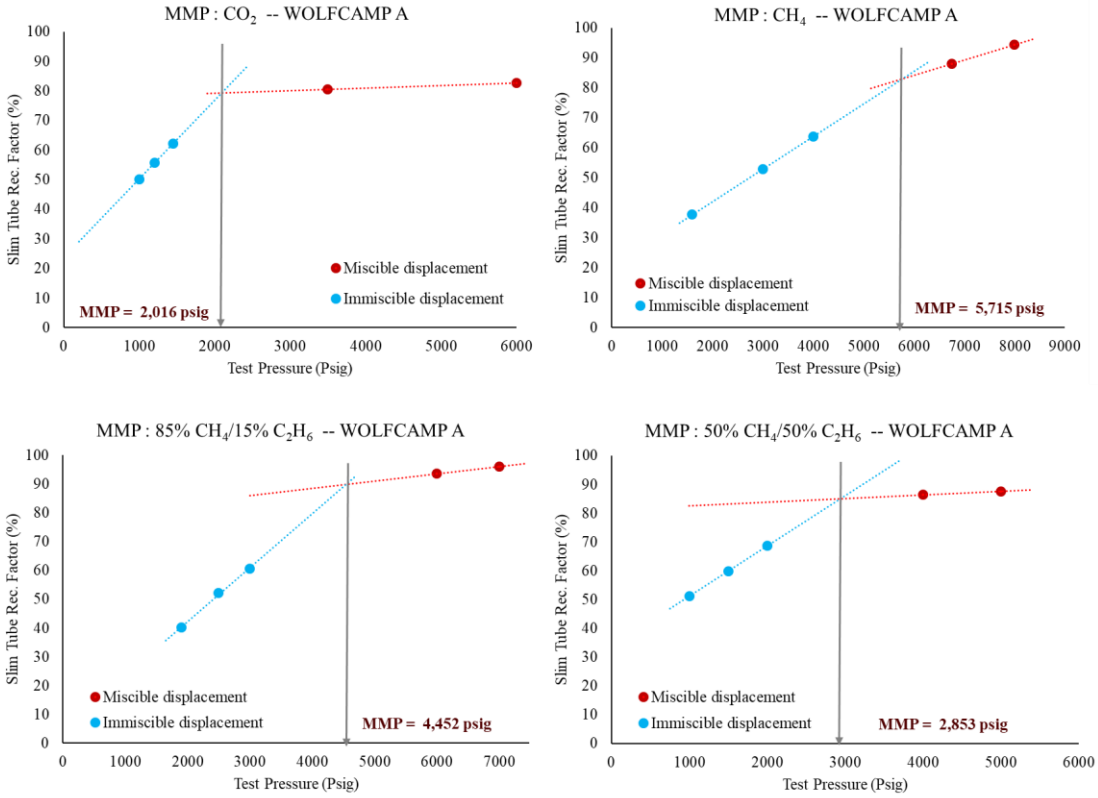

Figure 61 – Slim tube oil recovery vs. pressure for the CO_2 –Wolfcamp A system(top–left); the CH_4 –Wolfcamp A system (top–right); the 85% CH_4 15% C_2H_6 –Wolfcamp A system (bottom–left); the 50% CH_4 50% C_2H_6 –Wolfcamp A system (bottom–right).

A mixture of 85% CH_4 and 15% C_2H_6 was also tested in this study to represent produced gas from the Wolfcamp wells. Using a 15% ethane enrichment results in the MMP dropped to 4,452 psi. Due to the oil production boost in the Wolfcamp formations,

produced gas is easily accessible at moderate costs, which could make it a good candidate for gas injection processes in ULR. Compared to CH_4, a mixture of 85% CH_4 and 15% C_2H_6 is more effective to improve oil recovery in the Wolfcamp formation. Finally, enriched gas (50% CH_4 – 50% C_2H_6) was investigated to evaluate the effects on the MMP. When 50% ethane was added to pure methane, the MMP dropped from 5,715 psig to 2,862 psig, which was closed to the value obtained for the CO_2 case. Enriched gas (50% CH_4 – 50% C_2H_6) has a great potential of improving oil recovery in the Wolfcamp formation due to its low MMP when mixed with this particular oil and because it's cheap and readily available. The oil recovery potential of this mixture was examined by conducting the gas injection test.

Chemical Huff-n-Puff Experiments

The chemical Huff-n-Puff experiments followed the same experimental workflow as the gas Huff-n-Puff experiments, as described in the previous chapters. All the experiments were performed in the CT-scanner, enabling to scan the same position/slice of the cores at different time steps and conduct the tests at reservoir conditions of pressure and temperature.

Once the rock matrix-hydraulic fracture system was packed into the core-holder and connected to the core-flooding equipment, a vacuum was applied to remove the air. The surfactant solution with three gpt concentration was then injected into the until reaching the desired pressure. At this point, the soaking period lasted for 72 hours. CT-

scans were performed periodically to monitor fluid movement and saturation change during the soak period. After completing the soak period, the surfactant solution was displaced by nitrogen gas at a low flow rate, and the effluents were collected from the outlet to calculate the recovery factor of each experiment.

Table 12 – Results of chemical Huff-n-Puff experiments using pure brine and the best two types of surfactants in the brine solution.

Injection Fluid	Pressure, psi	Temperature, ^{o}F	Recovery Factor
Brine	5,000	155	6.9 %
Surf – B	5,000	155	12.3%
Surf – F	5,000	155	14.4%

Three chemical Huff-n-Puff experiments were performed using pure formation Brine, a solution of brine and Surf-B, and a solution of brine and Surf-F. The tests were performed at the reservoir temperature of 155 ^{o}F and 5,000 psi. The soak and production time of each Huff-n-Puff cycle was, respectively, 72 h and 3 h. The results of chemical Huff-n-Puff experiments are presented in **Table 12**.

Both types of surfactants increase the recovery factors of chemical injection experiments up to 14.4% compared to the recovery factor of 6.9% using brine alone. This observation indicates that adding surfactants into completion and injection fluids improves oil production in the Wolfcamp reservoir. Surf-F had a slightly better oil production enhancement effect than Surf-B. However, Surf-B showed a more stable performance in wettability alteration and IFT reduction at different salinities and was selected as a foam generation agent during the foam injection experiments.

CT images were taken periodically during the soak time, and the time-lapse CT images for the case of Surf-B is shown in **Fig. 62**. The CT number change throughout the experiment is invisible, and it may be caused by a small CT number contrast between the dopped Wolfcamp oil and the brine. The average CT number of the entire core plug was calculated for each time step. Similar to the observation from CT images, the average CT number of the whole core plug is almost constant throughout the duration of chemical injection experiments.

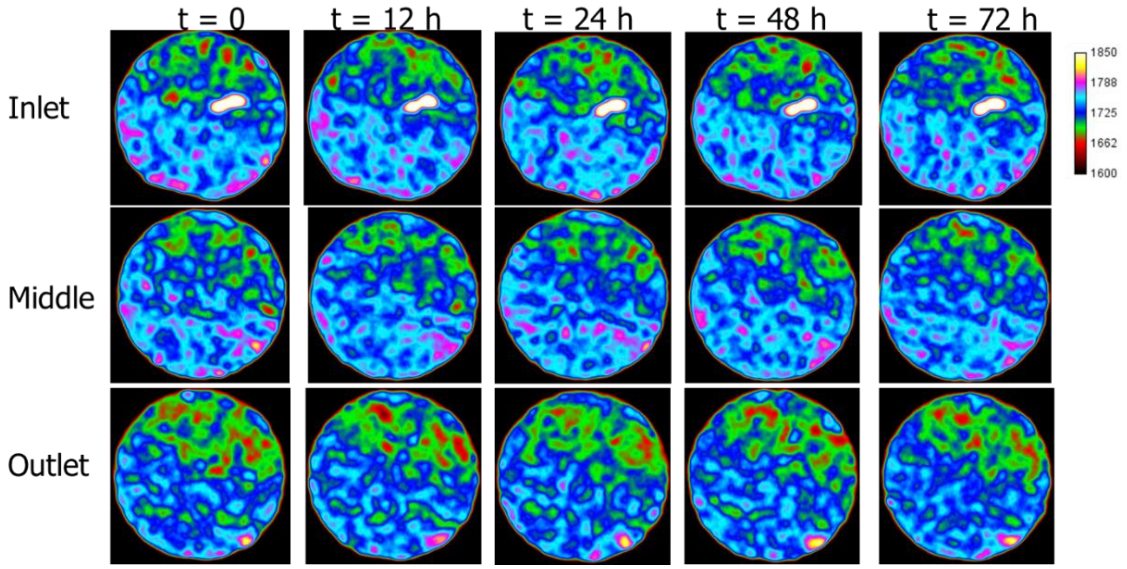

Figure 62 – CT images of three cross-sections (close to the inlet, in the middle of the core, and close to outlet) for chemical injection experiment using Surf-B.

Gas Huff-n-Puff Experiments

Previously, the efficiency of improving oil recovery in ULR using surfactant additives is evaluated by performing chemical injection tests. In this section, the recovery

performance of gas injection processes using various gases in the Wolfcamp formations is evaluated through gas Huff-n-Puff experiments following the same experimental workflow. Four gases (CH_4, a mixture of 85% CH_4 and 15% C_2H_6 (gas (50-50)) enriched gas (50-50) (50% CH_4 – 50% C_2H_6), and CO_2) were tested in this study to determine the optimal gas composition for gas injection EOR in ULR.

Gas tests were performed at reservoir temperature of 155 ^oF and 5,000 psig using 72h for soaking time and 3h for injection. It was chosen to use the same operating conditions as the surfactant experiments to be able to compare the EOR performances. The different EOR methods are compared using the recovery factors.

CH_4 Huff-n-Puff Experiment

The result of the CH_4 experiment is presented in **Table 13**. The average CT number of the entire core plug for each time step was calculated from the time-lapse CT images, and the average CT number change of the entire core during the experiment is shown in **Fig. 63**.

Table 13 – Results of the CH_4 injection experiment.

Injection Fluid	Pressure, psi	Temperature, ^oF	Recovery Factor
CH_4	5,000	155	9.7%

After the first cycle (72 h soak time and 3 h production time), the recovery factor of the CH_4 injection experiment was 9.7% of OOIP. Compared to recovery factors of

chemical experiments, injecting CH_4 is less effective in improving oil recovery in the Wolfcamp reservoirs. This could be caused by the experimental pressure, which is lower than the MMP obtained for pure methane. The injection pressure of this experiment was 5,000 psi that the multi-contact miscibility effect cannot be activated using CH_4. A higher oil recovery could be achieved if the injection pressure was above 6,000 psi.

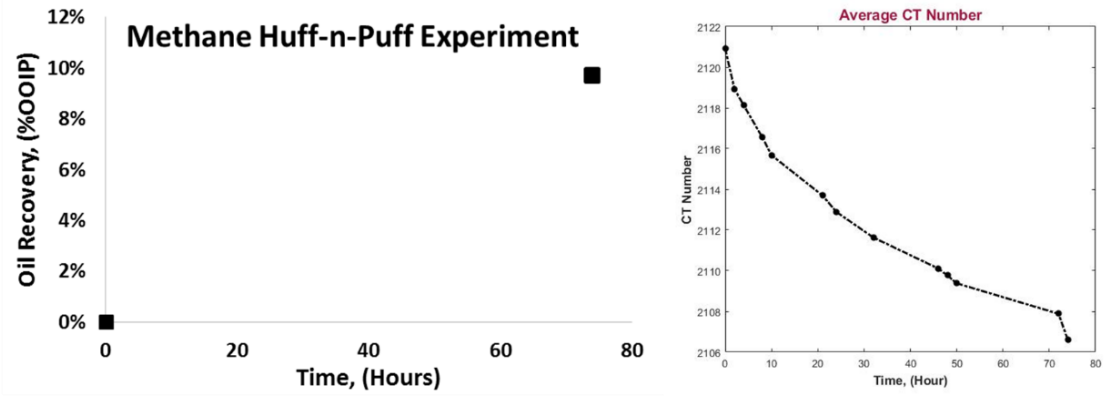

Figure 63 – Recovery factor for CH_4 test (left), and the average CT number of the entire core throughout the experiment (right).

In **Fig. 63**, the average CT number change of the entire core plug throughout the gas injection experiment was 14 Hounsfield unit (HU). An apparent average CT number change is observed in this test, indicating the injected gas invaded the core plug and extracted the oil. Time-lapse CT-scan images of three different cross-sections (close to the inlet, in the middle of the core, and close to outlet) for the CH_4 injection experiment are presented in **Fig. 64**. Although the recovery factor of the CH_4 injection experiment is less than those from chemical Huff-n-Puff experiments, the CT number change is more evident due to the significant contrast between dopped Wolfcamp oil and CH_4. These results

demonstrate that CT scan technology is more effective in monitoring saturation change in gas injection experiments compared to liquid-surfactant experiments.

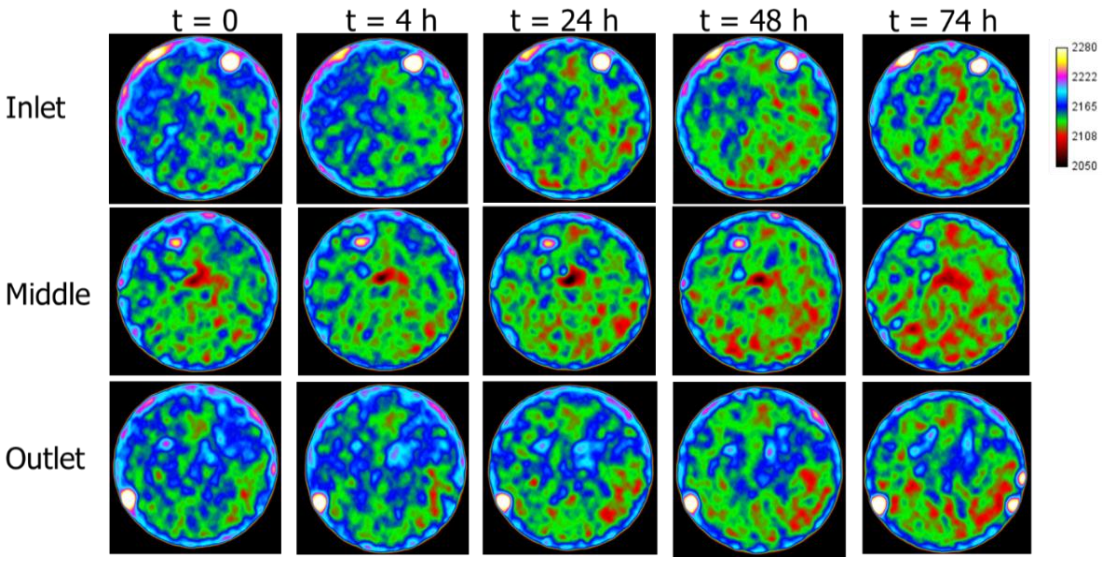

Figure 64 – Time-lapse CT images of three cross-sections (close to the inlet, in the middle of the core, and close to outlet) for gas Huff-n-Puff experiment using CH_4.

In **Fig. 64**, apparent color shifts occur from blue/green color to green/red color for the entire core. After 4 hours of soak, a color change was observed at the center of the core, indicating the CH_4 had invaded the center of the core plug. Time-lapse CT images also confirmed that oil was extracted from the plug during the CH_4 Huff-n-Puff experiment.

A picture of the produced oil was taken after the CH_4 experiment, which is shown in **Fig. 65**. The color of produced oil from the CH_4 test is much lighter than the color of original Wolfcamp A oil used to saturate the plug. Lighter components of the oil were

recovered during gas injection experiments through the multi-contact miscibility process, which was also observed in CO_2 injection experiments.

Figure 65 – Color of produced oil (lighter than original oil) from the CH_4 experiment.

A Mixture of 85% CH_4 and 15% C_2H_6 Huff-n-Puff Experiment

Huff-n-Puff experiment was performed using a mixture of 85% CH_4 and 15% C_2H_6 at 5,000 psig and reservoir temperature 155 ^oF, and the result of this experiment is presented in **Table 14**. The recovery factor of the injection experiment using 85% CH_4 and 15% C_2H_6 was 13% of OOIP after one cycle, which was higher than the recovery factor using CH_4. Adding 15% ethane into pure methane not only decreased MMP but also improved the oil recovery from gas injection experiments. Since a promising result was observed after the first cycle, more cycles were tested consequently until no more oil was recovered from the plug. The ultimate oil recovery was obtained after 5 cycles, which is presented in **Fig. 66**.

Table 14 – Results of the gas (85-15) experiment after the first Huff-n-Puff cycle.

Injection Fluid	Pressure, psi	Temperature, ^{o}F	Recovery Factor
85% CH_4-15% C_2H_6	5,000	155	13%

The ultimate oil recovery of the gas injection experiment using a mixture of 85% CH_4 and 15% C_2H_6 was achieved after 5 cycles, and the recovery factor was 23.2% of OOIP. This observation indicates produced gas is a promising EOR agent in improving oil recovery in the Wolfcamp reservoirs and further ethane enrichment could result in higher ultimate oil recovery from gas injection experiments.

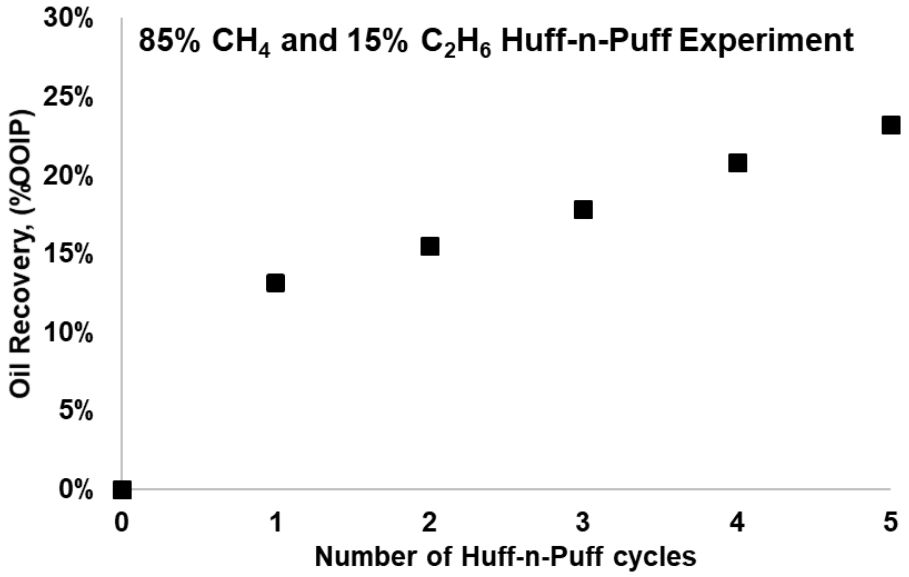

Figure 66 – Recovery factors of each cycle for the gas (85-15) Huff-n-Puff experiment.

The average CT number of the entire core plug for each time step was calculated from the CT images of this Huff-n-Puff experiment, and the average CT number change

of the entire core plug throughout the gas injection experiment is 18 HU. The average CT number change has a positive correlation with the recovery factor for gas injection experiments, and the other two gas Huff-n-Puff experiments will be used to examine this correlation. In addition, time-lapse CT-scan images of three different cross-sections (close to the inlet, in the middle of the core, and close to outlet) for the mixture injection experiment are presented in **Fig. 67**.

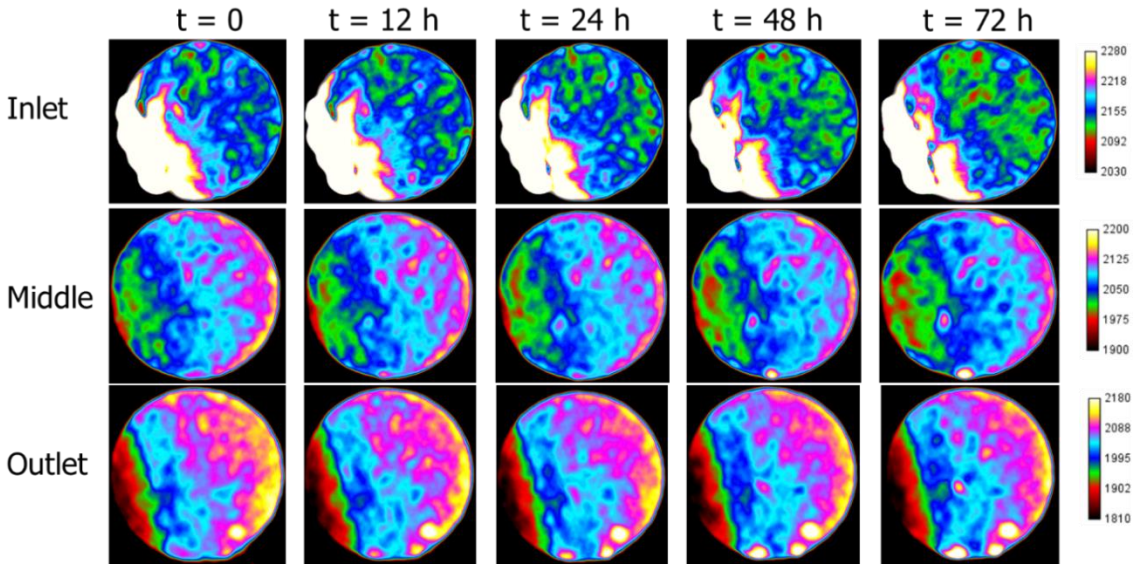

Figure 67 – Time-lapse CT images of three cross-sections (close to the inlet, in the middle of the core, and close to outlet) for gas injection experiment using the mixture of 85% CH_4 and 15% C_2H_6.

In **Fig. 67**, the CT images showed a clear heterogeneity of this core plug. An apparent color change was observed from pink/blue color to blue/green color in the whole core. During the soak period, gas invaded into the core resulting in a density decrease.

Therefore, the time-lapse CT images confirmed that oil was produced from the plug during the experiment.

The image of the produced oil was recorded for this experiment and is shown in **Fig. 68**. The color of the produced oil was lighter than the original Wolfcamp A oil, and it was similar to the color of the produced oil from the CH_4 test. This observation confirms that lighter components of the oil were recovered by the gas injection process.

Figure 68 – Color of produced oil (lighter than original oil) from the mixture of 85% CH_4 and 15% C_2H_6 experiment.

Enriched Gas (50% CH_4 – 50% C_2H_6) Huff-n-Puff Experiment

Enriched gas (50% CH_4 – 50% C_2H_6) Huff-n-Puff experiment was performed to evaluate the effect of ethane enrichment on the oil recovery in the Wolfcamp reservoirs, and the result of this experiment is presented in **Table 15**. After the first Huff-n-Puff cycle (72 h soak time and 3 h production time), the recovery factor of the experiment was 23%

of OOIP, which was much higher than the other two gases. This result proves that 50% ethane enrichment to dry gas can tremendously improve the oil recovery in the Wolfcamp reservoirs. Enriched gas (50% CH_4 – 50% C_2H_6) shows the enormous potential to be the optimum gas composition for gas injection EOR in ULR. In addition, the ultimate oil recovery of the enriched gas test is also investigated, and the recovery factor of each cycle are presented in **Fig. 69**.

Table 15 – Results of the Huff-n-Puff experiment using enriched gas (50% CH_4 and 50% C_2H_6) after the first cycle.

Injection Fluid	Pressure, psi	Temperature, ^oF	Recovery Factor
50% CH_4-50% C_2H_6	5,000	155	23%

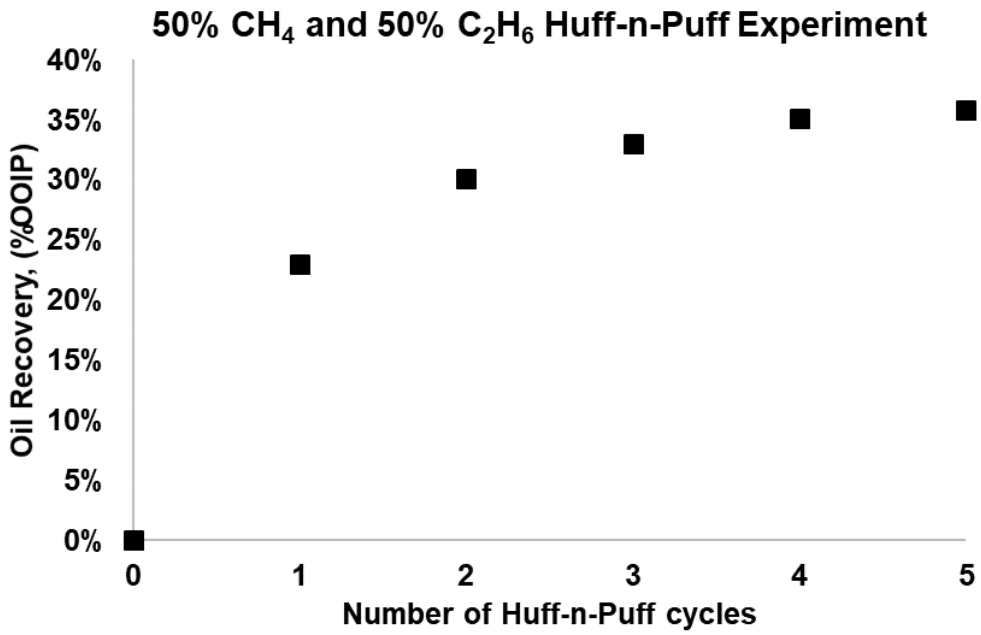

Figure 69 – Recovery factors for the enriched gas test.

The ultimate oil recovery of the enriched gas injection experiment was reached after 5 cycles, which was 36% of OOIP. More than 60% of the ultimate recovery is recovered during the first cycle, indicating that enriched gas injection EOR is a fast process to recover more oil from unconventional reservoirs.

The average CT number change of the entire core throughout the enriched gas injection experiment is 22 HU. It confirms the average CT number change has a positive correlation with the recovery factor for gas injection experiments. Time-lapse CT-scan images of the enriched gas test are presented in **Fig. 70**.

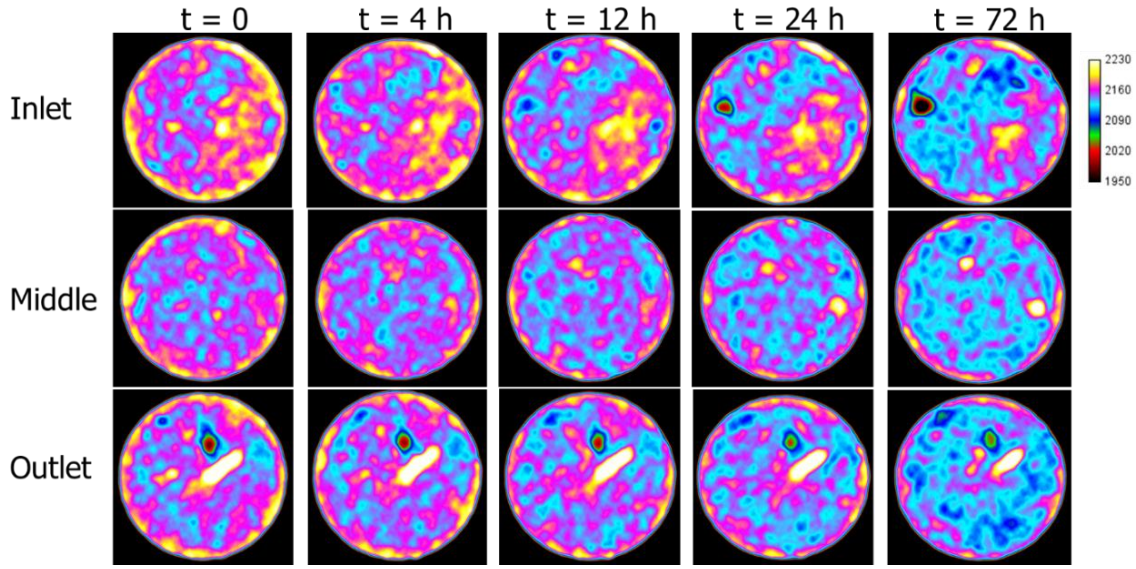

Figure 70 – Time-lapse CT images of three cross-sections (close to the inlet, in the middle of the core, and close to outlet) for gas Huff-n-Puff experiment using the enriched gas.

A more apparent color shift is observed in **Fig. 71**, the color of the entire core changes from a pinkish color to a bluish color. Higher recovery factors result in a stronger

color change in the CT images, demonstrating that CT scan technology not only tracks saturation change during the gas injection experiments but also may validate the recovery factor of those tests.

Figure 71 – Color of produced oil (slightly darker than other produced oil) from the enriched gas test.

The image of produced oil from the enriched gas injection experiment was taken after the test, and the oil is shown in **Fig. 71**. The color of the produced oil from this experiment is also lighter than the color of the original oil, but slightly darker than the oil recovered from the CH_4 and the mixture tests. As the injection pressure is much higher than the MMP, some heavier components of the oil reached the level of miscibility and vaporized into the gas phase.

CO_2 Huff-n-Puff Experiment

CO_2 is a promising EOR agent in ULR based on previous tests through experiments and numerical simulation. The Huff-n-Puff experiment using CO_2 was

performed at 5,000 psi and reservoir temperature 155 ^{o}F to evaluate the recovery performance of CO_2 at high pressure.

The result of the CO_2 test is presented in **Table 16**. After one cycle (72 h soak time and 3 h production time) the recovery factor of the CO_2 test was 9% of OOIP, which was the lowest recovery factor of all gas injection experiments. Because the CO_2 has the lowest MMP compared to the other gases, the recovery factor of this experiment was expected to be higher than that conducted with enriched gas. However, a surprising result was observed from the CO_2 test; the performance of CO_2 injection at 5,000 psi was even lower than that of using CH_4. Then, the ultimate oil recovery of the CO_2 experiment was compared to the ultimate recovery factor of the enriched gas experiment. The recovery factors for the CO_2 injection experiment are plotted in **Fig. 72**.

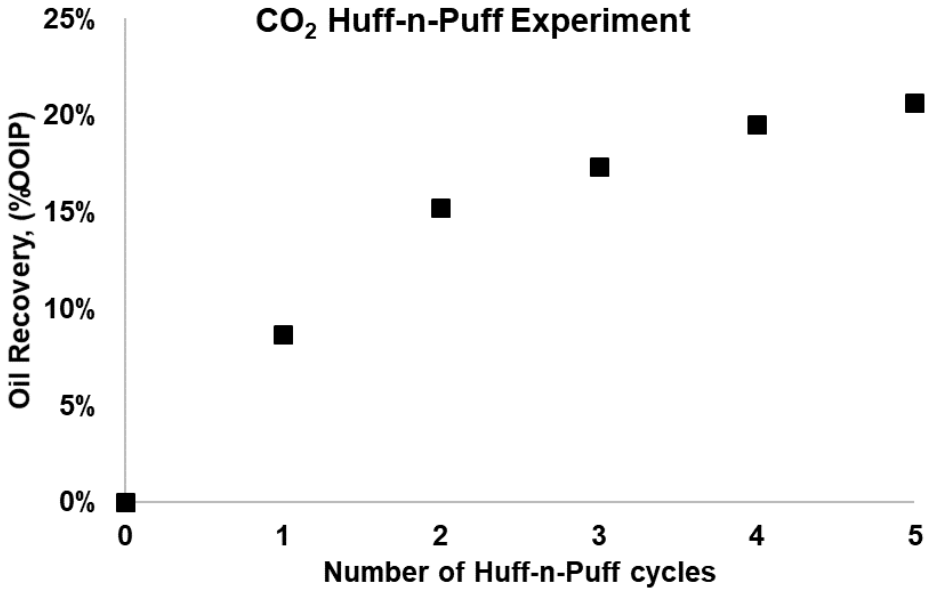

Figure 72 – Recovery factors for the CO_2 injection experiment.

Table 16 – Results of the CO_2 injection experiment and experimental operation conditions.

Injection Fluid	Pressure, psi	Temperature, ^oF	Recovery Factor
CO_2	5,000	155	9%

The ultimate oil recovery of the CO_2 injection experiment was reached after 5 injection/production cycles, and the recovery factor was 21% of OOIP, which was slightly less than the ultimate recovery factor of the mixture (85% CH_4 and 15% C_2H_6) test. In Chapter IV, the ultimate recovery of the CO_2 injection experiment at 3,500 psi was about 50% of OOIP. Then, the recovery factors for all CO_2 injection experiments at various pressures are plotted in **Fig. 73**, and these recovery factors are also listed in **Table 17**.

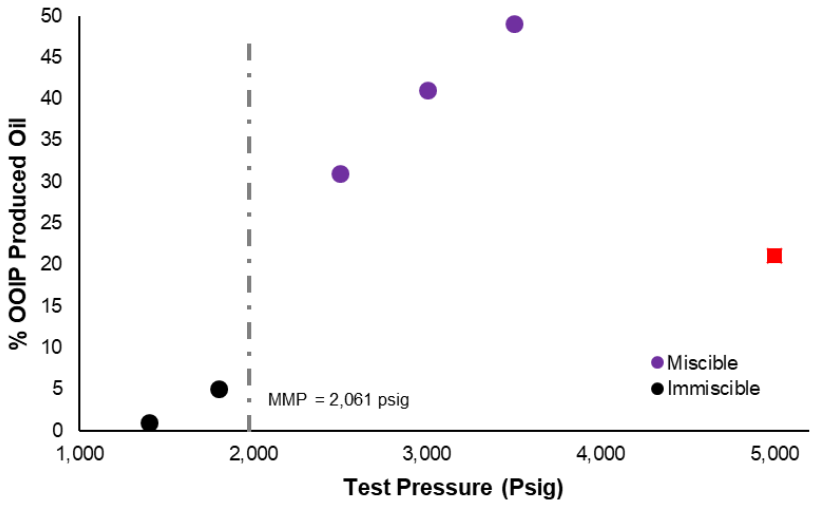

Figure 73 – Ultimate recovery factors for all CO_2 injection experiments at different injection pressures.

A positive correlation of experimental pressure and recovery factors was observed from the previous CO_2 tests. However, the result of the CO_2 experiment at 5,000 psi fails

to follow this trend, indicating higher injection pressure does not always lead to higher oil production enhancement. The optimum pressure of CO_2 injection EOR in ULR is between 3,500 and 5,000 psi based on the laboratory observations. In deep shale reservoirs (depth > 10,000 ft), the pressure of these reservoirs may still be high after four years of oil production. If the injection pressure is 3,500 psi, not enough volume of gas could be injected into those reservoirs to improve oil production from the gas injection process effectively. The corrosion issue of high pressure CO_2, which makes necessary low pressure injection (thus lesser oil yield), and the high cost of CO_2 in a large part of shale plays makes CO_2 an unsuitable choice as an EOR agent in ULR.

Table 17 – Recovery factors of CO_2 injection experiments at different pressures.

Miscibility Status	Test Pressure (psig)	Oil Recovery (% of OOIP)
Miscible	5,000	21
	3,500	49
	3,000	41
	2,500	31
Immiscible	1,800	5
	1,400	1

The average CT number change of the whole core throughout the first cycle of the CO_2 injection experiment is 17 HU, which is higher than the average CT difference of the CH_4 test. Heavier components of the oil were recovered from the CO_2 injection experiment, and the CT number has a positive correlation with density. Although the recovery factor of CH_4 experiments is higher than that from the CO_2 test, the average CT number difference of the CO_2 injection experiment is higher than using CH_4. Because the density of produced oil from the CO_2 injection experiment is larger than the produced oil

of the CH_4 test. In addition, time-lapse CT-scan images of the CO_2 test are presented in **Fig. 74**. The CT images confirmes that oil was extracted from the plug during the CO_2 injection process.

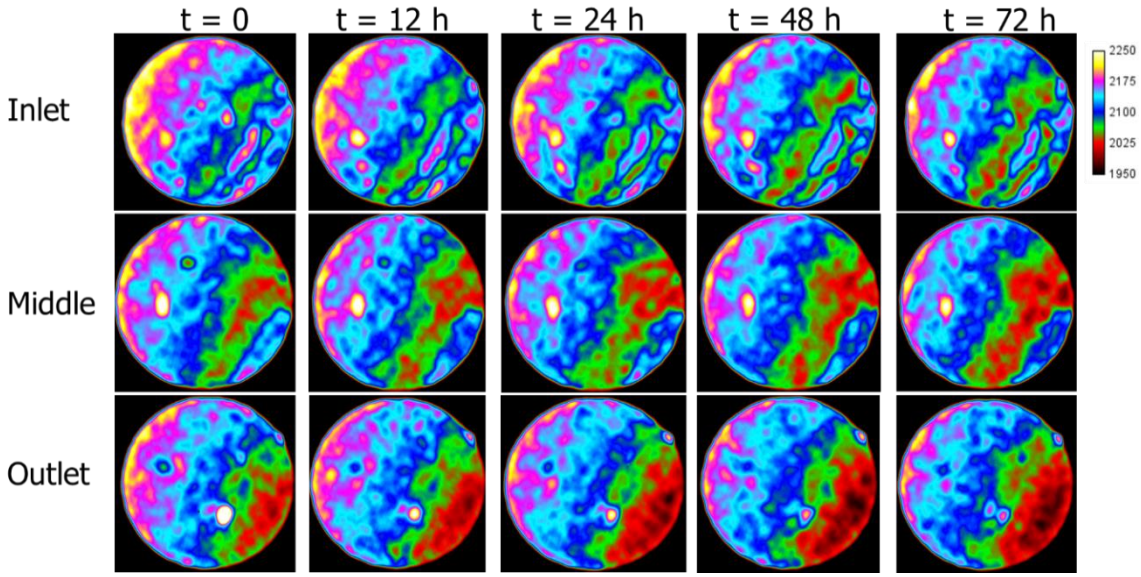

Figure 74 – Time-lapse CT images of three cross-sections (close to the inlet, in the middle of the core, and close to outlet) for the CO_2 test.

An image of produced oil from the CO_2 injection experiment was recorded and presented in **Fig. 75**. The produced oil from the Huff-n-Puff experiment using CO_2 has a darker color than the oil recovered from the other gas injection tests, and it was closed to the color of the original oil sample. This observation indicates that heavier components of the oil were extracted from the core during the CO_2 injection experiment. As described in Chapter V, the recovery mechanism of the gas injection process is multi-contact miscibility. The injection pressure was much higher than the MMP, which means that the majority of the oil components could reach the miscible state when the gas was injected.

As oil was recovered from the outer layer of the core plug, gas may occupy the pore spaces, reducing the effects of the multi-contact process. On the contrary, during the other gas experiments, only the lighter components of the oil vaporized into the gas phase (much lighter color of the produced oil), and this resulted in a smaller gas blockage effect and higher oil recovery. This could explain why the recovery factor of the CO_2 test at 5,000 psi was lower than the recovery factors of the other gas experiments.

Figure 75 – Color of produced oil (darker than all other gas experiments) from the CO_2 test.

Foam Huff-n-Puff Experiment

Injecting foam to improve oil recovery in depleted unconventional reservoirs is a new EOR technique. The main objectives of the foam injection experiments are a) investigating the feasibility of foam injection for improving diversion in ultralow permeability shale reservoirs and b) evaluating the recovery performance of combined the

gas and foam injection in ULR. A novel experimental workflow of foam injection experiments using the Huff-n-Puff protocol on saturated sidewall ULR core plugs was developed to reveal the capability of foam injection EOR in unconventional reservoirs. Two gases (gas (85-15) and enriched gas (50-50) with Surf-B are used in foam tests. Results of the contact angle and IFT measurements using Surf-B are presented in **Fig. 76**. The surfactant additives alter the wettability of rock from intermediate-wet to water-wet and reduce IFT from 18.1 to 1.1 mN/m. It should be emphasized that we are not investigating improvement in diversion, but rather the understanding of displacement efficiency with the combined synergy of both foam and miscible gas.

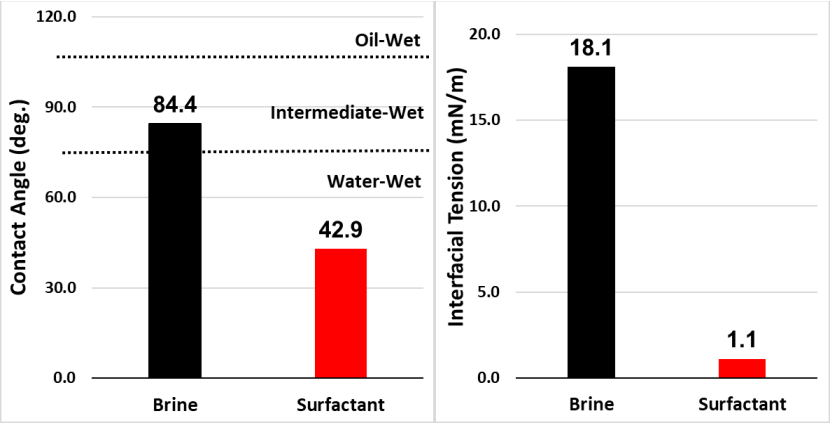

Figure 76 – Contact angle alteration and IFT reduction results using Surf-B at 3 gpt with brine.

It is very challenging to simulate the foam injection process using a Huff-n-Puff protocol at high temperature and pressure in the laboratory, especially the foam experiments that were set up within the CT scanner. A few foam injection tests were

performed using dummy cores to figure out the challenges and risks of foam injection experiments as well as update the experimental workflow.

Hydrate blocking is a serious issue and it is common during foam injection experiments. During preliminary tests, methane hydrates were formed in the lines and the visual cell when the surfactant solution and gas were co-injected into the lines at the room temperature. A picture of the methane hydrates formed in the visual cells is presented in **Fig. 77**. The foam injection experiment had to be stopped since the lines were completely plugged. To solve the hydrate problem and to be able to perform the final experiments, heating tapes were wrapped around all the lines and the visual cell to keep them at high temperature to dissolve the methane hydrates. After addressing all the issues, foam injection experiments using saturated cores were performed to assess the efficiency of the foam injection process on oil production improvement in the Wolfcamp formation.

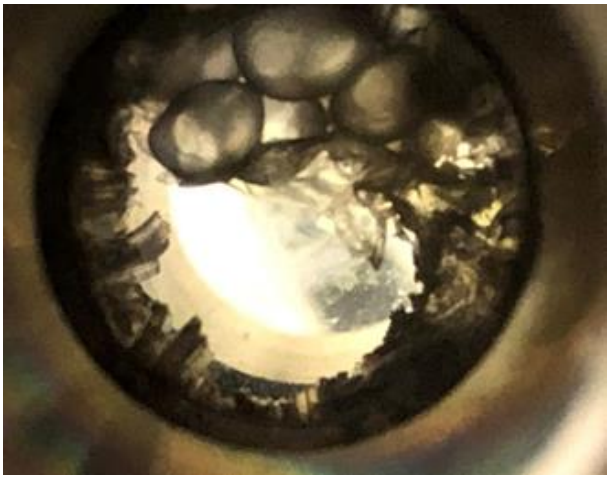

Figure 77 – Methane hydrates formed inside the visual cell during the foam injection preliminary test.

Foam-1 (Surf-B+ A Mixture of 85% CH_4 and 15% C_2H_6) Experiment

Foam-1 Huff-n-Puff experiment was performed 5,000 psig and reservoir temperature 155 ^oF following the comprehensive experimental workflow. The gas mixture of 85% CH_4 and 15% C_2H_6 and Surf-B were co-injected into the core holder at 13.9 ml/min and 5.9 ml/min, respectively, which corresponded to a 70% gas/liquid ratio. The result of the foam-1 Huff-n-Puff experiment is presented in **Table 18**. The time-lapse CT-scan images of three different cross-sections of the core plug and the glass beads in the foam-1 injection experiment are shown in **Fig. 79** - **Fig. 80**. In addition, the color of the produced oil from the foam-1 test is depicted in **Fig. 81**.

The recovery factor of the foam-1 injection experiment was 12.8% of OOIP, which was similar to the recovery factor obtained from the pure gas injection experiment using the same gas mixture (85% CH_4 and 15% C_2H_6) which was 13% of OOIP. The oil recovery was determined with some degree of uncertainty due to some residual oil left in the glass beads. This is a pessimistic recovery factor due to residual oil retained in the glass beads. **Fig. 78** shows a picture of the glass beads after the core holder was disassembled. Considering this residual oil, the actual recovery factor of the foam-1 experiment should be higher than that from the corresponding gas injection test. These observations confirm the potential of foam injection as an EOR method for unconventional reservoirs. Furthermore, foam could control mobility and could reduce the out of zone injection problems, making it more attractive than the pure gas injection.

Table 18 – Results of foam-1 Huff-n-Puff experiment using the gas mixture of 85% CH_4 and 15% C_2H_6 and Surf-B.

Injection Fluid	Pressure, psi	Temperature, ^oF	Recovery Factor
Surf-B and 85% CH_4-15% C_2H_6	5,000	155	12.8%

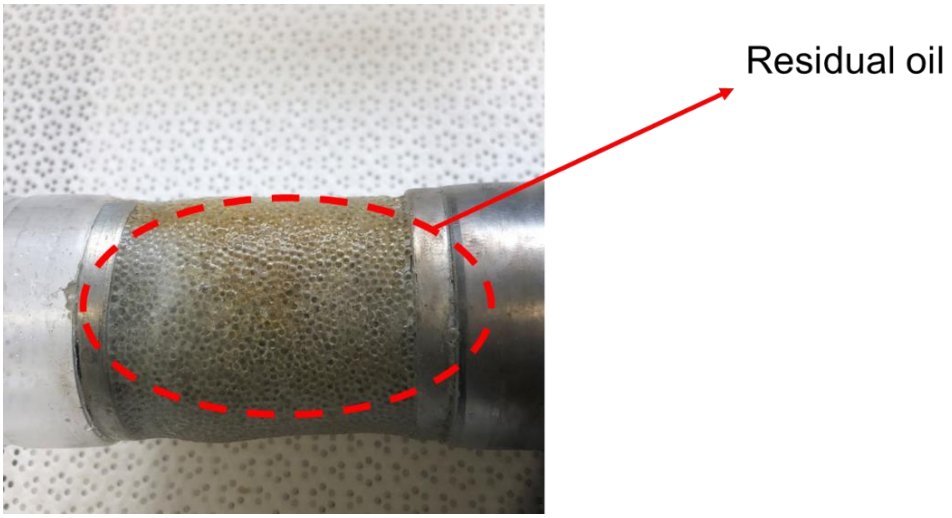

Figure 78 – Residual oil in glass beads for foam-1 Huff-n-Puff experiment.

Fig. 79 shows the CT images of the glass beads in the initial stages of the foam test (within 12 h). The first column (t = 0 gas) shows CT images of the glass beads invaded by pure gas (85-15) before the foam was injected in the core holder at 5,000 psi. The second column (t = 0 foam) presents CT images of three different positions in the glass beads when the foam was initially injected in the core holder. Columns 3 to 5 show the CT change during the first 12 h of soaking. It is possible to see that the foam was successfully injected and filled the core-holder by comparing the CT images in the first two columns. When the foam collapsed, gravity segregation was observed, resulting in the CT number decreasing on the top part of the glass beads (filled with gas) and increased in the bottom part (filled with liquid).

The preliminary foam quality test indicates the foam lasts 30 min to 1 hour at 2,000 psi and room temperature. Surprisingly, most of the foam still existed in the glass beads within the first 12 h of foam test. The foam tends to be more stable in the glass beads under pressure indicating a longer duration of foam in propped fractures.

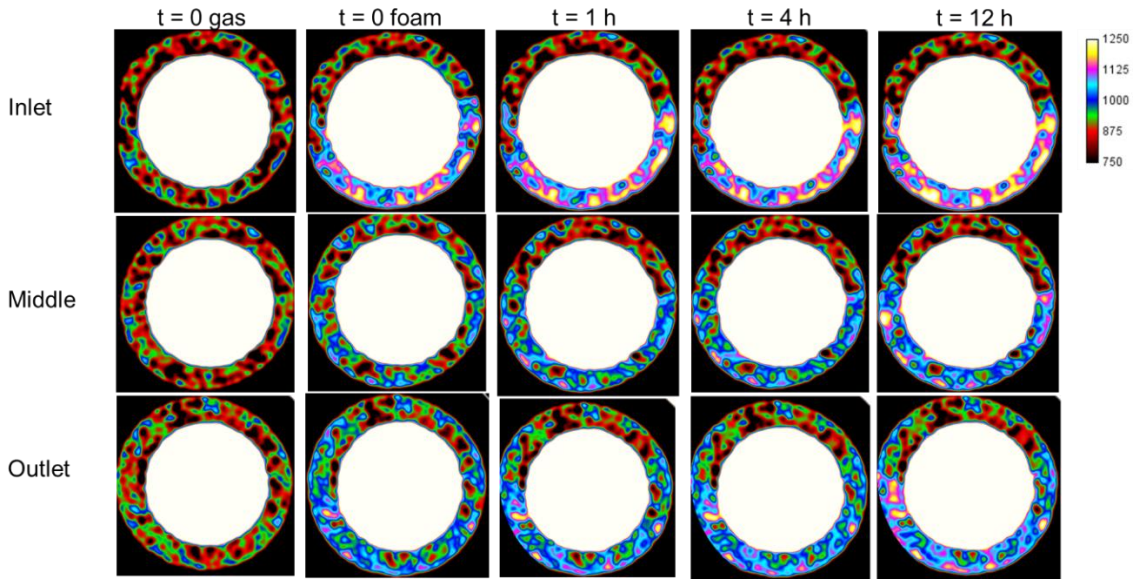

Figure 79 – Time-lapse CT images of three cross-sections (close to the inlet, in the middle of the core, and close to outlet) of the glass beads during first 12 h of the foam-1 Huff-n-Puff experiment.

Fig. 80 shows the CT images of the glass beads throughout the whole experiment. An apparent color change from blue to almost white was observed in the bottom half of the glass beads; this indicated a density increase in the fluid occupying the bottom half of the glass beads, especially after 24 h. We could deduct that the half-life of the foam used in this experiment at 5,000 psi was approximately 24 h. In addition, time-lapse CT images

confirmed that the CT scanner was capable of tracking phase separation during the foam collapse process.

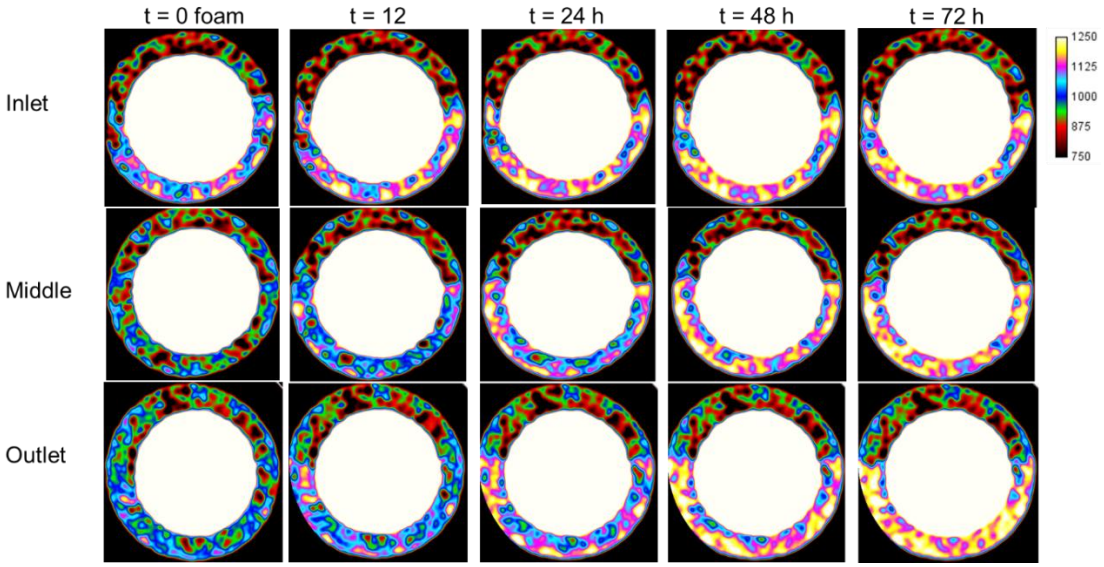

Figure 80 – Time-lapse CT images of three cross-sections (close to the inlet, in the middle of the core, and close to outlet) of the glass beads during the foam-1 Huff-n-Puff experiment.

Fig. 81 shows the CT images of the core plug throughout the test. The average CT number change of the entire core plug was 4 HU, which was significantly smaller than the one obtained for the corresponding gas injection experiment. This was due to the competing water imbibing, which increases the CT number as opposed to gas penetration which lowers the CT number. The small average CT number change was manifested by the small color shift in the CT images. The small average CT number change justified the little color shift in the CT images of **Fig. 81**.

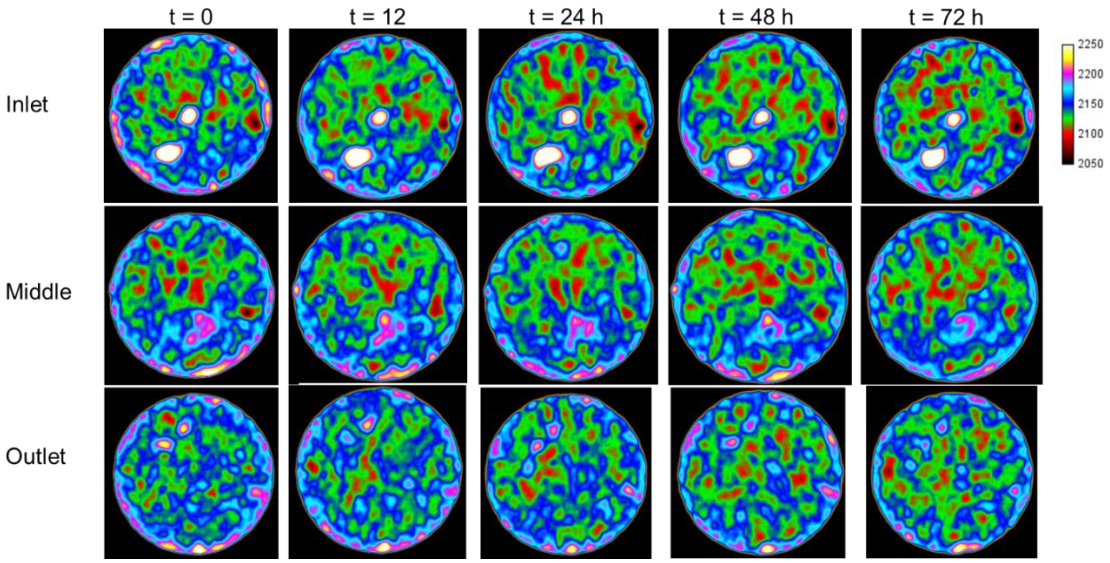

Figure 81 – Time-lapse CT images of three cross-sections (close to the inlet, in the middle of the core, and close to outlet) of the core during the foam-1 test.

The color of the produced oil was lighter than the original color of the Wolfcamp A oil, and it was similar to the produced oil from the corresponding gas test. However, darker oil was observed in the glass beads after the test, as shown in **Fig. 82**. These observations indicate that heavier components of the oil were recovered from the rock submerged in the surfactant solution, and the oil was trapped in the aqueous phase. Lighter components of the oil vaporized from the top half of the core and were produced with the gas. This indicated foam injection is a combination of chemical and gas injection EOR with the mechanisms of wettability alteration and multi-contact miscibility.

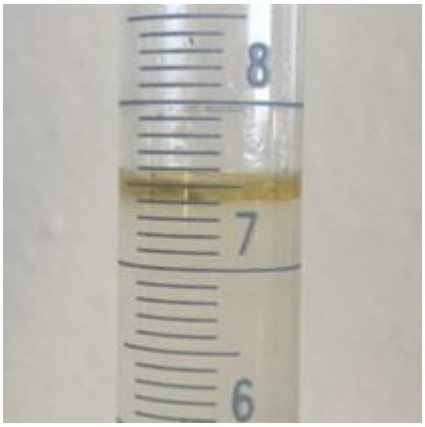

Figure 82 – Color of produced oil from the foam-1 test. The color is similar to the oil produced in the corresponding gas test.

Foam-2 (Surf-B+ Enriched Gas (50% CH_4 and 50% C_2H_6)) Experiment

In the Foam-2 Huff-n-Puff experiment, enriched gas (50% CH_4 and 50% C_2H_6) and Surf-B were co-injected into the core holder at 13.9 ml/min and 5.9 ml/min, respectively, which corresponded to a 70% gas/liquid ratio. The result of the foam-2 injection experiment is listed in **Table 19**. The time-lapse CT-scan images of three different cross-sections of the glass beads and the core plug are shown in **Fig. 84** and **Fig. 85**. In addition, the color of the produced oil from the foam-2 injection experiment is shown in **Fig. 86**.

Table 19 – Results of foam-2 Huff-n-Puff experiment using the enriched gas (50% CH_4 and 50% C_2H_6) and Surf-B.

Injection Fluid	Pressure, psi	Temperature, ^oF	Recovery Factor
Surf-B and 50% CH_4-50% C_2H_6	5,000	155	19.2%

The recovery factor of the foam-2 injection experiment increased to 19.2% of OOIP compared to the recovery factor of 12.8% from the foam-1 test. The injected gas composition dominated the ultimate recovery of foam injection experiments, and the enriched gas (50% CH_4 and 50% C_2H_6) having better performance on gas injection tests on ULR cores resulted in higher ultimate recovery factor of foam injection experiments. Furthermore, the recovery factor of the foam-2 test was smaller than the recovery factor of 23% obtained during the no-foam, enriched gas (50-50) experiment. Compared to the pure gas tests, however, the foam-2 experiment recovered darker oil which indicated that a larger number of oil components were recovered during the process. Considering the effect of foam on mobility control and out of zone injection elimination, the foam-2 could outperform the pure gas injection process in ULR.

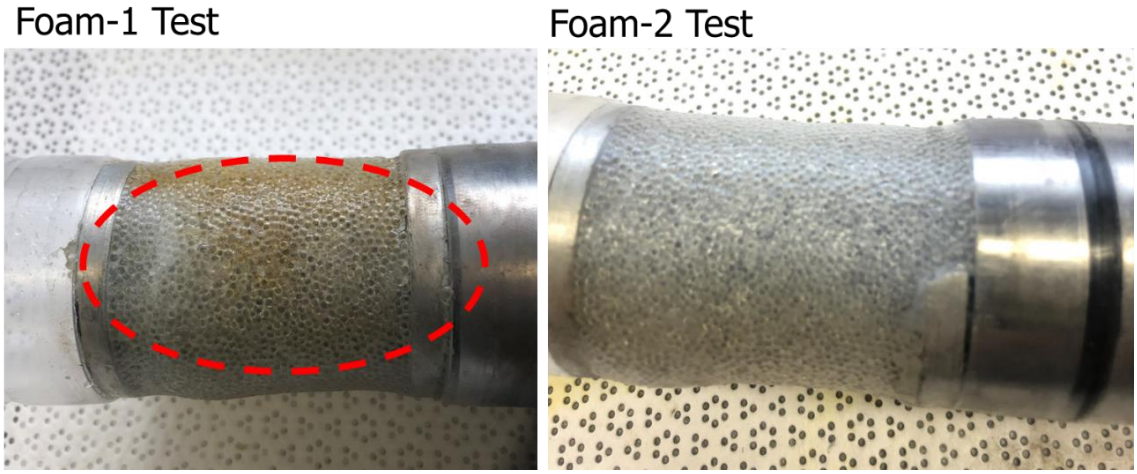

Figure 83 – Comparison of the glass beads for the foam-1 and foam-2 tests after disassembling the core holder.

Fig. 83 compares the glass beads for the foam-1 and foam-2 tests after disassembling the core holder. The residual oil was found in the glass beads only after the foam-1 injection experiment, while the second test did not show any trapped oil. The main difference between the foam-1 and foam-2 tests was the gas composition that the fraction of ethane in enriched gas (50-50) is higher than gas (85-15). The supercritical enriched gas (50-50) may have a better potential to access the oil trapped in the glass beads and to displace oil to the outlet.

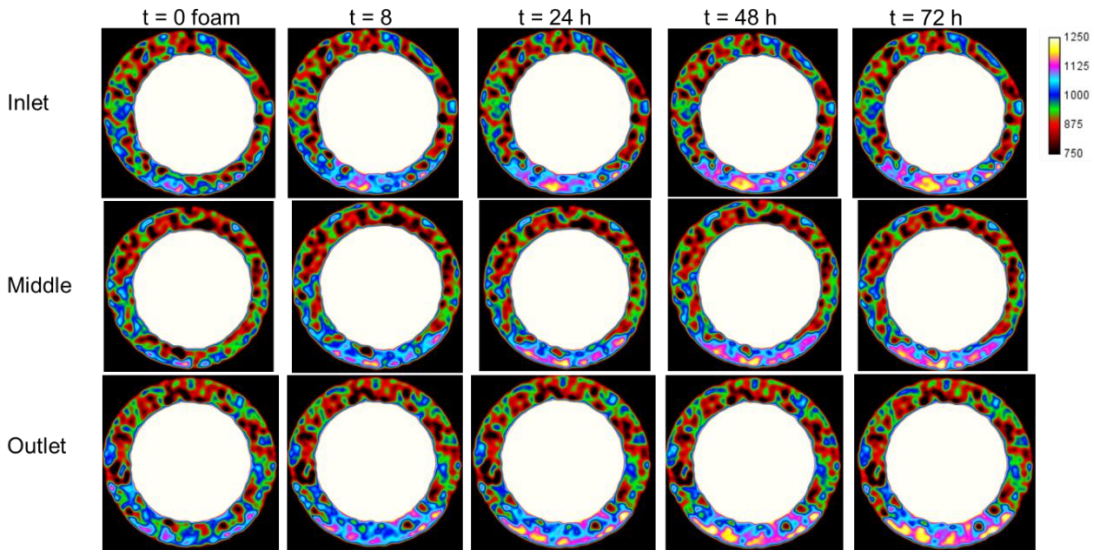

Figure 84 – Time-lapse CT images of three cross-sections (close to the inlet, in the middle of the core, and close to outlet) in the glass beads during the foam-2 Huff-n-Puff experiment.

Fig. 84 shows the CT images of the glass beads during the foam-2 experiment. The foam was successfully injected and filled the core-holder. An apparent color change from blue to bright white is observed at the bottom part of the glass beads, indicating that the foam collapsed after some time, leaving behind the aqueous phase. The half-life of the

foam-2 at 5,000 psi was also over 24 h, indicating the enriched gas (50-50) and the selected surfactant generated high quality foam. In addition, clear phase separation was observed in the glass beads during the soak period, with liquid occupying the bottom quarter of the glass beads.

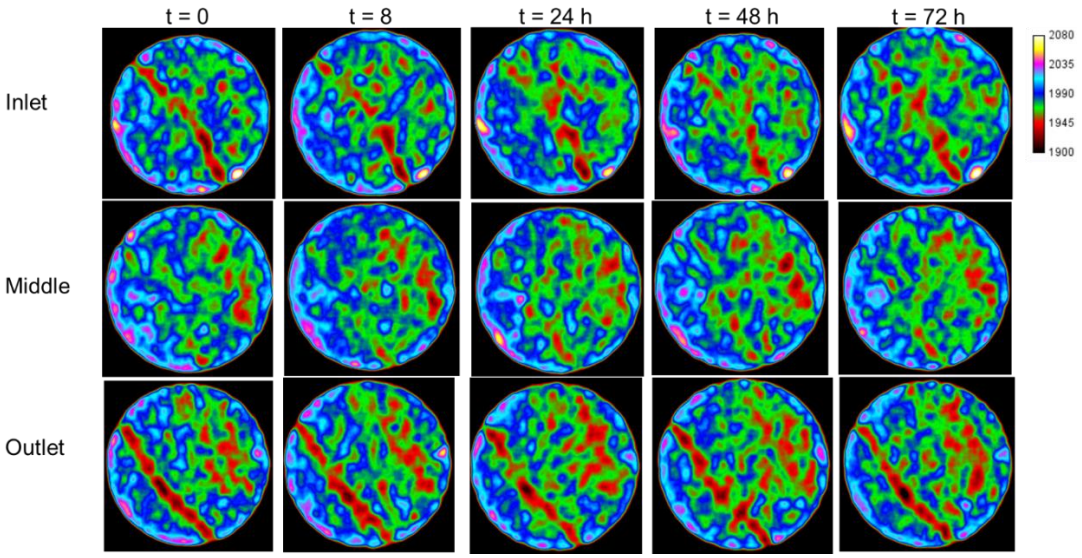

Figure 85 – Time-lapse CT images of three cross-sections (close to the inlet, in the middle of the core, and close to outlet)of the core during the foam-2 Huff-n-Puff experiment.

Fig. 85 shows the CT images of the core plug throughout the foam-2 experiment. The average CT number change of the core plug throughout the foam-2 injection experiment was 3 HU, which was smaller than that of the previous test. Brine spontaneous imbibition process and multi-contact miscibility process co-occurred during the foam injection experiments. As brine imbibed into the core plug, the average CT number of core increased. On the contrary, the average CT number decreased as the gas dissolved into the oil phase. Smaller average CT number change indicated that more brine imbibed into the

core plug during the foam-2 experiment compared to the foam-1 test. A strong color shift of the core was not observed from the time-lapse CT images during the foam-2 injection experiment.

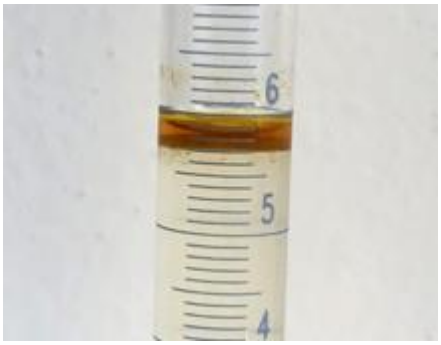

Figure 86 – Color of the produced oil (darker color than the corresponding gas test) from the foam-2 test.

The color of the produced oil, as shown in **Fig. 86**, is darker than the color of the produced oil from the corresponding enriched gas test. In Chapter VI, the color of produced oil from imbibition tests is much darker than the oil produced from gas injection experiments. As demonstrated previously, the spontaneous imbibition process and multi-contact miscibility process co-occur during the foam injection experiment. Heavier components of the oil were recovered through the imbibition process, and lighter components of the oil were extracted through the multi-contact miscibility process.

In order to compare the production behavior of the gas and the foam injection processes, the normalized average CT number change during gas and foam tests were plotted and analyzed. The slope of the normalized CT number curve represented the production rate, and a larger slope corresponded to a higher oil production rate.

Normalized average CT number curves of pure gas experiments (using CH_4, enriched gas (50-50), and CO_2) have a similar pattern (as shown in **Fig. 87)** that the recovery rate gradually decreases during gas injection experiments. This observation indicates that the gas injection process (regardless of gas composition) has a general normalized recovery rate curve.

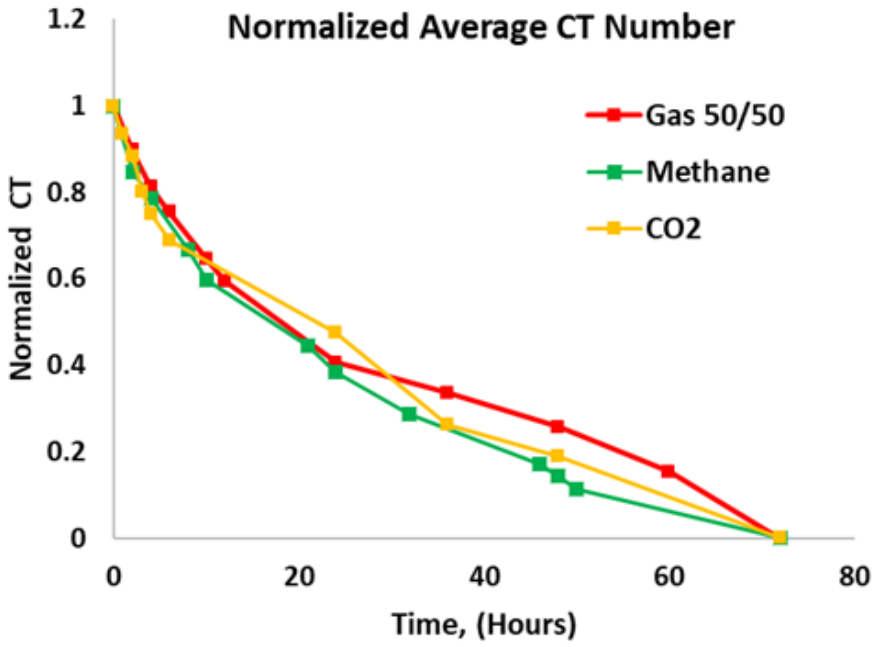

Figure 87 – The normalized average CT number change for pure gas experiments (using CH_4, enriched gas (50-50), and CO_2).

To systematically analyze the efficiency of foam-1 and foam-2 injection processes, the normalized average CT number curves were plotted for the CH_4, enriched gas (50-50), CO_2, foam-1, and foam-2 experiments in **Fig. 88** and **Fig. 89**, respectively. The time lapse

CT images of the glass beads during the two foam tests were also plotted in the corresponding figure.

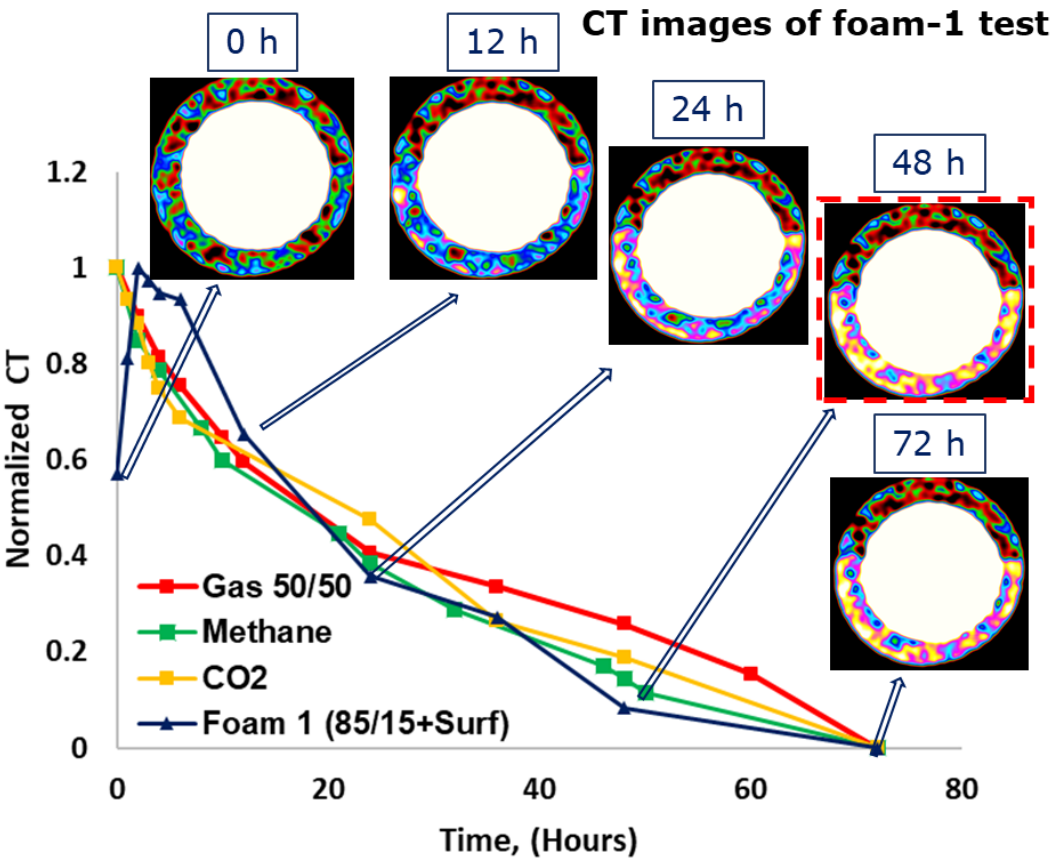

Figure 88 – The normalized average CT number curves during the CH_4, enriched gas, CO_2, and foam-1 Huff-n-Puff experiments and the time lapse CT images of the glass beads for the foam-1 test.

In **Fig. 89,** the slope of normalized average CT number curve for foam-2 test is larger than other curves. It is possible to observe that the recovery rate of the foam-2 injection experiment was larger than the rate of all pure gas injection tests during the first 20 h. This observation indicates that the foam injection process could recover most of the

oil in a shorter time compared to the gas injection process. On the other hand, the recovery rate of the foam-1 test is similar to gas injection experiments.

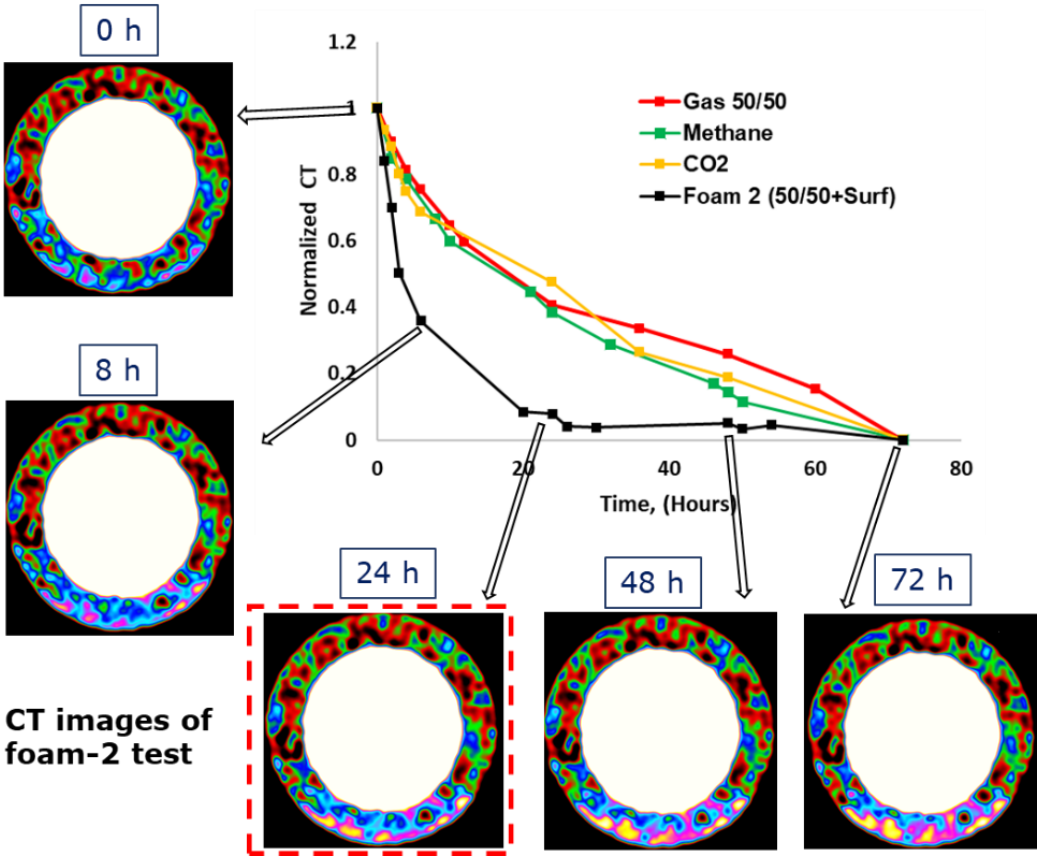

Figure 89 – The normalized average CT number curves during the CH_4, enriched gas, CO_2, and foam-2 Huff-n-Puff experiments and the time lapse CT images of the glass beads for the foam-2 test.

Fig. 88 and **Fig. 89** shows that most of the foam collapsed within 48 h during the foam-1 experiment based on the CT images of the glass beads. In addition, the foam lifetime of the foam-2 experiment was 24 h. The normalized average CT number of the two foam experiments reached almost zero when all the foam collapsed (foam-1 test at 48 h and foam-2 test at 24 h), indicating that the average CT number of the foam test ceased

to decrease when most of the foam collapsed. This observation demonstrates that the foam lifetime could affect the effectiveness of the foam injection processes on improving oil recovery.

In addition, the normalized average CT number curve of the foam-1 experiment was similar to all pure gas injection tests, demonstrating that the dominant recovery mechanism of foam-1 experiment is multi-contact miscibility, which is the same to gas tests. However, the foam-2 possess showed a different curve shape compared to the other tests. Foam injection using enriched gas (50-50) was a fast process and recovered most of the oil within 24 hours. Considering the color of the produced oil from the foam-2 test, heavier components were recovered during the foam-2 Huff-n-Puff experiment. These observations indicate that the recovery mechanisms of the foam-2 test are the combination of the recovery mechanisms of the gas injection and surfactant EOR. A proper foam generation formula is essential to improve oil recovery significantly and speed up this enhanced oil recovery process efficiently.

Color of the Produced Oil

Fig. 90 presents the color of the produced oil from all four gas Huff-n-Puff experiments after the first cycle (72 h soak and 3 h production). The oil recovered from the CO_2 injection experiment was darker than the oil produced from all the other gas experiments, indicating that heavier components of the oil were extracted from the core by the high pressure CO_2. The oils produced from the pure gas test using CH_4 and gas (85-

15) had a similar color (light yellow), and the colors of these oils were much lighter than the original oil. This observation demonstrates that only the lighter components were recovered by the gas injection process because the injection pressure was around the MMP. In addition, the color of the produced oil from the enriched gas experiment was slightly darker than the oil recovered from the CH_4 and the mixture tests. Some heavier components of the oil reached the miscible condition through the multi-contact miscibility process and consequently were collected in the graduated cylinder. In this case, the injection pressure (5,000 psig) was much higher than the MMP (2,853 psig) measured between the enriched gas and the Wolfcamp oil.

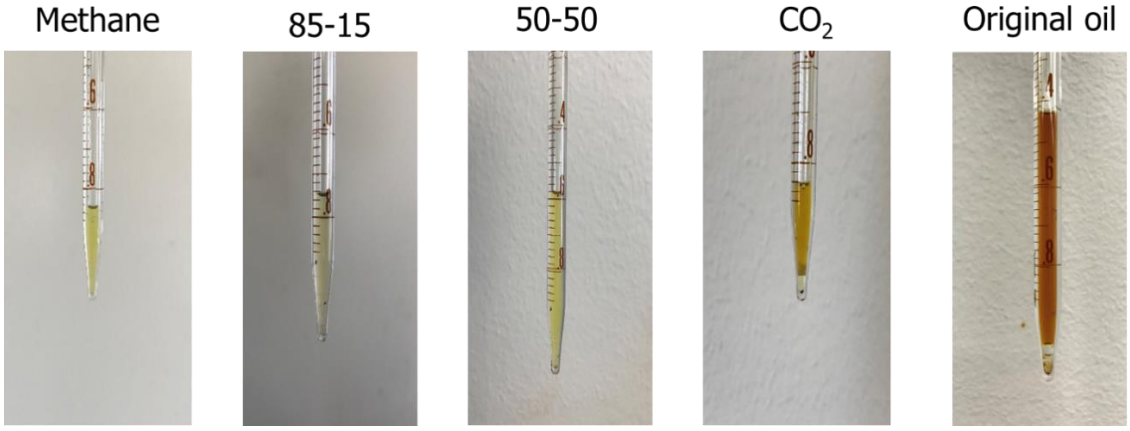

Figure 90 – The color of produced oil from all four gas Huff-n-Puff experiments. Gas 85/15 refers to the gas mixture of 85% CH_4 and 15% C_2H_6, Gas 50/50 refers to enriched gas (50% CH_4 and 50% C_2H_6), and original Wolfcamp oil.

The color of the oil produced from the foam injection experiments and the corresponding pure gas tests is presented in **Fig. 91**. The oil produced from the foam-1 experiment had a similar color to the oil produced from the gas mixture (85% CH_4 - 15%

C_2H_6) experiment. On the contrary, the oil produced from the foam-2 test was much darker than the oil produced from the enriched gas (50% CH_4 - 50% C_2H_6) Huff-n-Puff experiment. The foam-2 generated from enriched gas (50% CH_4 - 50% C_2H_6) and Surf-B recovered heavier hydrocarbon components through the Huff-n-Puff experiments.

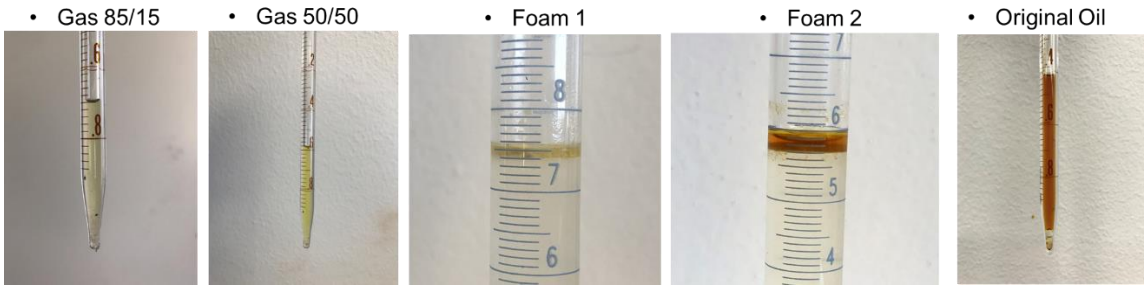

Figure 91 – The color of produced oil from foam Huff-n-Puff experiments and the corresponding gas experiments. Gas 85/15 refers to the gas mixture of 85% CH_4 and 15% C_2H_6, and Gas 50/50 refers to enriched gas (50% CH_4 and 50% C_2H_6).

Summary of Laboratory Experiments

The results of all Huff-n-Puff experiments are presented in **Table 20**. The highest recovery factor was achieved from the enriched gas (50% CH_4 - 50% C_2H_6) Huff-n-Puff experiment and was equal to 23% of OOIP. Surprisingly, even if the MMP of CO_2 – Wolfcamp oil was the lowest, the recovery factor of the CO_2 experiment was the lowest of all the gas-related Huff-n-Puff tests.

Chemical injection showed the great potential of improving oil recovery in unconventional liquid reservoirs. A proper surfactant formulation is required to effectively improve the EOR effect through wettability alteration and IFT reduction. Surfactants can

be implemented into completion fluids, injection fluid, and foam generation to boost production in new drilling wells and as remediation of existing depleted wells. In addition, heavier components of crude oil can be recovered from chemical EOR methods using surfactant additives.

Table 20 – Results of all Huff-n-Puff experiment (one cycle) performed at 5,000 psi and reservoir temperature of 155 ºF.

Injection Fluid	Recovery Factor	Ave. CT No. Change (HU)
Brine	6.9 %	0
Surf – B	12.3%	0
Surf – F	14.4%	0
CH_4	9.7%	14
85% CH_4-15% C_2H_6	13%	18
50% CH_4-50% C_2H_6	23%	22
CO_2	9%	17
Surf-B and 85% CH_4-15% C_2H_6	12.8%	4
Surf-B and 50% CH_4-50% C_2H_6	19.2%	3

Based on the observations of pure gas experiments, the injection pressure should be higher than the MMP to improve oil production in ULR significantly. However, injecting at very high pressure may have detrimental effects on the oil recovery, as shown in the CO_2 experiment. The MMP for the crude oil and CO_2 is 2,061 psi, and the Huff-n-Puff experiment is performed at a much higher pressure (5,000 psi). Surprisingly, even if the high pressure CO_2 could recover heavier components of the oil, the ultimate oil recovery was less than all the other pure gas tests. Generally, the gas injection EOR

technique has a better performance in improving oil production than chemical EOR methods in ULR. The optimum gas composition for gas injection EOR in the Wolfcamp reservoir is the enriched gas (50% CH_4-50% C_2H_6).

The results of the foam tests proved the feasibility of the foam injection EOR method in ULR and demonstrated that additional oil could be produced by this new technique. As the foam interacts with the reservoir rock, the imbibition process and gas vaporization process co-occur to expel oil from the matrix. Foam can be used as a mobility control agent, to improve the relative permeability, and to eliminate the out of zone injection. Injecting foam can further improve the oil recovery in ULR compared to the corresponding pure gas injection and opens the possibility of achieving optimum oil recovery for depleted well in ULR.

Core-Scale History Match

Laboratory-scale simulation models were developed to determine the upscaling parameters of the chemical, gas, and foam Huff-n-Puff experiments. Core-scale modeling followed the same simulation workflow, as described in Chapter III. The CT-Scan images of each core plug used in the tests were converted into porosity and permeability distribution and assigned to the grids for the numerical simulator. The upscaling parameters for each EOR method were determined by history matching the Huff-n-Puff experimental data.

Fig. 92 presents a comparison between the core-scale model and the 3D CT image of the rock samples. Capillary pressure and relative permeability curves of both the base case (brine) and the surfactant cases were generated and implemented to the core-scale simulation models for chemical injection experiments. The history match process of the chemical tests using surfactants was performed on the laboratory-scale model. In the core-scale history match of gas Huff-n-Puff experiments, the diffusion coefficients of gases and oil pseudo-components were modified to match the experimental results. All the upscaling parameters achieved from the core-scale history match of chemical and gas injection tests were implemented in the foam simulation model. These scaling parameters were verified by matching the results of the foam tests with the co-injection of surfactant solution and gas.

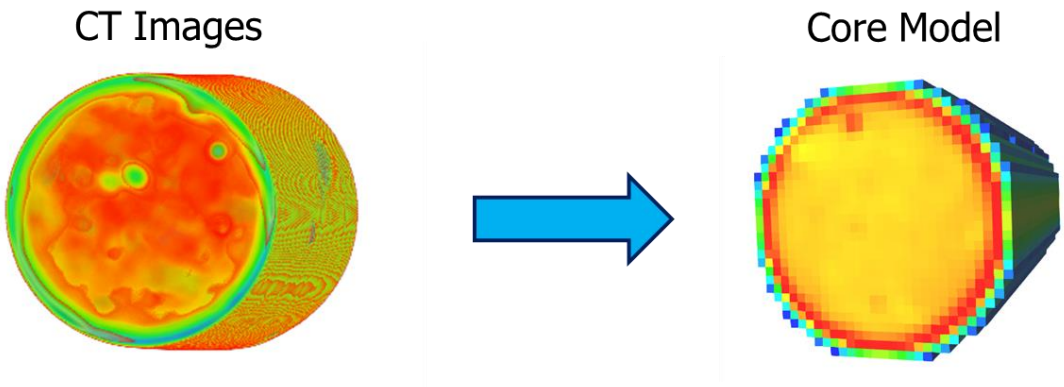

Figure 92 – Converting CT images of the core-plug to digiting the core-scale grid model.

Core-Scale History Match of Chemical Huff-n-Puff Experiments

Simulation results from the core-scale history match of surfactant experiments are presented in **Fig. 93** – **Fig. 95**. The layout of each sub-figure follows history match laboratory data on the left, relative permeability curves in the middle, and capillary pressure curves on the right.

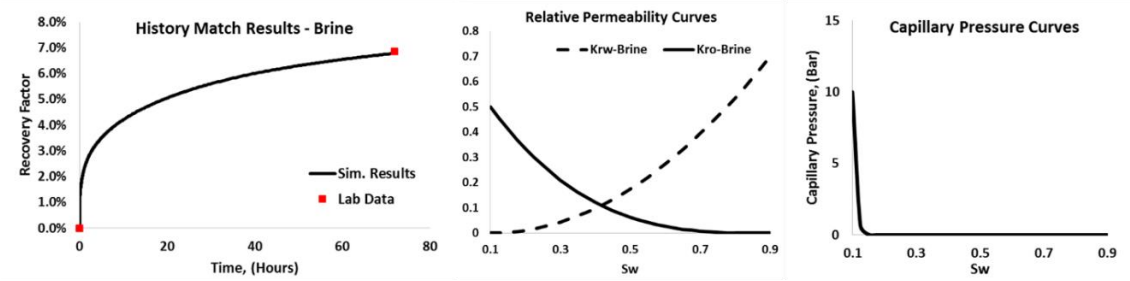

Figure 93 – Best history match results (left), corresponding relative permeability curves (middle), and capillary pressure curves of brine base case.

The simulation results of all three cases agreed with the experimental results of chemical Huff-n-Puff tests using surfactants and brine alone. As shown in **Fig. 93**, the intersection point of the oil and water relative permeability curves is located in the intermediate/oil-wet zone, and the positive capillary pressure range is very narrow because the initial wettability of the rock samples is intermediate-wet. Adding both types of surfactants (Surf-B and Surf-F) to the brine solution resulted in an increment of the capillary pressure curve due to wettability alteration. In addition, the saturation endpoint of the capillary pressure curve was also shifted to the right, spreading the capillary pressure to a broader range of water saturation. The oil relative permeability of the surfactant case

was significantly higher than the base case, while the opposite behavior was displayed for the water relative permeability curve.

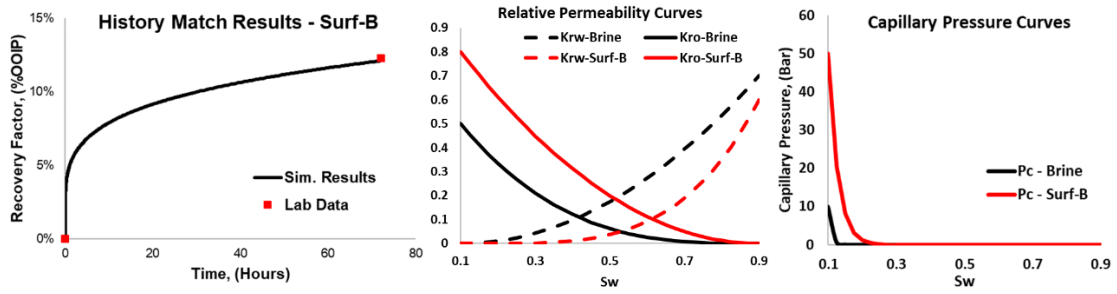

Figure 94 – Best history match results (left), corresponding relative permeability curves (middle), and capillary pressure curves of the chemical test using Surf-B.

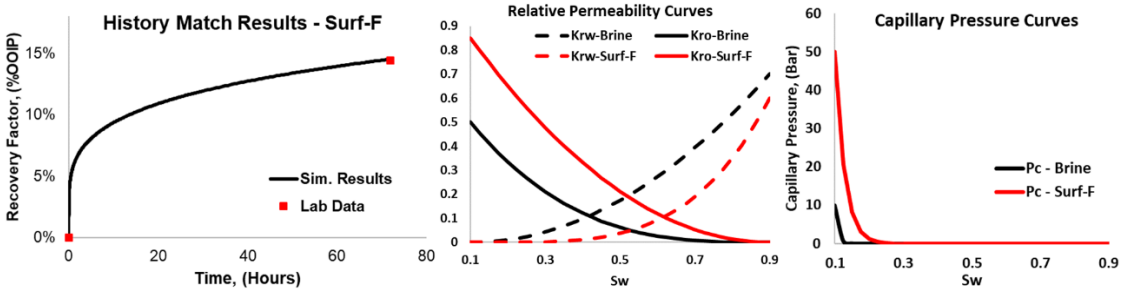

Figure 95 – Best history match results (left), corresponding relative permeability curves (middle), and capillary pressure curves of the chemical test using Surf-F.

As the rock surface was altered to water-wet, the flow of water across the rock was hindered, resulting in a lower water relative permeability. On the contrary, oil relative permeability was improved by wettability alteration. Although IFT reduction led to an increase in the relative permeability, the effect of IFT reduction on the relative permeability was negligible compared to the impact of wettability alteration.

Core-Scale History Match of Gas Huff-n-Puff Experiments

The history-match of the gas injection experiments was performed on the core-scale model, which was constructed based on each core plug following the same gas injection simulation workflow. In the core-scale models, the injection pressure, the soak time, the production time, and the dimensions were all the same as for the gas injection experiments. Due to the limitations of the simulator, there was no available function to tune the effect of multi-contact miscibility. For the gas injection experiments, the diffusion coefficient was chosen as the dominant variable to history match the laboratory data. The history match results of all pure gas experiments are presented in **Fig. 96**.

History match results decently agreed with the experimental data of all gas tests. The consistency of the simulation results with the experimental results demonstrated that the diffusion coefficient was a good parameter for representing the effect of the gas injection on improving oil recovery in ULR. As demonstrated in Chapter V, the diffusion coefficient from the history match results combined the impact of Fick's law defined diffusion and multi-contact miscibility process. The dominant mechanism of gas injection EOR is multi-contact miscibility. The diffusion coefficients of each component are listed in **Table 21** and were applied to the foam core-scale model.

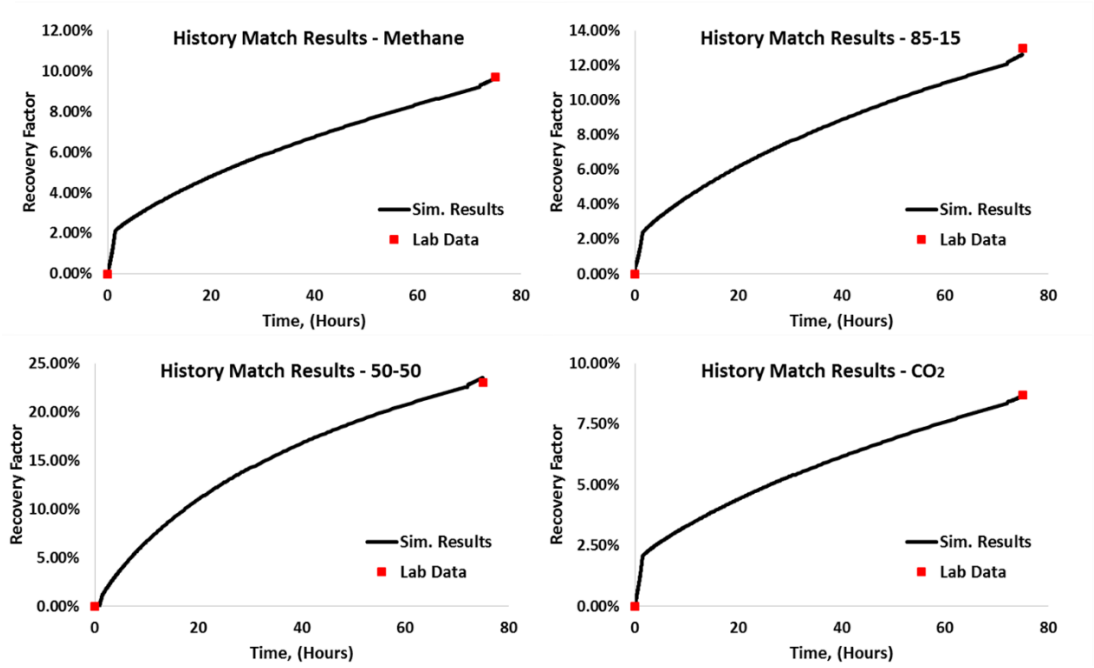

Figure 96 – History match results of all gas experiments. 85-15 refers to the gas (85-15) and 50-50 refers to enriched gas (50-50).

Table 21 – Diffusion coefficient of each composition from history matching results.

COMPONENTS						
CO_2	C1	C2	C3-C6	C7-C11	C12-C17	C18+
DIFFUSION COEFFICIENT OF GAS PHASE (1 cm^2/s)						
6.00E-05	6.50E-05	7.50E-04	1.50E-05	5.00E-06	5.00E-06	2.50E-06
DIFFUSION COEFFICIENT OF OIL PHASE (1 cm^2/s)						
5.00E-05	6.00E-05	7.00E-04	1.00E-05	6.50E-06	4.50E-06	1.00E-06

Core-Scale History Match of Foam Huff-n-Puff Experiments

Two foam injection experiments were performed at 5,000 psi and reservoir temperature 155 ^oF using the gas (85-15) and enriched gas (50- 50) with Surf-B.

The capillary pressure and relative permeability curves used in core-scale history match of foam tests were achieved from the chemical experiment history match results. Also, the diffusion coefficients of all the components, obtained from gas injection simulation results, were implemented to the foam scale-scale simulation. Gases and Surf-B were co-injected with the same rate as the foam tests into the core holder at 13.9 ml/min and 5.9 ml/min, respectively. The best history match results of both foam tests are presented in **Fig. 97**.

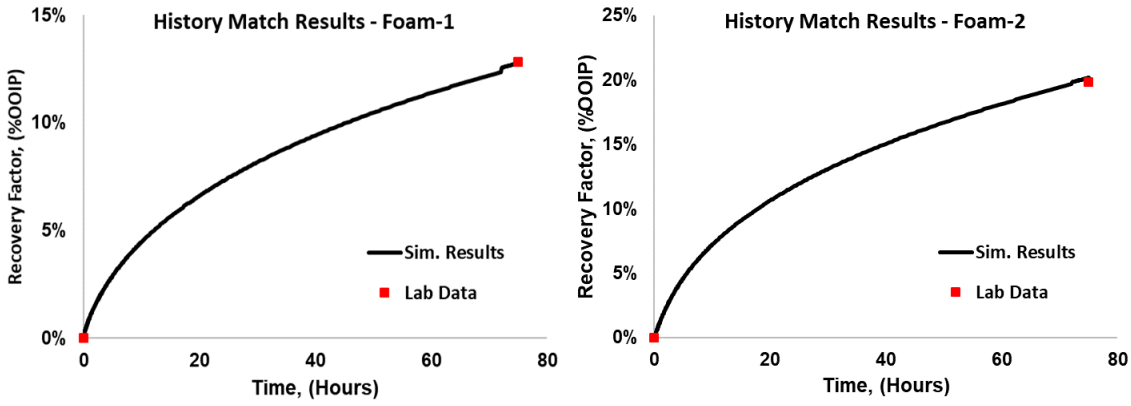

Figure 97 – History match results of the two foam Huff-n-Puff experiments. Foam-1 using the gas mixture (85% CH_4 - 15% C_2H_6) with Surfactant Surf B and Foam-2 using enriched gas (50% CH_4 - 50% C_2H_6) with Surfactant Surf B.

History match results decently agreed with the foam injection data for both the experiments. The diffusion coefficient, capillary pressure, and relative permeability curves achieved from previous history matches were validated from the core-scale history match results of the foam experiments. All the scaling parameters from the history match captured the performances of the different EOR methods and could be implemented into

the reservoir model to forecast possible recovery improvements in unconventional liquid reservoirs.

CHAPTER VIII

CONCLUSIONS AND RECOMMENDATIONS

This study dealt with the effects of surfactants, gas injection, sequencing surfactant/gas injection, and foam on improving oil recovery in unconventional liquid reservoirs through numerical simulation and laboratory experiments. A set of correlated experiments, including spontaneous imbibition, gas injection, and foam injection tests, were performed to evaluate the efficiency of various EOR methods on recovery and gather enough data to determine upscaling parameters from core-scale history match using numerical simulation. This research developed comprehensive simulation workflows for chemical, gas injection, and hybrid EOR applications in order to target unconventional shale reservoirs. The reservoir model considered the results of laboratory experiments, core-scale history match, and hydraulic fracturing simulation to represent the flow behavior of unconventional liquid reservoirs better and forecast the actual performance effect of various EOR methods.

In order to evaluate the potential of surfactant related chemical EOR applications, surfactant screening tests were performed to understand the mechanisms of chemical EOR on improving oil recovery and collect data for reservoir simulation. Surfactant additives can change the wettability of rock from oil and intermediate-wet to water-wet and moderately reduce IFT, resulting in enhancing oil flow paths and extracting additional oil from smaller pores. CT scan technology is utilized to track saturation change during the imbibition experiments. In addition, the CT images of the core plug were utilized to

convert individual voxel to the porosity and permeability in the core-scale model to model the heterogeneity of core samples. Capillary pressure and relative permeability curves before and after surfactant treatment were determined by scaling group analysis and core-scale history match, coupled with surfactant adsorption data to simulate the effects of wettability alteration and IFT reduction on reservoir simulation.

The results indicate wettability alteration and IFT reduction are the primary mechanisms of chemical EOR in ULR. A proper surfactant formulation is essential to improve oil production significantly through chemical EOR using surfactant additives. A surfactant screening test is needed to select the most suitable type of surfactant utilizing the oil and rock samples from the target formation. The addition of surfactants into completion and injection fluids results in oil production boost for new wells and remediation of existing depleted wells in shale reservoirs. Laboratory data, reservoir properties, and numerical simulation results are systematically analyzed to optimize chemical EOR design in ULR.

This research also provided the assessment of improved oil recovery in unconventional liquid reservoirs through the gas injection process, including gas Huff-n-Puff experiments, ternary diagram analysis, core-scale history match, and forecasting oil production enhancement by application of the reservoir simulation. The dominant mechanism of the gas injection process was concluded by analyzing experimental data, ternary diagrams, and simulation results. In addition, the optimum gas composition was also investigated by comparing the results of slim tube miscibility pressure measurements and gas injection experiments for different gases.

The results reveal that the primary recovery mechanism of the gas injection process in ULR is multi-contact miscibility rather than diffusion. As injection pressure is above the MMP, the multi-contact miscibility process causes the lighter components of the oil to vaporize into the gas phase along with viscosity reduction and oil swelling. The effect of the diffusion defined by Fick's law contributes less than 10% of the ultimate recovery in the gas injection tests.

MMP is the critical parameter determining the performance of gas injection EOR in shale reservoirs, and the injection pressure should be higher than the MMP to improve oil production effectively. This finding challenges the paradigm in the conventional reservoirs that operating pressure at the MMP is the optimum injection pressure for EOR designs. However, increasing injection pressure above the MMP does not always result in higher ultimate oil recovery, for instance, the optimum pressure of gas injection using CO_2 is between 3,500 psi and 5,000 psi in the Wolfcamp reservoirs. Although CO_2 has a lower MMP and a significant impact of oil recovery enhancement at 3,500 psi, CO_2 was observed to be less effective at high pressure (beyond 5,000 psi). Enriched gas (50% CH_4 – 50% C_2H_6), which is easy to access and achieved the highest recovery factor from the Huff-n-Puff experiment at 5,000 psi, possesses the greatest potential as the optimum gas composition for gas injection in the Wolfcamp formations.

Next, the evaluation of the hybrid EOR (sequencing surfactant/gas injection) technique on improving oil recovery in the Eagle Ford formation was described in this study (as shown in Chapter VI). The laboratory observations demonstrated the feasibility of combining chemical and gas injection EOR methods to enhance oil recovery in ULR.

CT images and produced oil were analyzed to reveal the target oil components and pore size for each method. In addition, the numerical simulation workflow of this hybrid EOR method was developed to upscale the experimental results to evaluate the efficiency of this hybrid technique on recovery and provide guidance of EOR design for the Eagle Ford.

The results confirm that the hybrid EOR technique is a feasible and fast method to improve oil recovery in ULR effectively. Even the core plug that was recovered 50% of OOIP from the gas injection experiment was capable of producing an additional 10% OOIP using chemical EOR. Generally, core plugs were saturated in crude oil for more than three months to restore the original reservoir conditions. However, up to 60% of OOIP was recovered from the core plug within ten days. In addition, the laboratory observations indicate that chemical and gas injection techniques recover two different spectra. Heavier components of the oil are recovered from smaller pores through the surfactant imbibition process, whereas most of the oil is recovered from larger pores with lighter components during gas injection.

Finally, a novel foam Huff-n-Puff experimental workflow was designed for assessing the efficiency of the foam EOR method in ULR. The potential of foam injection as a remedial treatment for depleted horizontal wells in ULR was investigated through foam Huff-n-Puff experiments. As with previous EOR experiments, CT images analysis along with observation of the color of produced oil from the tests was used to analyze transfer mechanisms.

The experimental results demonstrate foam injection is an attractive technique that can improve oil recovery in unconventional liquid reservoirs. As the foam interacts with

the reservoir rock, the imbibition process and gas vaporization process are co-occurred to expel oil from the matrix. Foam injection is a combination of chemical and gas injection EOR with the mechanisms of wettability alteration and multi-contact miscibility. Considering the effect of foam on mobility control and out of zone injection elimination, the foam injection could outperform the pure gas injection process in ULR. Methane hydrate observed in the laboratory may be a potential risk at foam injection field operation. Therefore, the foam injection EOR design needs to consider the temperature limitation for the surface facilities. Based on the analysis of CT images and normalized average CT number curves, recovery rate shows a strong correlation with foam quality that stable foam results in a higher recovery rate. The foam injection process opens the possibility of achieving optimum oil recovery for depleted well in ULR.

The results and observations from this study confirm the potential of various EOR methods on improving oil recovery in ULR and provide insight into optimal EOR design for different unconventional liquid shale plays. The main conclusions and recommendations of the research are presented following:

- The primary recovery mechanisms of chemical EOR technique in unconventional reservoirs are wettability alteration and interfacial tension reduction. The addition of surfactant into the completion and injection fluids enhances oil production by improving water imbibition that extracts more oil from the matrix as well as improving the flow capacity of oil in the fracture system.

- Surfactant type, surfactant concentration, and soak time must be taken into consideration in order to incorporate surfactants into the chemical EOR designs properly.
- Gas injection is a feasible EOR technique to significantly improve oil recovery in unconventional liquid reservoirs. The primary recovery mechanism of the gas injection process in ULR is multi-contact miscibility, resulting in lighter components of the oil vaporized into the gas phase along with viscosity reduction and oil swelling by dissolved gas.
- Diffusion is a minor recovery mechanism of the gas injection process. The effect of the diffusion defined by Fick's law contributes less than 10% of the ultimate recovery in the gas Huff-n-Puff experiments.
- The injection pressure should be higher than the MMP to enhance oil production in ULR effectively. Increasing injection pressure above the MMP does not always result in higher oil recovery. For example, the optimum pressure of gas injection using CO_2 is between 3,500 psi and 5,000 psi in the Wolfcamp reservoirs.
- The oil recovered from the CO_2 injection experiment at 5,000 psi was much darker than the oil produced from all the other gas experiments, indicating that heavier components of oil were extracted from the core by the high pressure CO_2.
- The enriched gas (50% CH_4 – 50% C_2H_6) achieved the highest recovery factor from the Huff-n-Puff experiment at 5,000 psi and possesses the greatest potential as the optimum gas composition for gas injection EOR in the Wolfcamp formations.

- Numerical simulation indicates greater injection pressure results in a larger gas injection volume into the reservoir thereby improving ultimate recovery.
- The hybrid EOR technique (sequencing chemical/gas injection) laboratory test conducted by gas Huff-n-Puff experiment followed by spontaneous imbibition tests results in 50% recovery from gas injection followed by an additional 10% OOIP during SASI.
- The hybrid EOR method has the combined effects of chemical and gas injection EOR techniques due to two different spectra of the hydrocarbons recovered by chemical and gas injection techniques. Heavier components of the oil are recovered from smaller pores through the surfactant imbibition process, while most of the oil recovered from the larger pores of the core plug with lighter components during the gas injection process.
- Foam injection is an attractive technique that can improve oil recovery in unconventional liquid reservoirs. As the foam interacts with the reservoir rock, the imbibition process and gas vaporization process co-occurred to expel the oil from the matrix.
- Methane hydrate was observed in the laboratory experiments and could be a potential risk during foam injection field operations. Foam injection EOR design needs to take into account the temperature limitation for surface facilities.
- The color of produced oil from foam tests is darker than the color of produced oil from no foam, pure gas injection experiments indicating the imbibition mechanism as previously described.

- The average CT number change during foam tests is smaller than the pure gas injection experiments. These observations indicate that the foam injection is a combination of chemical and gas injection EOR with the mechanisms of wettability alteration and multi-contact miscibility.
- Normalized average CT number curves of pure gas experiments (using CH_4, enriched gas (50-50), and CO_2) have a similar pattern, indicating that the gas injection process (regardless of gas composition) has a general normalized recovery rate curve.
- Recovery rate shows a positive trend with foam quality that stable foam results in a higher recovery rate. The recovery rate dramatically decreases when the foam collapses. In addition, the foam tends to be more stable in the glass beads at higher pressure indicating a longer duration of foam in propped fractures.
- Foam injection is a combination of chemical and gas injection EOR with the mechanisms of wettability alteration and multi-contact miscibility. Considering the effect of foam on mobility control and out of zone injection elimination, foam injection presumably could outperform pure gas injection process in ULR.
- The upscaling parameters dominating each EOR method are determined by history match Huff-n-Puff experimental data using the core-scale model. These parameters can be implemented into a large reservoir model to predict the performance of various EOR techniques in improving the oil recovery in unconventional liquid reservoirs.

REFERENCES

Adel, I. A., Tovar, F. D., Schechter, D. S. 2016. Fast-Slim Tube: A Reliable and Rapid Technique for the Laboratory Determination of Mmp in Co2 - Light Crude Oil Systems. Presented at the SPE Improved Oil Recovery Conference, Tulsa, Oklahoma, USA, 2016/4/11/. https://doi.org/10.2118/179673-ms.

Adel, I. A., Tovar, F. D., Zhang, F. et al. 2018a. The Impact of Mmp on Recovery Factor During Co2 – Eor in Unconventional Liquid Reservoirs. Presented at the SPE Annual Technical Conference and Exhibition, Dallas, Texas, USA, 2018/9/17/. https://doi.org/10.2118/191752-MS.

Adel, I. A., Zhang, F., Bhatnagar, N. et al. 2018b. The Impact of Gas-Assisted Gravity Drainage on Operating Pressure in a Miscible Co2 Flood. Presented at the SPE Improved Oil Recovery Conference, Tulsa, Oklahoma, USA, 2018/4/14/. https://doi.org/10.2118/190183-ms.

Afanasev, P., Scerbacova, A., Tsyshkova, A. et al. 2019. Compositions of Anionic and Non-Ionic Surfactants within a Hybrid Eor Technology for Unconventional Hydrocarbon Reservoirs. Presented at the SPE Russian Petroleum Technology Conference, Moscow, Russia, 2019/10/22/. 10.2118/196759-MS.

Alfarge, D., Alsaba, M., Wei, M. et al. 2018a. Miscible Gases Based Eor in Unconventional Liquids Rich Reservoirs: What We Can Learn. Presented at the SPE International Heavy Oil Conference and Exhibition, Kuwait City, Kuwait, 2018/12/10/. 10.2118/193748-MS.

Alfarge, D., Wei, M., Bai, B. 2017. Ior Methods in Unconventional Reservoirs of North America: Comprehensive Review. Presented at the SPE Western Regional Meeting, Bakersfield, California, 2017/4/23/. 10.2118/185640-MS.

Alfarge, D., Wei, M., Bai, B. 2018b. A Parametric Study on the Applicability of Miscible Gases Based Eor Techniques in Unconventional Liquids Rich Reservoirs. Presented at the SPE Canada Unconventional Resources Conference, Calgary, Alberta, Canada, 2018/3/13/. 10.2118/189785-MS.

Alharthy, N., Teklu, T., Kazemi, H. et al. 2015. Enhanced Oil Recovery in Liquid-Rich Shale Reservoirs: Laboratory to Field. Presented at the SPE Annual Technical Conference and Exhibition, Houston, Texas, USA, 2015/9/28/. 10.2118/175034-MS.

Alharthy, N., Teklu, T. W., Kazemi, H. et al. 2018. Enhanced Oil Recovery in Liquid-Rich Shale Reservoirs: Laboratory to Field. *SPE Reservoir Evaluation & Engineering* **21** (01):137-159. 10.2118/175034-PA.

Alhashim, H. W., Zhang, F., Schechter, D. S. et al. 2019. Investigation of the Effect of Pore Size Distribution on the Produced Oil from Surfactant-Assisted Spontaneous Imbibition in Ulrs. Presented at the SPE Annual Technical Conference and Exhibition, Calgary, Alberta, Canada, 2019/9/23/. 10.2118/195931-MS.

Alvarez, J. O., Saputra, I. W. R., Schechter, D. S. 2018a. The Impact of Surfactant Imbibition and Adsorption for Improving Oil Recovery in the Wolfcamp and Eagle Ford Reservoirs. *SPE Journal* **23** (06):2103-2117. 10.2118/187176-PA.

Alvarez, J. O., Schechter, D. S. 2016a. Application of Wettability Alteration in the Exploitation of Unconventional Liquid Resources. *Petroleum Exploration and Development* **43** (5):832-840. https://doi.org/10.1016/S1876-3804(16)30099-4.

Alvarez, J. O., Schechter, D. S. 2016b. Wettability, Oil and Rock Characterization of the Most Important Unconventional Liquid Reservoirs in the United States and the Impact on Oil Recovery. Presented at the Proceedings of the 4th Unconventional Resources Technology Conference, San Antonio, Texas, USA, 2016/8/1/. https://doi.org/10.15530/urtec-2016-2461651.

Alvarez, J. O., Tovar, F. D., Schechter, D. S. 2018b. Improving Oil Recovery in the Wolfcamp Reservoir by Soaking/Flowback Production Schedule with Surfactant Additives. *SPE Reservoir Evaluation & Engineering* **21** (04):1083-1096. 10.2118/187483-PA.

AlYousif, Z., Almobarky, M., Schechter, D. 2018. Nanoparticles-Stabilized Co2/Brine Emulsions at Reservoir Conditions: A New Way of Mitigating Gravity Override in Co2 Floods. Presented at the SPE Kingdom of Saudi Arabia Annual Technical Symposium and Exhibition, Dammam, Saudi Arabia, 2018/8/16/. 10.2118/192383-MS.

Atan, S., Ajayi, A., Honarpour, M. et al. 2018. The Viability of Gas Injection Eor in Eagle Ford Shale Reservoirs. Presented at the SPE Annual Technical Conference and Exhibition, Dallas, Texas, USA, 2018/9/24/. 10.2118/191673-MS.

Bai, B., Elgmati, M., Zhang, H. et al. 2013. Rock Characterization of Fayetteville Shale Gas Plays. *Fuel* **105**:645-652. https://doi.org/10.1016/j.fuel.2012.09.043.

Barragan, M., Woods, S., Julien, H. L. et al. 2002. Thermodynamic Equations of State for Hydrazine and Monomethylhydrazine. *Combustion and Flame* **131** (3):316-328. https://doi.org/10.1016/S0010-2180(02)00410-8.

Bidhendi, M. M., Kazempour, M., Ibanga, U. et al. 2019. A Set of Successful Chemical Eor Trials in Permian Basin: Promising Field and Laboratory Results. Presented at the SPE/AAPG/SEG Unconventional Resources Technology Conference, Denver, Colorado, USA, 2019/7/31/. 10.15530/urtec-2019-881.

Carpenter, C. 2019. Gas Injection Evaluated for Eor in Organic-Rich Shale. *Journal of Petroleum Technology* **71** (07):72-73. 10.2118/0719-0072-JPT.

Chevallier, E., Bouquet, S., Gland, N. et al. 2019. Advanced Eor Foam in Naturally Fractured Carbonates Reservoirs : Optimal Balance between Foam and Interfacial Tension Properties. Presented at the SPE Middle East Oil and Gas Show and Conference, Manama, Bahrain, 2019/3/15/. 10.2118/194992-MS.

EIA. 2019. Horizontally Drilled Wells Dominate U.S. Tight Formation Production. *Energy Information Administration*. https://www.eia.gov/todayinenergy/detail.php?id=39752.

EIA. 2020. Drilling Productivity Report. *Energy Information Administration*. https://www.eia.gov/petroleum/drilling/archive/2020/01/.

Ellafi, A., Jabbari, H. 2019. Coupling Geomechanics with Diffusion/Adsorption Mechanisms to Enhance Bakken Co2-Eor Modeling. Presented at the 53rd U.S. Rock Mechanics/Geomechanics Symposium, New York City, New York, 2019/8/28/.

EOG. 2019. Eog Resources Earnings (3q 2019) Presentation. https://s24.q4cdn.com/589393778/files/doc_financials/2019/q3/presentation_q3_2019.pdf.

Fick, A. 1855. Ueber Diffusion. *Annalen der Physik* **170** (1):59-86. 10.1002/andp.18551700105.

Gamadi, T. D., Sheng, J. J., Soliman, M. Y. et al. 2014. An Experimental Study of Cyclic Co2 Injection to Improve Shale Oil Recovery. Presented at the SPE Improved Oil Recovery Symposium, Tulsa, Oklahoma, USA, 2014/4/12/. 10.2118/169142-MS.

Hoffman, B. T., Reichhardt, D. 2019. Quantitative Evaluation of Recovery Mechanisms for Huff-N-Puff Gas Injection in Unconventional Reservoirs. Presented at the SPE/AAPG/SEG Unconventional Resources Technology Conference, Denver, Colorado, USA, 2019/7/25/. 10.15530/urtec-2019-147.

Jacobs, T. 2019. To Solve Frac Hits, Unconventional Engineering Must Revolve around Them. *Journal of Petroleum Technology* **71** (04):27-31. 10.2118/0419-0027-JPT.

Jin, L., Sorensen, J. A., Hawthorne, S. B. et al. 2017. Improving Oil Recovery by Use of Carbon Dioxide in the Bakken Unconventional System: A Laboratory Investigation. *SPE Reservoir Evaluation & Engineering* **20** (03):602-612. 10.2118/178948-PA.

Katiyar, A., Patil, P., Rohilla, N. et al. 2019. Industry-First Hydrocarbon-Foam Eor Pilot in an Unconventional Reservoir: Design, Implementation, and Performance Analysis. Presented at the SPE/AAPG/SEG Unconventional Resources Technology Conference, Denver, Colorado, USA, 2019/7/25/. 10.15530/urtec-2019-103.

Kazempour, M., Kiani, M., Nguyen, D. et al. 2018. Boosting Oil Recovery in Unconventional Resources Utilizing Wettability Altering Agents: Successful Translation from Laboratory to Field. Presented at the SPE Improved Oil Recovery Conference, Tulsa, Oklahoma, USA, 2018/4/14/. 10.2118/190172-MS.

Leverett, M. C. 1939. Flow of Oil-Water Mixtures through Unconsolidated Sands. *Transactions of the American Institute of Mining and Metallurgical Engineers* **132**:149-169. https://doi.org/10.2118/939149-G.

Li, L., Su, Y., Sheng, J. J. 2018. Investigation of Gas Penetration Depth During Gas Huff-N-Puff Eor Process in Unconventional Oil Reservoirs. Presented at the SPE Canada Unconventional Resources Conference, Calgary, Alberta, Canada, 2018/3/13/. 10.2118/189804-MS.

Luo, S., Lutkenhaus, J. L., Nasrabadi, H. 2018. Effect of Nano-Scale Pore Size Distribution on Fluid Phase Behavior of Gas Ior in Shale Reservoirs. Presented at the SPE Improved Oil Recovery Conference, Tulsa, Oklahoma, USA, 2018/4/14/. https://doi.org/10.2118/190246-MS.

Mohanty, K. K., Tong, S., Miller, C. et al. 2019. Improved Hydrocarbon Recovery Using Mixtures of Energizing Chemicals in Unconventional Reservoirs. *SPE Reservoir Evaluation & Engineering* **Preprint** (Preprint):13. 10.2118/187240-PA.

Monsalve, A., Schechter, R. S., Wade, W. H. 1984. Relative Permeabilities of Surfactant/Steam/Water Systems. Presented at the SPE Enhanced Oil Recovery Symposium, Tulsa, Oklahoma, 1984/1/1/. 10.2118/12661-MS.

Morrow, N. R. 1976. Capillary Pressure Correlations for Uniformly Wetted Porous Media. *Journal of Canadian Petroleum Technology* **15** (04):22. 10.2118/76-04-05.

Nguyen, D., Wang, D., Oladapo, A. et al. 2014. Evaluation of Surfactants for Oil Recovery Potential in Shale Reservoirs. Presented at the SPE Improved Oil Recovery Symposium, Tulsa, Oklahoma, USA, 2014/4/12/. 10.2118/169085-MS.

Ning, Y., Kazemi, H. 2018. Ethane-Enriched Gas Injection Eor in Niobrara and Codell: A Dual-Porosity Compositional Model. Presented at the SPE Improved Oil Recovery Conference, Tulsa, Oklahoma, USA, 2018/4/14/. 10.2118/190226-MS.

Orozco, D., Aguilera, R., Selvan, K. 2018. Material Balance Forecast of Huff-and-Puff Gas Injection in Multiporosity Shale Oil Reservoirs. Presented at the SPE

Canada Unconventional Resources Conference, Calgary, Alberta, Canada, 2018/3/13/. 10.2118/189783-MS.

Orozco, D., Fragoso, A., Selvan, K. et al. 2019. Eagle Ford Huff 'N' Puff Gas-Injection Pilot: Comparison of Reservoir-Simulation, Material Balance, and Real Performance of the Pilot Well. *SPE Reservoir Evaluation & Engineering* **Preprint** (Preprint):14. 10.2118/191575-PA.

Pankaj, P., Phatak, A., Verma, S. 2018. Application of Natural Gas for Foamed Fracturing Fluid in Unconventional Reservoirs. Presented at the SPE Argentina Exploration and Production of Unconventional Resources Symposium, Neuquen, Argentina, 2018/8/13/. 10.2118/191863-MS.

Park, K. H., Schechter, D. S. 2019. Investigation of the Interaction of Surfactant at Variable Salinity with Permian Basin Rock Samples: Completion Enhancement and Application for Enhanced Oil Recovery. *SPE Drilling & Completion* **Preprint** (Preprint):14. 10.2118/191801-PA.

Parsegov, S. G., Nandlal, K., Schechter, D. S. et al. 2018a. Physics-Driven Optimization of Drained Rock Volume for Multistage Fracturing: Field Example from the Wolfcamp Formation, Midland Basin. Presented at the SPE/AAPG/SEG Unconventional Resources Technology Conference, Houston, Texas, USA, 2018/7/23/. https://doi.org/10.15530/urtec-2018-2879159.

Parsegov, S. G., Niu, G., Schechter, D. S. et al. 2018b. Benefits of Engineering Fracture Design. Lessons Learned from Underperformers in the Midland Basin. Presented at the SPE Hydraulic Fracturing Technology Conference and Exhibition, The Woodlands, Texas, USA, 2018/1/23/. https://doi.org/10.2118/189859-ms.

Pu, H., Li, Y. 2016. Novel Capillarity Quantification Method in Ior Process in Bakken Shale Oil Reservoirs. Presented at the SPE Improved Oil Recovery Conference, Tulsa, Oklahoma, USA, 2016/4/11/. 10.2118/179533-MS.

Rathmell, J. J., Stalkup, F. I., Hassinger, R. C. 1971. A Laboratory Investigation of Miscible Displacement by Carbon Dioxide. Presented at the Fall Meeting of the Society of Petroleum Engineers of AIME, New Orleans, Louisiana, 1971/1/1/. 10.2118/3483-MS.

Rubin, B. 2010. Accurate Simulation of Non Darcy Flow in Stimulated Fractured Shale Reservoirs. Presented at the SPE Western Regional Meeting, Anaheim, California, USA, 2010/1/1/. https://doi.org/10.2118/132093-MS.

Sahni, V., Liu, S. 2018. Miscible Eor Process Assessment for Unconventional Reservoirs: Understanding Key Mechanisms for Optimal Field Test Design. Presented at the SPE/AAPG/SEG Unconventional Resources Technology Conference, Houston, Texas, USA, 2018/8/9/. 10.15530/URTEC-2018-2870010.

Saputra, I. W. R., Park, K., Zhang, F. et al. 2019. Surfactant-Assisted Spontaneous Imbibition to Improve Oil Recovery on the Eagle Ford and Wolfcamp Shale Oil Reservoir: Laboratory to Field Analysis. *Energy & Fuels* **33** (8):6904-6920.

Schechter, D. S., Zhou, D., Orr, F. M. 1994. Low Ift Drainage and Imbibition. *Journal of Petroleum Science and Engineering* **11** (4):283-300. https://doi.org/10.1016/0920-4105(94)90047-7.

Shu, G., Dong, M., Hassanzadeh, H. et al. 2017. Effects of Operational Parameters on Diffusion Coefficients of Co2 in a Carbonated Water–Oil System. *Industrial & Engineering Chemistry Research* **56** (44):12799-12810. 10.1021/acs.iecr.7b02546.

Sun, H., Zhou, D., Chawathe, A. et al. 2017. Understanding the 'Frac-Hits' Impact on a Midland Basin Tight-Oil Well Production. Presented at the SPE/AAPG/SEG Unconventional Resources Technology Conference, Austin, Texas, USA, 2017/7/24/. 10.15530/URTEC-2017-2662893.

Sun, J. L., Zou, A., Sotelo, E. et al. 2016. Numerical Simulation of Co2 Huff-N-Puff in Complex Fracture Networks of Unconventional Liquid Reservoirs. *Journal of Natural Gas Science and Engineering* **31**:481-492. https://doi.org/10.1016/j.jngse.2016.03.032.

Thakur, G. 2019. Enhanced Recovery Technologies for Unconventional Oil Reservoirs. *Journal of Petroleum Technology* **71** (09):66-69. 10.2118/0919-0066-JPT.

Todd, H. B., Evans, J. G. 2016. Improved Oil Recovery Ior Pilot Projects in the Bakken Formation. Presented at the SPE Low Perm Symposium, Denver, Colorado, USA, 2016/5/5/. 10.2118/180270-MS.

Tovar, F. D., Barrufet, M. A., Schechter, D. S. 2018. Gas Injection for Eor in Organic Rich Shales. Part Ii: Mechanisms of Recovery. Presented at the SPE/AAPG/SEG Unconventional Resources Technology Conference, Houston, Texas, USA, 2018/8/9/. 10.15530/URTEC-2018-2903026.

Tovar, F. D., Eide, O., Graue, A. et al. 2014. Experimental Investigation of Enhanced Recovery in Unconventional Liquid Reservoirs Using Co2: A Look Ahead to the Future of Unconventional Eor. Presented at the SPE Unconventional Resources Conference, The Woodlands, Texas, USA, 2014/4/1/. https://doi.org/10.2118/169022-MS.

Valluri, M. K., Alvarez, J. O., Schechter, D. S. 2016. Study of the Rock/Fluid Interactions of Sodium and Calcium Brines with Ultra-Tight Rock Surfaces and Their Impact on Improving Oil Recovery by Spontaneous Imbibition. Presented at the SPE Low Perm Symposium, Denver, Colorado, USA, 2016/5/5/. https://doi.org/10.2118/180274-ms.

Wang, D. M., Zhang, J., Butler, R. et al. 2016. Scaling Laboratory-Data Surfactant-Imbibition Rates to the Field in Fractured-Shale Formations. *Spe Reservoir Evaluation & Engineering* **19** (3):440-449. https://doi.org/10.2118/178489-Pa.

Wang, S., Di, Y., Wu, Y.-S. et al. 2019. A General Framework Model for Fully Coupled Thermal-Hydraulic-Mechanical Simulation of Co2 Eor Operations. Presented at the SPE Reservoir Simulation Conference, Galveston, Texas, USA, 2019/3/29/. 10.2118/193879-MS.

Whitfield, T., Watkins, M. H., Dickinson, L. J. 2018. Pre-Loads: Successful Mitigation of Damaging Frac Hits in the Eagle Ford. Presented at the SPE Annual Technical Conference and Exhibition, Dallas, Texas, USA, 2018/9/24/. 10.2118/191712-MS.

Wilson, K. G. 1969. Non-Lagrangian Models of Current Algebra. *Physical Review* **179** (5):1499-1512. 10.1103/PhysRev.179.1499.

Xu, T., Hoffman, T. 2013. Hydraulic Fracture Orientation for Miscible Gas Injection Eor in Unconventional Oil Reservoirs. Presented at the SPE/AAPG/SEG Unconventional Resources Technology Conference, Denver, Colorado, USA, 2013/8/12/. 10.1190/urtec2013-189.

Xu, T., Lindsay, G., Zheng, W. et al. 2019a. Proposed Refracturing-Modeling Methodology in the Haynesville Shale, a Us Unconventional Basin. *SPE Production & Operations* **Preprint** (Preprint):10. 10.2118/187236-PA.

Xu, T., Zheng, W., Baihly, J. et al. 2019b. Permian Basin Production Performance Comparison over Time and the Parent-Child Well Study. Presented at the SPE Hydraulic Fracturing Technology Conference and Exhibition, The Woodlands, Texas, USA, 2019/1/29/. 10.2118/194310-MS.

Yadav, H., Motealleh, S. 2017. Improving Quantitative Analysis of Frac-Hits and Refracs in Unconventional Plays Using Rta. Presented at the SPE Hydraulic Fracturing Technology Conference and Exhibition, The Woodlands, Texas, USA, 2017/1/24/. 10.2118/184812-MS.

Young, T. 1805. Iii. An Essay on the Cohesion of Fluids. *Phil. Trans. R. Soc.* **95**. https://doi.org/10.1098/rstl.1805.0005.

Zhang, F., Adel, I. A., Park, K. H. et al. 2018a. Enhanced Oil Recovery in Unconventional Liquid Reservoir Using a Combination of Co2 Huff-N-Puff and Surfactant-Assisted Spontaneous Imbibition. Presented at the SPE Annual Technical Conference and Exhibition, Dallas, Texas, USA, 2018/9/17/. https://doi.org/10.2118/191502-MS

Zhang, F., Adel, I. A., Saputra, I. W. R. et al. 2019a. Numerical Investigation to Understand the Mechanisms of Co2 Eor in Unconventional Liquid Reservoirs. Presented at the SPE Annual Technical Conference and Exhibition, Calgary, Alberta, Canada, 2019/9/23/. 10.2118/196019-MS.

Zhang, F., Saputra, I. W. R., Adel, I. A. et al. 2018b. Scaling for Wettability Alteration Induced by the Addition of Surfactants in Completion Fluids: Surfactant Selection for Optimum Performance. Presented at the SPE/AAPG/SEG Unconventional Resources Technology Conference, Houston, Texas, USA, 2018/8/9/. 10.15530/URTEC-2018-2889308.

Zhang, F., Saputra, I. W. R., Adel, I. A. et al. 2019b. Numerical Investigation of Eor Applications in Unconventional Liquid Reservoirs through Surfactant-Assisted Spontaneous Imbibition Sasi and Gas Injection Following Primary Depletion. Presented at the SPE Annual Technical Conference and Exhibition, Calgary, Alberta, Canada, 2019/9/23/. 10.2118/196055-MS.

Zhang, F., Saputra, I. W. R., Niu, G. et al. 2018c. Upscaling Laboratory Result of Surfactant-Assisted Spontaneous Imbibition to the Field Scale through Scaling Group Analysis, Numerical Simulation, and Discrete Fracture Network Model. Presented at the SPE Improved Oil Recovery Conference, Tulsa, Oklahoma, USA, 2018/4/14/. https://doi.org/10.2118/190155-ms.

Zhang, F., Saputra, I. W. R., Parsegov, S. G. et al. 2019c. Experimental and Numerical Studies of Eor for the Wolfcamp Formation by Surfactant Enriched Completion Fluids and Multi-Cycle Surfactant Injection. Presented at the SPE Hydraulic Fracturing Technology Conference Woodlands, TX, USA, 2019/2/5/. https://doi.org/10.2118/194325-ms.

Zhang, Y., Di, Y., Yu, W. et al. 2017. A Comprehensive Model for Investigation of Co2-Eor with Nanopore Confinement in the Bakken Tight Oil Reservoir. Presented at the SPE Annual Technical Conference and Exhibition, San Antonio, Texas, USA, 2017/10/9/. 10.2118/187211-MS.